6525

Report No. FRA/ORD-81/73

A LOW COST CATENARY DESIGN -ANALYSIS

R.L. RETALLACK
AMERICAN ELECTRIC POWER
SERVICE CORPORATION
2 BROADWAY
NEW YORK, N.Y. 10004

GEORGE R. DOYLE, JR.
BATTELLE COLUMBUS
LABORATORIES
505 KING AVENUE
COLUMBUS, OHIO 43201

LYNN A. SCHNEIDER
JOHN M. SHEADEL
THE OHIO BRASS
COMPANY
380 N. MAIN STREET
MANSFIELD, OHIO

October, 1981

Final Report, Tasks 1 & 2

Prepared for

U.S. DEPARTMENT OF TRANSPORTATION
FEDERAL RAILROAD ADMINISTRATION
OFFICE OF FREIGHT AND PASSENGER
SYSTEMS, R & D
WASHINGTON, D.C. 20590

U.S. DEPARTMENT OF ENERGY
OFFICE OF TRANSPORTATION PROGRAMS
WASHINGTON, D.C. 20585

LEGAL NOTICE

This report was prepared by American Electric Power Service Corporation, Battelle Columbus Laboratories and the Ohio Brass Company, as an account of work sponsored by the Department of Energy (DOE) and the Department of Transportation (DOT). Neither DOE, DOT, any member of DOE or DOT, American Electric Power Service Corporation, Battelle Columbus Laboratories, The Ohio Brass Company, nor any person acting on behalf of either:

1. Make any warranty or representation, expressed or implied, with respect to the accuracy, completeness, or usefulness of the information contained in this report, or that the use of any information, apparatus, method, or process disclosed in this report may not infringe privately owned rights, or

2. Assume any liabilities with respect to the use of, or for damages resulting from the use of, any information, apparatus, method or process disclosed in this report.

This document is disseminated under the sponsorship of the Department of Transportation in the interest of the information exchange. The United States Government assumes no liability for the contents or use thereof.

Technical Report Documentation Page

1. Report No.	2. Government Accession No.	3. Recipient's Catalog No.
FRA/ORD-81/73		

4. Title and Subtitle	5. Report Date
A LOW COST CATENARY DESIGN-ANALYSIS Final Report, Tasks 1 & 2	October, 1981
	6. Performing Organization Code
7. Author(s) R.L. Retallack, George R. Doyle, Jr., Lynn A. Schneider, and John M. Sheadel	8. Performing Organization Report No.
9. Performing Organization Name and Address American Electric Power Service Corporation * 2 Broadway, New York, New York, 10004	10. Work Unit No. (TRAIS)
	11. Contract or Grant No. DTFR53-80-C-00045
12. Sponsoring Agency Name and Address U.S. Department of Transportation ** Federal Railroad Administration Office of Freight and Passenger Systems, R&D Washington, D.C., 20590	13. Type of Report and Period Covered Final Report October, 1980 to October, 1981
	14. Sponsoring Agency Code ** Co-Sponsors: U.S. Department of Energy Office of Transportation Programs Washington, D.C., 20585
15. Supplementary Notes * Subcontractors: Battelle Columbus Laboratories, Columbus, Ohio, 43201 The Ohio Brass Company, Mansfield, Ohio, 44902	

16. Abstract

A new system of railroad electrification has been studied that requires only a single contact conductor as opposed to the conventional catenary system. Preliminary designs for the various components have been developed and are described. These include the traveller (that rides on the contact conductor), the traveller arm and the supports for the contact conductor. Various dynamic analysis models were developed including a six-degree of freedom model and a finite-element model to study the dynamic performance of the total system. Results of the interaction of the components are presented for various contact conductor diameters and tensions, for different span lengths between supports and for various vehicle (traveller) speeds. These results indicate the concept is feasible and the design is viable. Further, the report recommends that the full-scale field test (tasks 3-7 inclusive of the contract) be funded to complete the dynamic analysis and to provide a working mechanical model.

17. Key Words	18. Distribution Statement
Railroad Electrification System, Catenary, Contact Conductor, Traveller/Conductor Design, Dynamic Analysis	Document is made available to the U.S. public through the National Technical Information Service, Springfield, Virginia, 22161

19. Security Classif. (of this report)	20. Security Classif. (of this page)	21. No. of Pages	22. Price
Unclassified	Unclassified		

Form DOT F 1700.7 (8-72) Reproduction of completed page authorized

EXECUTIVE SUMMARY

A new system of railroad electrification has been studied that requires only a single contact conductor as opposed to the conventional catenary system. Preliminary designs for the various components have been developed and are described. These include the traveller (that rides on the contact conductor), the traveller arm and the supports for the contact conductor. Various dynamic analysis models were developed including a six-degree of freedom model and a finite-element model to study the dynamic performance of the total system. Results of the interaction of the components are presented for various contact conductor diameters and tensions, for different span lengths between supports and for various vehicle (traveller) speeds.

As a result of the preliminary design studies and the dynamic analyses, the following were concluded:

1. The mechanical loads determined by the dynamic analysis are within the limits of reasonable design practice. These loads are not in thousands of pounds but in the order of hundreds of pounds.

2. As expected, to minimize these loads the weight of the assembly and the sag angle of the conductor must be low. Sag angle is minimized by high conductor tension and low conductor weight.

3. Further reduction of these mechanical loads can be effected by providing a transition curve in the conductor at the supports. The arc radius and length of the transition are within the limits of reasonable design practice.

4. Velocities above 50 MPH and lateral deflections of the conductor for curved track sections were briefly investigated. These conditions increase the mechanical loads, but it is believed a properly designed conductor support and transition curve will offset their effect.

5. The preliminary design, the dynamic analysis and the cost comparison indicate the concept is feasible and the design is viable. The cost comparison indicates the installed cost of the low cost catenary system is less than one-half that of the conventional catenary system.

6. The design and the results technically justify proceeding with the physical testing of the system. Testing should include initial design testing of the contact conductor support and of the traveller wheel assembly. Following this an outdoor full-scale laboratory test with rail vehicle speeds up to 50 MPH is required to confirm concept feasibility.

PREFACE

On August 24, 1979 an unsolicited proposal for the Research and Development of the Elevated Conductor System for Electric Railroads (Phase I) was submitted jointly to the Federal Railroad Administration and to the Department of Energy by the American Electric Power Service Corporation. This proposal describes a new system of railroad electrification, the elevated conductor system, that if developed would reduce substantially the high initial cost and maintenance cost of the conventional electrification systems. The estimated savings are believed significant enough to warrant an investigation of the technical and operational feasibility of this new system. The elements of the elevated conductor system are described in the U.S. Patent No. 3,829,631 (included as Appendix A).

The objectives of the proposed research and development program are:

Phase I - To conduct a theoretical dynamic analysis supplemented by laboratory testing to demonstrate the technical feasibility of the elevated conductor system and to determine the financial benefits of this new system.

Phase II - To make a preliminary full scale test to demonstrate the operational feasibility of the elevated conductor system.

Phase III -

1. To make a final full scale test of all the features of the elevated conductor system.
2. To establish a practical form for the elevated conductor system.
3. To determine the useful life of the various components.
4. To provide a full-size working model of the elevated conductor system for demonstration purposes.
5. To refine the cost and financial benefits.

Fundamental questions to be answered through this research are:

1. Is the elevated conductor system technically feasible?
2. Can this system be developed into an operationally and financially feasible railroad electification system?

Benefits of this total research program are:

1. The test facility (Phase III) will demonstrate to railroads, electric power utilities, equipment manufacturers and other practioners a simplified system of railroad electrification that markedly will reduce installation and maintenance costs from those of present designs.

2. This program will provide preliminary design and financial information for establishing this simplified system of railroad electrification.

3. The proven system will encourage railroad electrification hence will reduce the national demand for diesel fuel--petroleum, especially if the electric energy can be derived from energy sources other than petroleum, such as coal, nuclear or hydroelectric.

Funding, as applied for the original proposal, is for Phase I only--the theoretical dynamic analysis and the laboratory testing. The dynamic analysis is to be done by Battelle Columbus Laboratories, the design and fabrication of the components is to be done by The Ohio Brass Company and the management of the project and the laboratory test facility is to be provided by American Electric Power Service Corporation.

On September 9, 1980 a contract entitled, "A Low Cost Catenary Design--Analysis" was awarded for the work described under Phase I of the proposal.

The efforts of the following people are acknowledged for furthering this project and providing technical assistance:

Donald Ahlbeck
Willard Kaiser — Battelle Columbus Laboratories
Robert Prause

M. F. Gowing
Donald L. Herbert — The Ohio Brass Company
John R. Turk

METRIC CONVERSION FACTORS

Approximate Conversions to Metric Measures

Symbol	When You Know	Multiply by	To Find	Symbol
LENGTH				
in	inches	*2.5	centimeters	cm
ft	feet	30	centimeters	cm
yd	yards	0.9	meters	m
mi	miles	1.6	kilometers	km
AREA				
in^2	square inches	6.5	square centimeters	cm^2
ft^2	square feet	0.09	square meters	m^2
yd^2	square yards	0.8	square meters	m^2
mi^2	square miles	2.6	square kilometers	km^2
	acres	0.4	hectares	ha
MASS (weight)				
oz	ounces	28	grams	g
lb	pounds	0.45	kilograms	kg
	short tons (2000 lb)	0.9	tonnes	t
VOLUME				
tsp	teaspoons	5	milliliters	ml
Tbsp	tablespoons	15	milliliters	ml
fl oz	fluid ounces	30	milliliters	ml
c	cups	0.24	liters	l
pt	pints	0.47	liters	l
qt	quarts	0.95	liters	l
gal	gallons	3.8	liters	l
ft^3	cubic feet	0.03	cubic meters	m^3
yd^3	cubic yards	0.76	cubic meters	m^3
TEMPERATURE (exact)				
°F	Fahrenheit temperature	5/9 (after subtracting 32)	Celsius temperature	°C

*1 in. = 2.54 cm (exactly). For other exact conversions and more detail tables see NBS Misc. Publ. 286, Units of Weight and Measures. Price $2.25 SD Catalog No. C13 10 286.

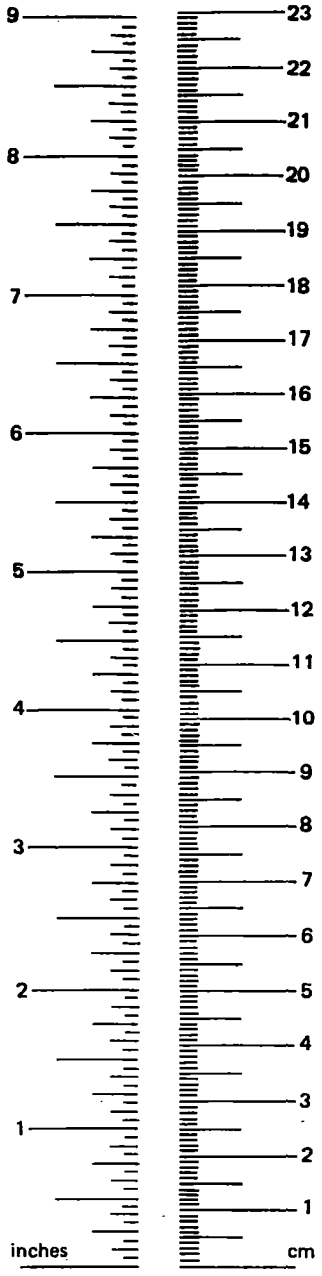

Approximate Conversions from Metric Measures

Symbol	When You Know	Multiply by	To Find	Symbol
LENGTH				
mm	millimeters	0.04	inches	in
cm	centimeters	0.4	inches	in
m	meters	3.3	feet	ft
m	meters	1.1	yards	yd
km	kilometers	0.6	miles	mi
AREA				
cm^2	square centimeters	0.16	square inches	in^2
m^2	square meters	1.2	square yards	yd^2
km^2	square kilometers	0.4	square miles	mi^2
ha	hectares (10,000 m^2)	2.5	acres	
MASS (weight)				
g	grams	0.035	ounces	oz
kg	kilograms	2.2	pounds	lb
t	tonnes (1000 kg)	1.1	short tons	
VOLUME				
ml	milliliters	0.03	fluid ounces	fl oz
l	liters	2.1	pints	pt
l	liters	1.06	quarts	qt
l	liters	0.26	gallons	gal
m^3	cubic meters	36	cubic feet	ft^3
m^3	cubic meters	1.3	cubic yards	yd^3
TEMPERATURE (exact)				
°C	Celsius temperature	9/5 (then add 32)	Fahrenheit temperature	°F

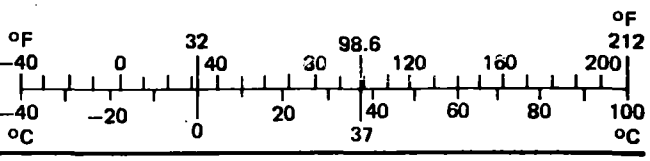

TABLE OF CONTENTS

TABLE OF CONTENTS
(Continued)

LIST OF ILLUSTRATIONS

LIST OF ILLUSTRATIONS
(Continued)

LIST OF ILLUSTRATIONS
(Continued)

LIST OF TABLES

1. INTRODUCTION

On September 9, 1980 a contract was awarded by the Federal Railroad Administration (FRA) to the American Electric Power Service Corporation (AEP) for "A Low Cost Catenary Design--Analysis". The objective is to determine if the electrification system described in U.S. Patent No. 3,829,631 (see Appendix A) is technically feasible and more economical to build than conventional railroad electrification systems. The purpose of this new system is to improve railroad's operating efficiency and to encourage the application of a transportation system not dependent on petroleum.

To achieve the above stated objective, the contract identifies seven tasks listed below:

Task 1: Preliminary Design Analysis. Conduct a literature search of the Railroad Research Information Service (RRIS) and other appropriate sources in order to preclude re-doing work already done and in order to broaden the contractor's technical knowledge base in this area. Conduct a preliminary theoretical dynamic analysis of a traveller in motion and its effect on the contact conductor and the supports for the contact conductor. Concurrent with this analysis, prepare a preliminary design of a traveller, the traveller arm and the supports for the contact conductor. Iterate the design and the analysis, as necessary, and identify areas requiring laboratory testing.

Task 2: Preliminary Concept Feasibility. Based on the results of Task 1, determine if preliminary analysis and design indicate concept feasibility and a viable design.

Task 3: System Design. Complete the design and fabricate the traveller, the traveller arm and the supports for the contact conductor.

Task 4: Test Facility. Design and build a suitable laboratory facility for dynamic testing the traveller, the contact conductor, and the supports of the contact conductor. Conduct tests at various speeds of the traveller and at various dimension values, and observe, monitor, and record test results.

Task 5: Final Design Analysis. Complete the theoretical dynamic analysis using laboratory results to supplement the analysis.

Task 6: TSC Hardware. Provide a second set of hardware (traveller, traveller arm, plus short section of conductor and conductor support) to the Transportation Systems Center, Cambridge, Massachusetts, of the various components of the system for laboratory testing as necessary.

Task 7: Concept Feasibility and Cost/Benefits. Through the dynamic analysis and the laboratory test results of Task 4, determine the technical feasibility of the traveller, the traveller arm, and the conductor support system to perform in an electrified rail system. Update cost estimate and conduct a cost/benefit analysis of the proposed system versus an equivalent existing conventional system. Present financial impacts that this new technology can have on railroad electrification.

Although seven tasks were listed in the contract, funding was approved only for Tasks 1 and 2. Further, the contract stipulates that before work may commence on tasks 3-7 inclusive, a cost and technical/management proposal must be submitted to and be approved by FRA. The contract also specifies that a final report shall be submitted at the completion of Tasks 1 and 2. This report covers only the work completed under Tasks 1 and 2.

For this work, subcontracts were let by AEP to Battelle Columbus Laboratories, Columbus, Ohio (Battelle) to conduct a theoretical dynamic analysis and to The Ohio Brass Company, Mansfield, Ohio (Ohio Brass) to prepare a preliminary design. This work was started October 1, 1980 and was completed as of the date of this report.

The work proceeded essentially as described under Task 1. First the literature search was conducted jointly by AEP, Battelle and Ohio Brass using the Railroad Research Information Service as the principal source. Then the preliminary design was initiated by Ohio Brass followed by the dynamic analysis conducted by Battelle. The preliminary design and the analytical results were iterated several times before selecting the design. The following sections will describe this work.

2. LITERATURE SEARCH AND INTERFACE WITH OTHER PROJECTS

A literature search was made using the Railroad Research Information Service and through other technical information sources available to AEP, Battelle and Ohio Brass. The documents reviewed are listed in Appendix B.

No literature was found that provided information, analytical techniques or design techniques that are directly applicable to the work described herein. The system of railroad electrification being investigated under this contract is significantly different from past or present systems of railroad electrification.

A meeting was held with Alcoa, the contractor of the Aluminum Catenary System Project, to interface the projects. Both projects were described and discussed, but it was found that the same major differences for the two projects exist as for conventional catenary systems vs. the catenary system under this project. However, the aluminum alloy contact conductor for the Aluminum Catenary System was recommended as an alternate contact conductor for this project. The aluminum alloy is 6201T81 and support attachments may be swaged directly onto this aluminum alloy contact conductor.

There are no other known projects requiring interface.

3. PRELIMINARY DESIGN

Basic System Requirements

Background

Since the beginning of electric traction, the transmission of electric power to the moving vehicle has been a critical function. To meet the reliability, safety and maintainability requirements as well as the electrical demand, many different systems of overhead power distribution have been tried.

For example, some early street railways had four wheel travellers riding on a pair of overhead wires. The mechanical connection, traveller current collector to street car, was also the conducting cable. A similar complete system was disclosed for electrifying buses in the U.S. Patent No. 1,817,093.

The original 1895 Baltimore and Ohio Railroad Howard Street tunnel electrification in Baltimore employed an overhead conductor of two Z-bars arranged to form a box shape with a slot in the bottom. A brass shoe held by a simple diamond shaped pantograph rides in this slot to pick up the current.

Both of these systems operated at low voltage, about 600 volts dc, and used heavy components. However, problems of corrosion, traveller mass and inertia, high currents, need for higher speeds and economics directed overhead current collection development toward a catenary system. Underrunning current collecting shoes, supported by a pantograph or a trolley arm arrangement from the top of the moving vehicle, pressed against the energized contact wire held over the train and parallel to the track by a catenary electrification system. The contact wires generally have been copper or copper alloy and more recently the shoes have been a carbon compound.

With the recent economic application of solid state rectifiers on moving vehicles, high AC traction voltages became practical. For many applications a single contact wire at 25kV or 50kV will meet the current carrying and mechanical strength requirements. This single contact conductor may employ the new concepts disclosed in the U.S. Patent No. 3,829,631 (Appendix A). New materials, such as high-strength lightweight metals and polymers, can be used to reduce mass and provide desirable mechanical properties. This new concept described in the patent of a current collector traveller mounted on an extensible arm from the vehicle and clamped around a single contact conductor provides freedom for the contact conductor to move to either side or above the vehicle, thus permitting choice of location by lowest cost.

To conduct the theoretical dynamic analysis, as required under this contract, each element, pole to vehicle, was reviewed for available

materials and possible design, and a choice or a range of choices was specified in order to conduct the analysis. The first dynamic analysis results were reviewed, and design changes and repeated analyses were made to determine the preliminary design as described herein.

Figure 3-1 shows a general arrangement of the subassemblies considered.

Contact Conductor

For 25kV or 50kV applications it was felt that short time high current demands for a traveller current collector would be limited to about 500 amp. Average current for one hour would be expected to be less than 200 amp. Mechanical requirements include conductor temperature changes from -29 C (-20 F) to 65.5 C (150 F), wind loads of 383 Pa (8 lb/ft^2), and combined ice and wind loading for heavy loading districts of 192 Pa (4 lb/ft^2) and 12.7 mm (0.5 in.) radial thickness of ice. For low cost installation, support points spaced apart on the order of 50 m (164 ft) to 90 m (295 ft) are normal power utility distribution line practice. The material must be favorable for good current collection and must have strength characteristics permitting economic span lengths. The diameter of the conductor must be great enough that no significant electrical discharge or corona will occur at the maximum operating voltage which may be as high as 55kV-to-ground.

Traveller Wheel Assembly

This assembly engages the contact conductor and must continue to engage the conductor as it passes down the line. Critical points are at the conductor support especially for rail curves. The current collection from the contact conductor must be continuous and reliable. Minimum mass will help reduce mechanical forces at changes in conductor direction. It must have an arrangement to permit placing it on and removing it from an energized contact conductor.

Arm Assembly

This assembly provides the connection between the traveller wheel assembly and the rail vehicle. It may be used, if desirable, to maintain the wheel assembly in a relationship to the vehicle axis. It must function with the contact conductor as close as 914 mm (36 in.) to the vehicle and continue to function until fully extended, 4270 mm (14 ft). It must provide a means of current conduction from the wheel assembly to the vehicle. At rest, extended horizontally and clamped on the contact conductor, the arm assembly may reasonably have a deflection of 25 mm (1 in.). It must withstand the mechanical loading resulting from speeds of 81 kph (50 mi/h) and potentially up to 162 kph (100 mi/h).

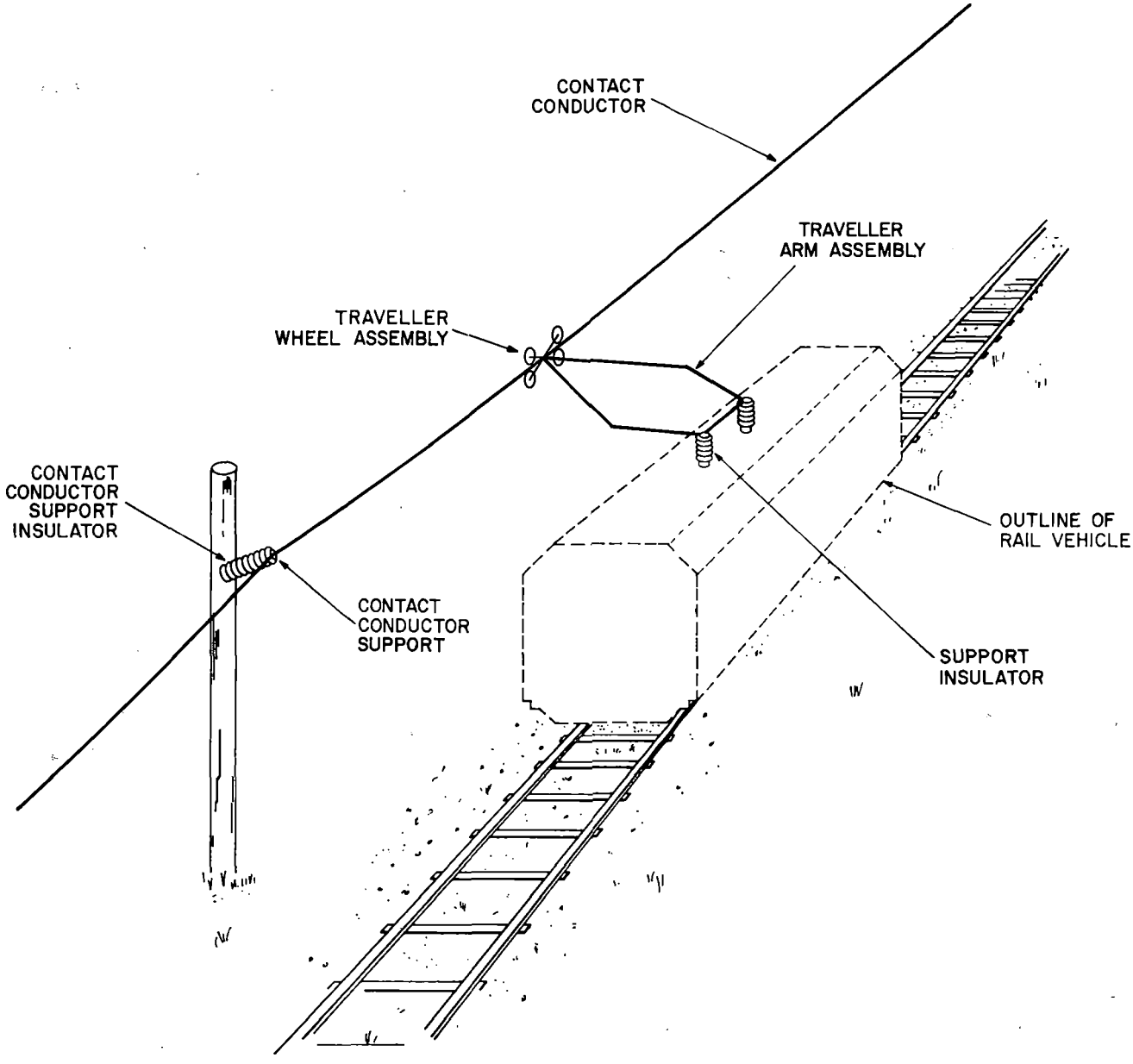

FIGURE 3-1. GENERAL ARRANGEMENT OF SUBASSEMBLIES FOR A LOW COST CATENARY SYSTEM.

High Voltage Insulators

The insulators must meet the electrical requirements for 25kV and 50kV line-to-ground operation. Basic impulse insulation levels (BIL) chosen are 250kV and 400kV, respectively. For railroad applications insulators having high resistance to impact damage are especially desirable. For the contact conductor support insulator, low stiffness will assist in reducing mechanical forces as the wheel assembly passes by a support point. Mechanical loads produced by the conductor and by the reaction from the moving wheel assembly must be withstood.

Contact Conductor Support

This device must meet the mechanical requirements of supporting the contact conductor at the conductor support insulator. The conductor shape and material is critical in this choice. The means to reduce any abrupt conductor direction change at the take-off (sag) angle also is important in reducing mechanical forces as the wheel assembly passes the support point.

Contact Conductor Design

Consideration was given to different materials and shapes for the contact conductor. First considered were round, grooved, Figure 9 deep-section grooved and Figure 8 trolley wires as defined by ANSI/ASTM B9, B47, and B116. Also, the conductor types illustrated in the patent (Appendix A) were considered. Figure 4 of the patent shows a solid contact conductor of a figure-8 type cross-section. Figure 4a shows a stranded type contact conductor. A review of these conductor types indicates that these conductors would not be suitable for the low cost catenary system under study. The stranded conductor, because of the traveller wheels rolling on the outer layer of helical strands, will cause accelerated mechanical wear of the strands and the wheels. The figure-8 conductor or any non-round conductor will experienced aerodynamic lift under wind conditions and may oscillate. This oscillation could result in operational problems and could cause metal fatigue at the supports.

Because of these concerns, it was concluded that the contact conductor must be of a solid (non-stranded), round configuration. Although contact conductors of tubular section or steel cladded with copper or aluminum may have applciation, it was decided to simplify the study and consider only solid, round conductors of copper or aluminum material. Subsequently, a nominal conductor size was chosen of 15.9 mm (0.625 in.) diameter solid hard drawn copper. Copper was chosen not only because this size will meet the current carrying requirements of short time demands of 500 amp, but also because of the long time experience with current collection. Present state-of-the-art current collection techniques can be applied with confidence.

Since the wheel assembly must travel engaging the contact conductor continuous, a fixed dead-end electrification system, not a constant tension system, is the simplest construction. Also, for the selected size of hard drawn copper contact conductor, a span length of about 61 m (200 ft) represents an average span for practical applications. Figure 3-2 illustrates the sag and tension curves for the temperature range specified. These values are calculated based on approximately half ultimate tension at -29 C (-20 F).

An illustration of a half span of the contact conductor is shown on Figure 3-3. The take-off (sag) angle at the support and the sag dimensions are identified. The sag angle at the support point of the contact conductor has been calcualted and is shown on Figure 3-4. This represents half of the total angle that the wheel assembly must pass at a tangent support point.

The contact conductor size selected will be free of any significant corona even under wet conditions when operating up to 55kV line-to-ground.

High Voltage Insulator Design

Contact Conductor Support Insulator

Of great significance in the study of a traveller current collecting system using a wheel assembly clamped on the contact conductor is the mechanical reaction as the wheel assembly passes the conductor support. The forces which occur must be within the capability of the system. The means to control the stress must be simple and economic compared to presently operating catenary systems. In contrast to former standard porcelain insulator assemblies which are relatively rigid and brittle, insulator assemblies using fiberglass reinforced plastics are now available that can provide spring constants at the wire support points that will markedly reduce the mechanical forces caused by the passage of the wheel assembly. These insulators have fiberglass reinforced epoxy rods at the core to provide the mechanical strength with desirable deflection properties. These insulators also employ weathersheds of a combination ethylene propylene copolymer (EPM) which provide the needed leakage surface characteristics required of high voltage insulators. These insulators are highly resistant to abuse such as stone throwing or rifle fire. They may be dropped on rails or other hard objects without damage. This style of insulator is now in regular production and is employed for general high voltage insulator applications.

The application of this insulator to the traveller assembly current collection system is best in the form of a horizontal line post shown in Figure 3-5 and Figure 3-6, when the contact conductor is along side the track. Not only is the deflection characteristic of the insulator helpful in reducing mechanical forces, but the insulator can

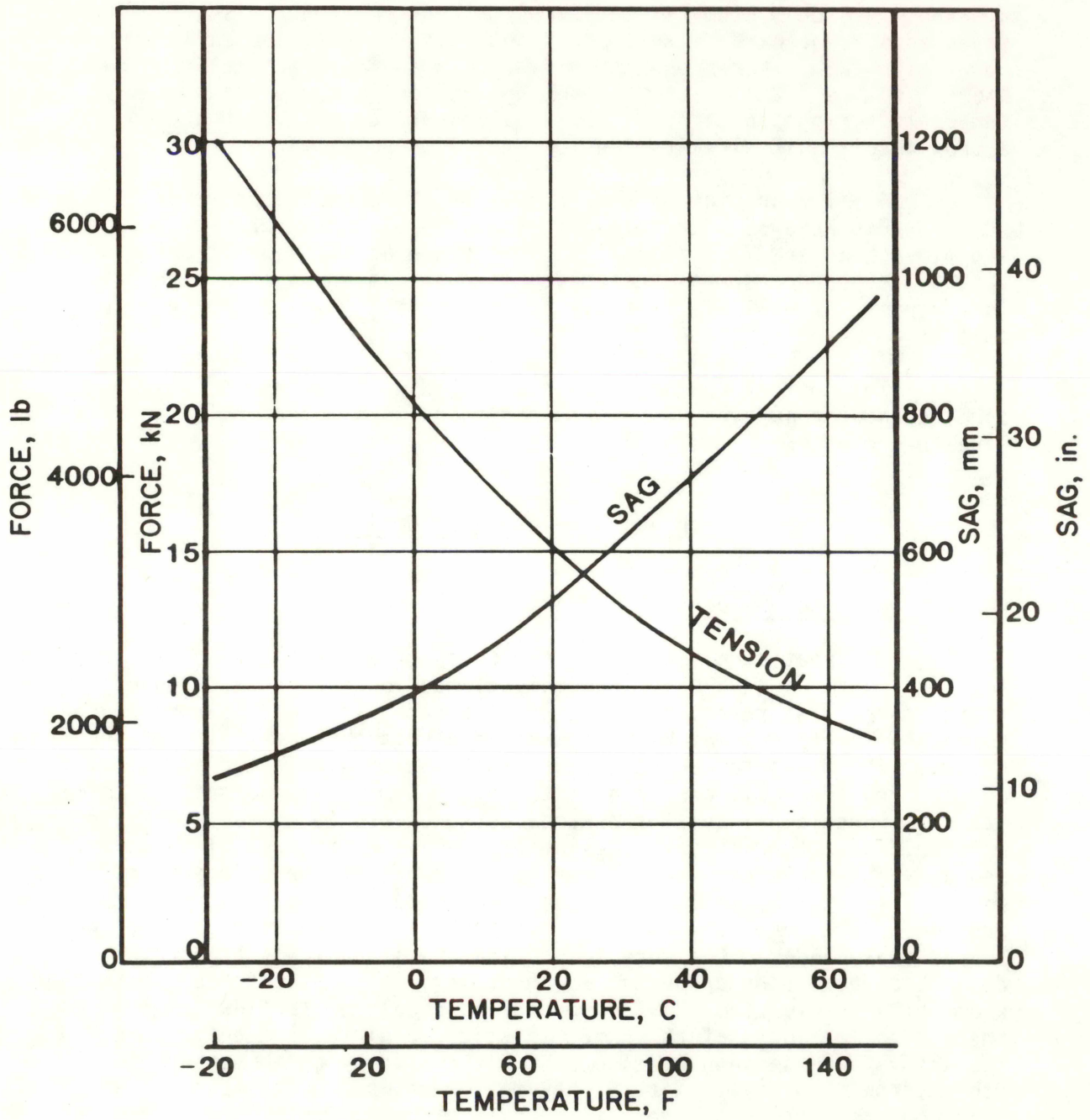

FIGURE 3-2. REPRESENTATIVE SAG AND TENSION CURVES: ROUND HARD DRAWN COPPER CONDUCTOR, 15.9 mm (0.625 in.) DIAMETER, 61 m (200 ft) SPAN. TENSION STRESS - 151690 kPa (22000 lb/in.^{2}) AT -29C (-20F)

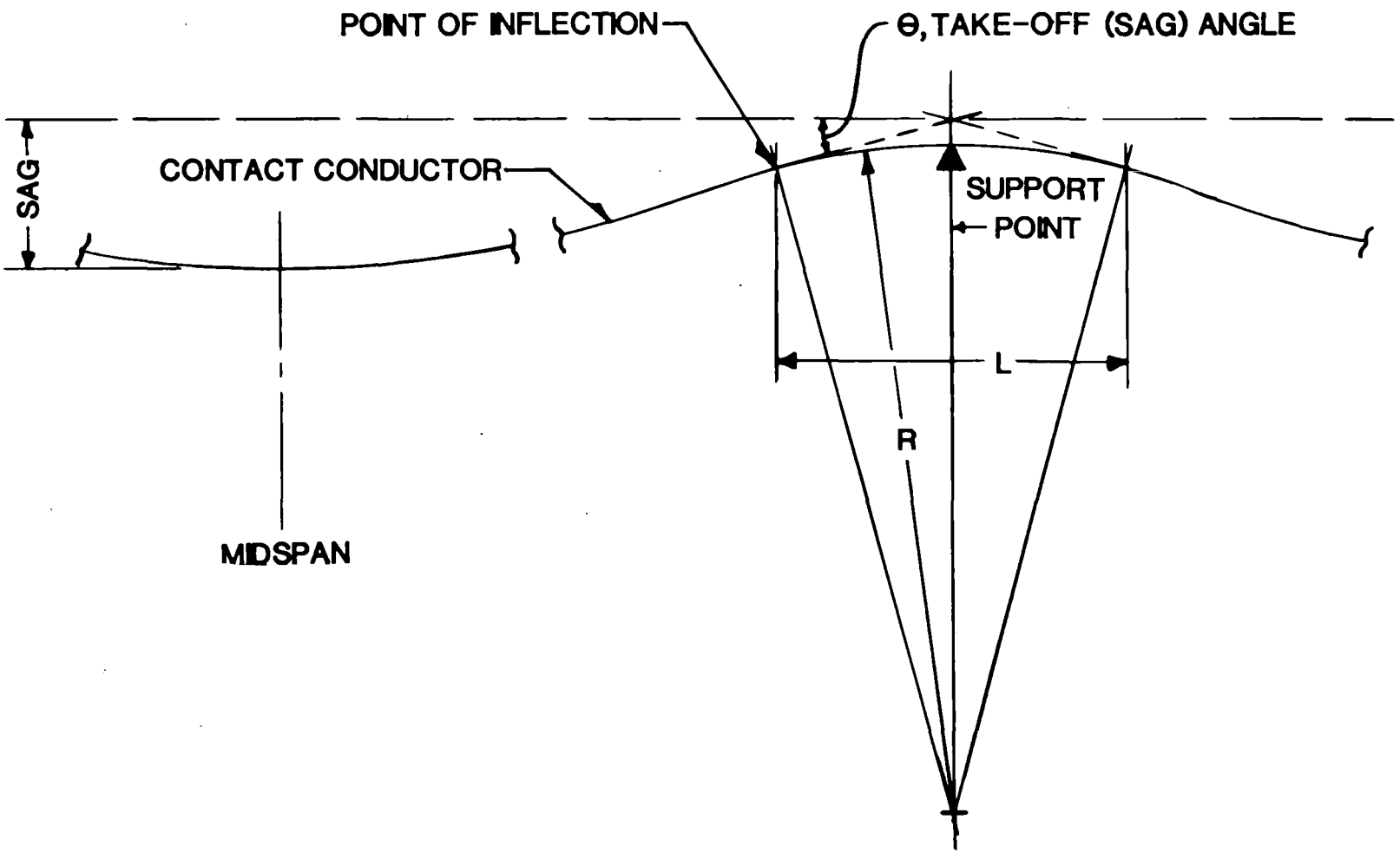

FIGURE 3-3. ILLUSTRATION OF HALF SPAN OF CONTACT CONDUCTOR INCLUDING POINT OF SUPPORT (NOT TO SCALE)

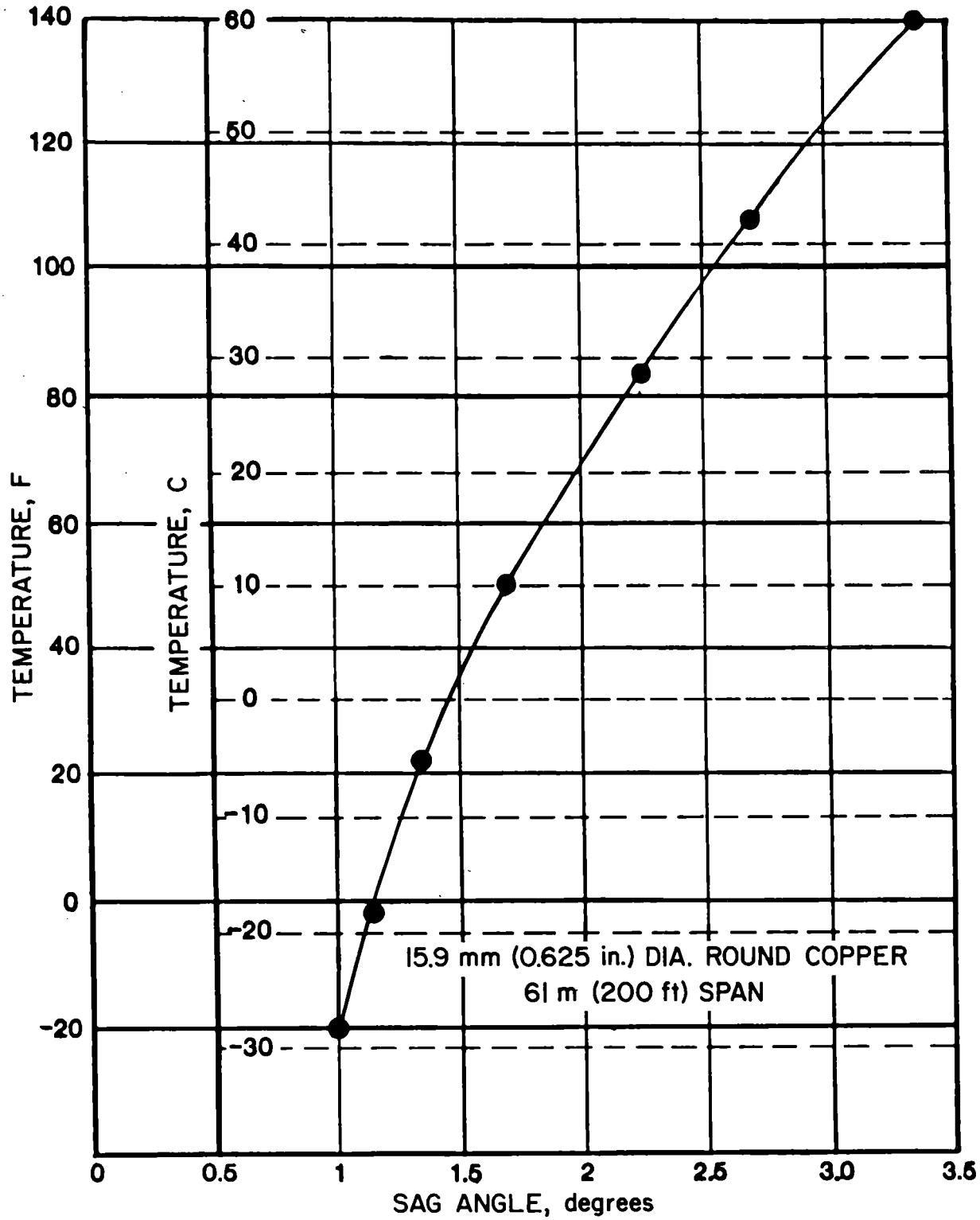

FIGURE 3-4. REPRESENTATIVE SAG ANGLE VS TEMPERATURE FOR 15.9 mm (0.625 in) DIA ROUND HD DRN COPPER CONDUCTOR ON A 61 m (200 ft) SPAN

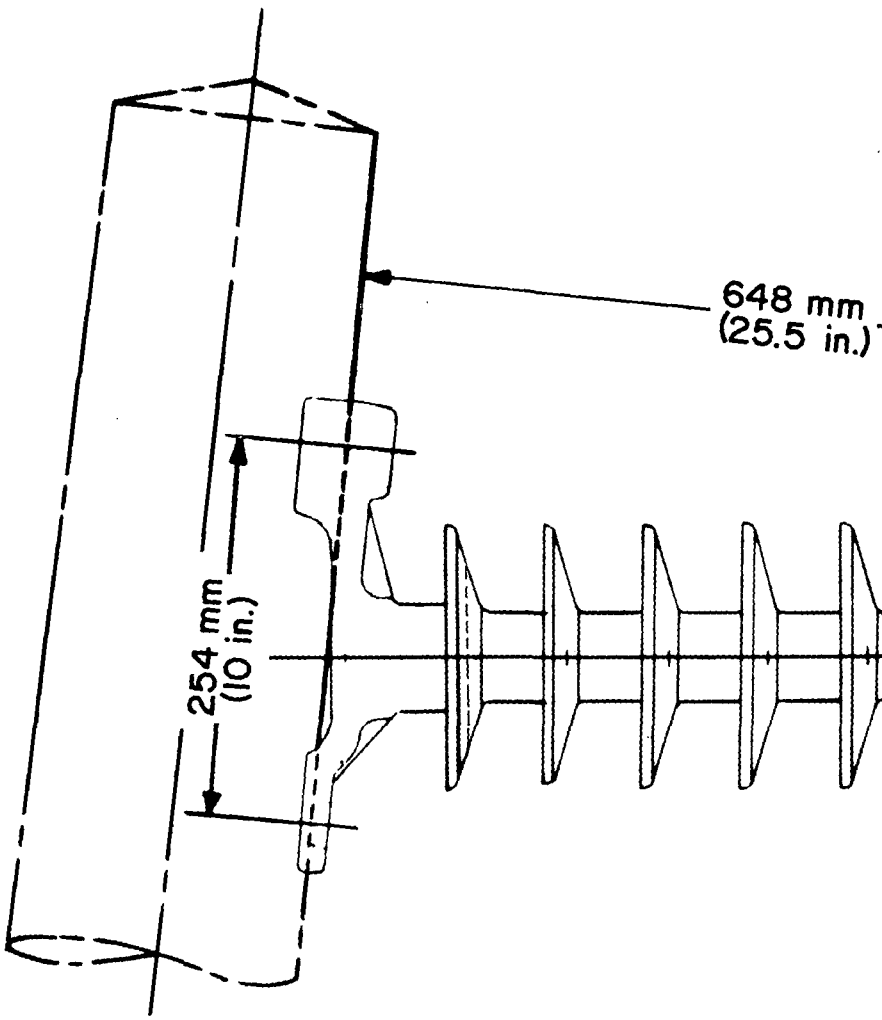

FIGURE 3-5. 25 kV HORIZONTAL LINE POST INSULATOR.

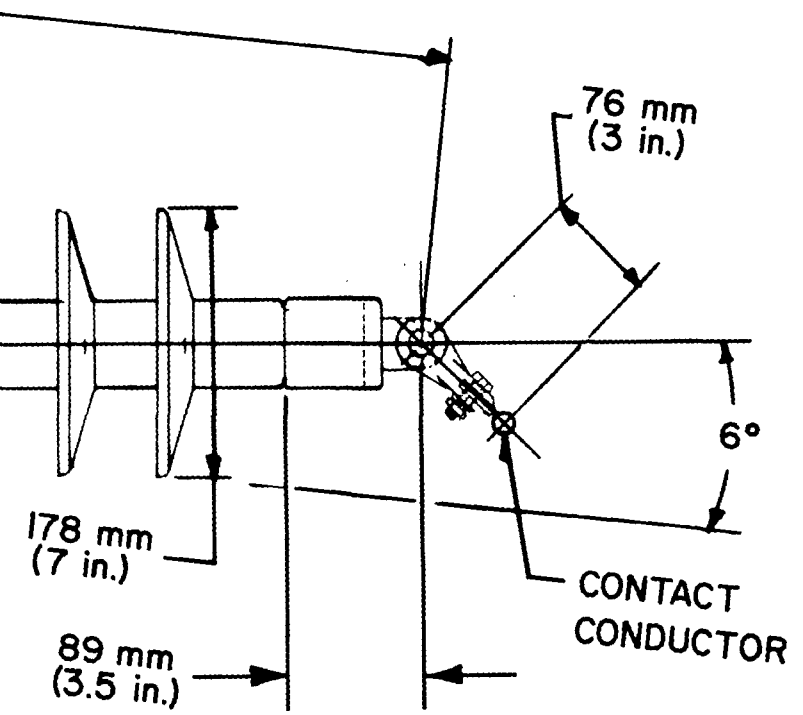
76 mm
(3 in.)
6°
178 mm
(7 in.)
CONTACT
CONDUCTOR
89 mm
(3.5 in.)

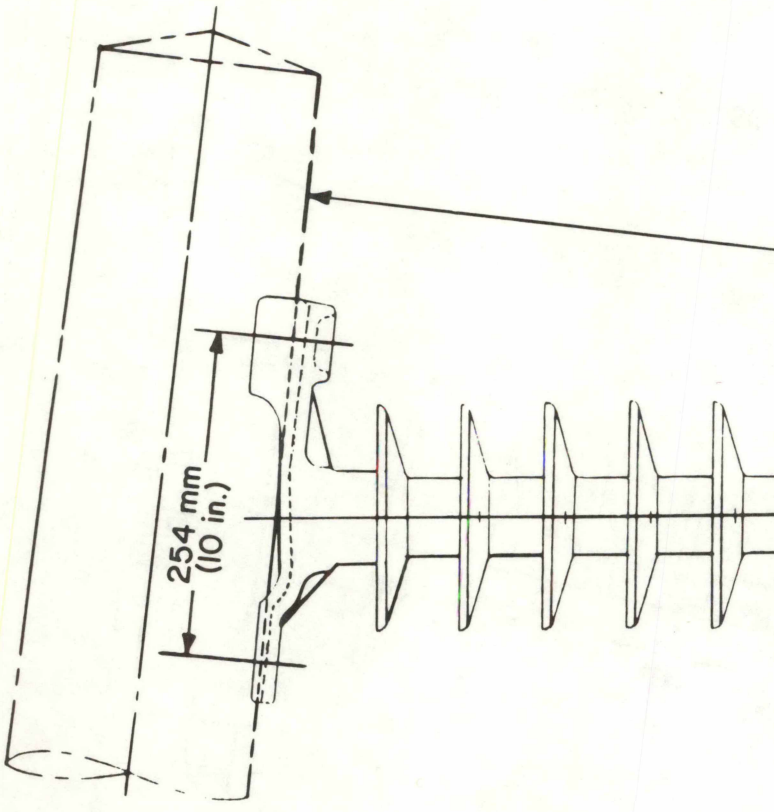

FIGURE 3-6. 50kV HORIZONTAL LINE POST INSULATOR.

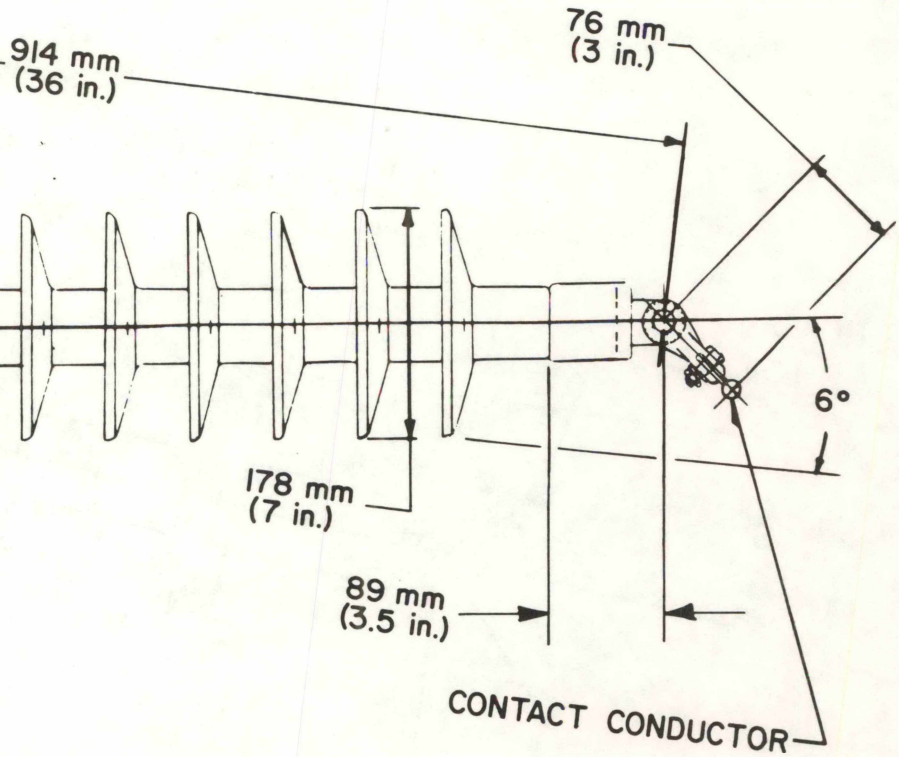
914 mm
(36 in.)
76 mm
(3 in.)
6°
178 mm
(7 in.)
89 mm
(3.5 in.)
CONTACT CONDUCTOR

be mounted toward the track, so that for a required pole clearance the traveller arm length will be a minimum value.

For the 15.9 mm (0.625 in.) diameter hard drawn copper contact conductor with 61 m (200 ft) spans, the resultant insulator load based on 12.7 mm (0.5 in.) radial thickness of ice and 192 Pa (4 lb/ft^2) wind velocity pressure is 2010 N (452 lb). Table 3-1 shows the characteristics of polymer horizontal line post insulators which meet the electrical and mechanical requirements for this wire and span for 25kV and 50kV voltage ratings.

TABLE 3-1. CHARACTERISTICS OF REPRESENTATIVE POLYMER HORIZONTAL LINE POST INSULATORS FOR 25KV AND 50KV VOLTAGE RATINGS (LINE-TO-GROUND)

	Figure 3-5	Figure 3-6
Voltage Application, Line-to-Ground, kV	25	50
Basic Impulse Insulation Level, kV	250	400
Leakage Distance, mm (in.)	1270 (50)	2000 (79)
Maximum Design Cantilever Load, N (lb)	4270 (960)	2890 (650)
Stiffness, N/mm (lb/in.)	140 (800)	43(245)

Insulator Support Assembly on Rail Vehicle

Similar styles of high voltage insulators are available for supporting the traveller assembly from the rail vehicle roof. Made of the same materials as the contact conductor support insulators, these insulators have the advantages of resilent reaction to sudden forces, high mechanical strength and excellent electrical properties. Also present is resistance to abuse such as stone throwing or rifle fire, which is a significant advantage for reliability and maintainability.

Where clearance permits, these insulators may be mounted vertically on the car roof, and tilted or horizontal installations may be used where necessary. Designs suitable for 25kV and 50kV are shown on Figure 3-7. Characteristics are listed in Table 3-2.

The traveller assembly drawing, Figure 3-13, shows two of these insulators mounted side by side on the vehicle roof in line with the axis of the car. The lower frame of the traveller assembly, which includes the pivot and equalizer assembly, is mounted directly on the top caps of these insulators.

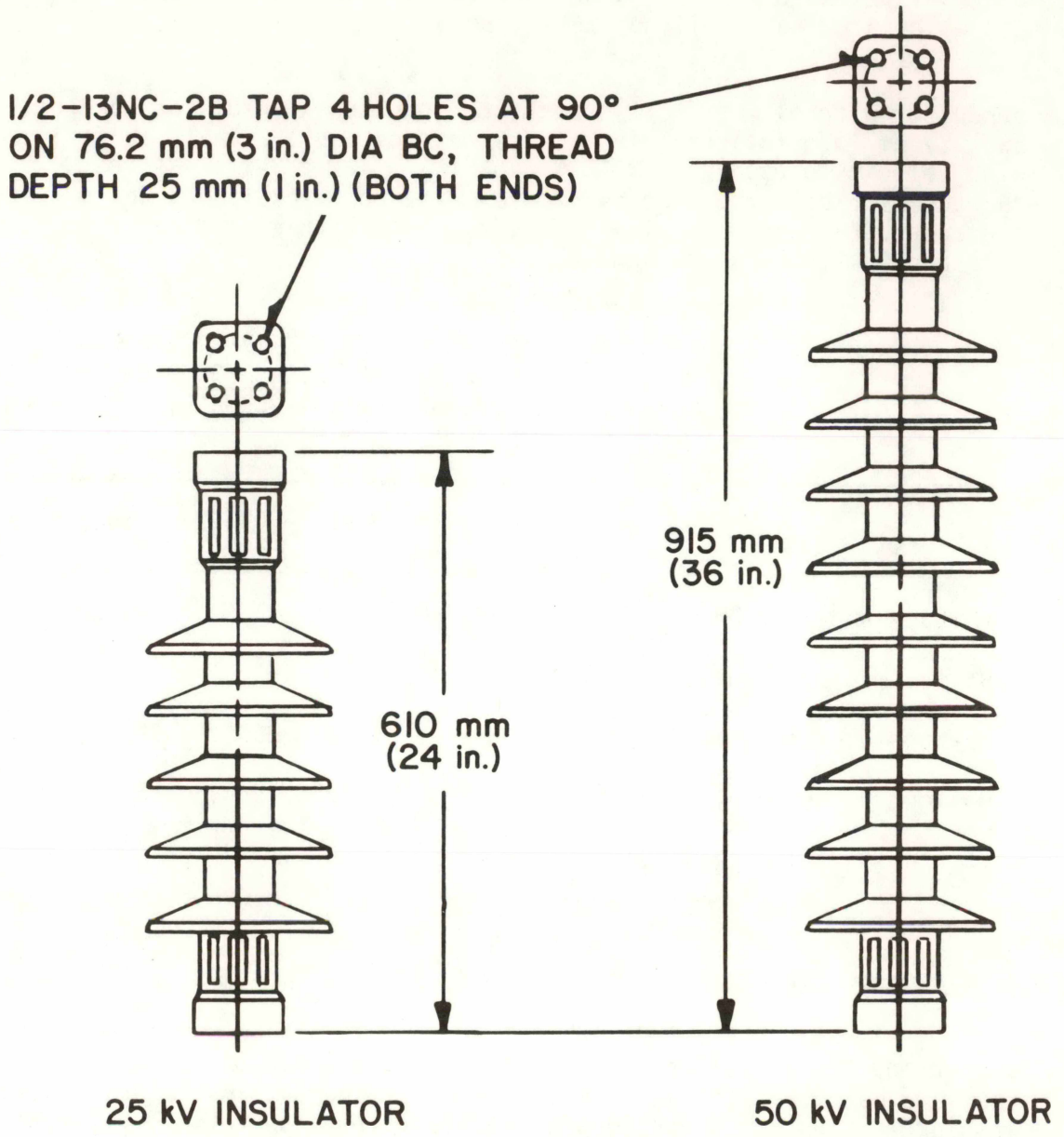

FIGURE 3-7. 25kV AND 50kV INSULATOR SUPPORT ASSEMBLIES AT RAIL VEHICLE.

TABLE 3-2. CHARACTERISTICS OF POLYMER STATION POST INSULATORS SUITABLE FOR SUPPORTING THE TRAVELLER ASSEMBLY ON THE RAIL VEHICLE

	Figure 3-7	
Voltage Application, Line-to-Ground, kV	25	50
Basic Impulse Insulation Level, kV	250	400
Leakage Distance, mm (in.)	1140 (45)	2060 (81)
Maximum Design Cantilever Load, N (lb)	8900 (2000)	5340 (1200)
Stiffness, N/mm (lb/in.)	840 (4800)	198 (1130)

Contact Conductor Support Design

Since the conductor is to be of round section, a challenging problem is a method of supporting this conductor--or more specifically, a method to attach this conductor to the support and still allow passage of the traveller past the support point. Figure 3-8A is a cross-section of a round conductor with traveller wheels shown by dashed lines. Based on the general proportions of the conductor and the wheels, it was decided arbitrarily that a sector 120 degrees above and below the conductor would be reserved for the traveller wheels and that a sector of 60 degrees right or left would be reserved for the attachment to the support.

Two methods of providing attachment to solid copper or aluminum conductors were investigated. One method is by soldering, brazing or welding and the other is by swaging. The Copper Development Association advises that welding would destroy the hard-drawn properties of the copper conductor, but with proper controls soldering or brazing may be used and still preserve the hard-drawn properties. Swaging also may be utilized to form the attachment for copper conductors, but this may require a more ductile alloy to avoid fracturing the copper.

The Aluminum Association advises that welding, soldering or brazing of 6201T81 aluminum alloy suitable for use as contact conductor, would destroy its heat-treatable strength properties. Swaging of 6201T81 aluminum alloy conductor is possible.

Figure 3-8B is a cross-section of a copper or aluminum conductor after swaging to provide an attachment point. The total cross-sectional area is the same as Figure 3-8A and the two 120 degree sectors for the traveller wheels must be maintained with the same radius

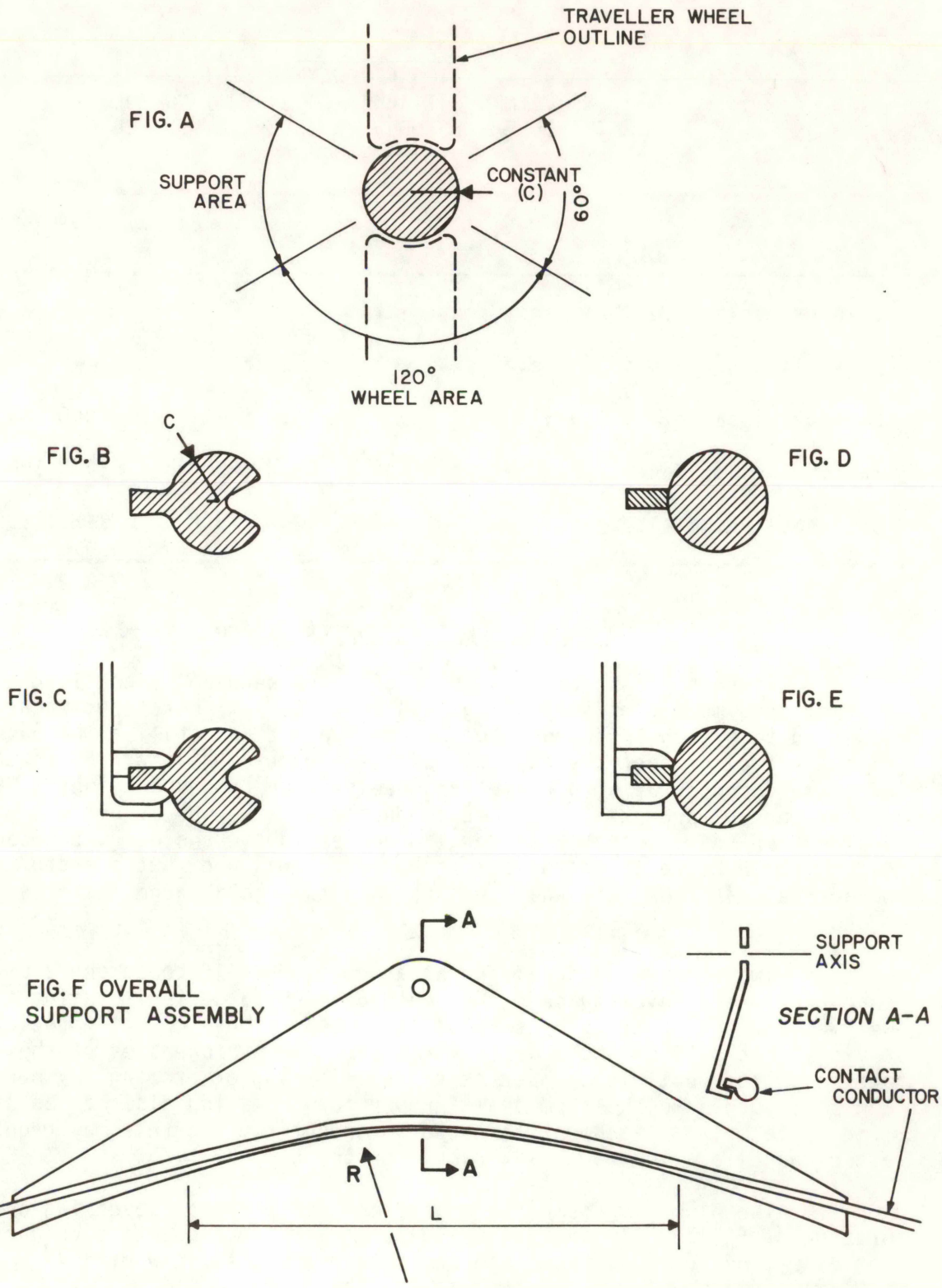

FIGURE 3-8. CONTACT CONDUCTOR ATTACHMENTS AND SUPPORT ASSEMBLY

(c) as the original round shape. In Figure 3-8C a bolted or swaged clamp is added to provide an attachment to the support assembly. The clamp and the swaging operation must be limited to the 60 degree sectors of the contact conductor.

Figure 3-8D is a cross-section of a copper conductor after a secondary support member has been soldered or brazed to the conductor. Again the 120 degree sectors for the traveller wheels must be left untouched. Figure 3-8E shows the clamp for the attachment to the support and this must be confined to the 60 degree sectors.

The control of forces which occur when the traveller wheel assembly passes the support point depends most significantly on the conductor support design. The conductor sag angles involved for the normal tangent span are summarized on Figure 3-4. As the conductor temperature increases, the sag and sag angle increase. The angle changes from about one degree at -29 C (-20 F) to over three degrees at 60 C (140 F). In order to provide a smooth transition at the insulator support, it is desirable to have the conductor supported at a proper radius of curvature. This can be accomplished by the design of a mounting tab attached to the conductor using the methods described before.

The mounting tab or support should be long enough to equal dimension L on Figure 3-3 so that the conductor take-off is tangential to the clamp support. Figure 3-9 shows a method of conductor support to provide this. A tapered strap support is shown joined to the conductor to provide a gradual change in conductor slope at the support. The means of support must be resilient enough to meet the changes in tension and sag angle caused by changes in temperature.

A second method of support providing a more direct solution is shown in Figure 3-8F. With this assembly the contact conductor is supported only for the distance necessary to maintain the radius of curvature R. If the span between supports is large (greater sag angle) more of the support arc is required. If the span between supports is small (less sag angle) less of the support arc is required. This support assembly with its conductor attachments can be designed to meet the support point criteria established by the dynamic analysis.

The dynamic analysis is used to define possible dimensions for length L and radius R of Figure 3-3. Further study and design testing is recommended to develop both of these conductor support methods described herein.

Wheel Assembly Design

The wheel assembly must continuously engage the contact conductor as the rail vehicle moves the wheel assembly along the conductor. The current collection from the conductor must function reliably and the mechanical reaction forces must be within the capabilities of the system.

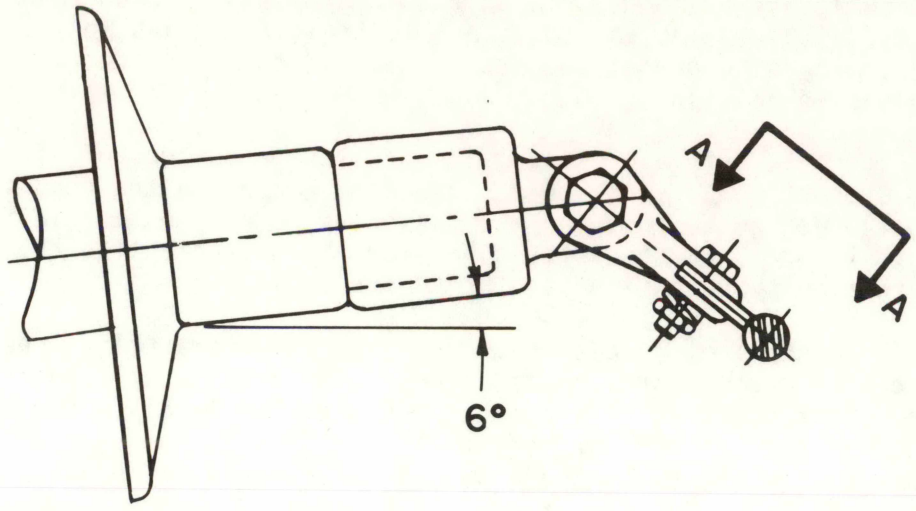

SIDE VIEW

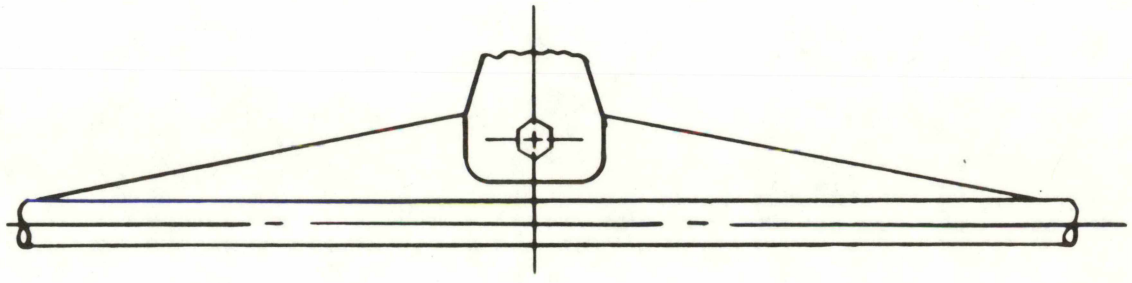

FRONT VIEW – SECTION A-A

FIGURE 3-9. TYPICAL CONTACT CONDUCTOR SUPPORT AT THE INSULATOR

The Patent describes an assembly with two pairs of grooved wheels and sliding contacts pressed against the contact conductor to hold the wheel assembly in engagement with the conductor and to establish electrical contact. This design principle is shwon in Figure 3-10. Type A uses wheels as the current collector. Since experience has indicated that sliding current collectors of suitable materials may have better current collection than that of rolling collectors, Type B shows two pairs of carbon shoes spring mounted in holders to clamp around the conductor and to collect the current. Type C shows a combination of wheels to serve as guides and shoes to collect the current.

Type A Wheel Current Collector

This assembly incorporates cast bronze collector wheels to guide the traveller assembly and to collect current from the conductor. Bronze is specified because of the electrical conductivity needs. This current collection method subjects the wheel and conductor to arcing and to erosion of the material. Higher currents can be collected with shoes. Type A assemblies also are relatively heavy. This produces high reaction forces on the conductor as the assembly passes through the support points. The high inertia of rapidly rotating wheels will cause tracking problems as the contact conductor changes direction.

Type B Shoe Current Collector

This design utilizes a set of holders with carbon inserts to collect from the contact conductor. It offers an improved current collection method when compared with a wheel type arrangement. It also provides a minimum mass assembly. The difficulty with this design is that it must rely on sliding contact between the insert holder and the conductor to guide the assembly. This will present problems with wear, especially at the support point where the contact conductor changes direction.

Type C Shoe Collector With Guide Wheels

This design incorporates carbon inserts to collect the current from the contact conductor and low mass wheels to guide the assembly along the wire. It utilizes the best feature of the wheel collector and the shoe collector. The superior current collection feature of carbon inserts and the superior guiding feature of a grooved wheel are used. Since the wheels do not collect current, they can be made of a minimum mass metal or non-metalic material to minimize the inertial and reaction forces. This was the design selected for the project.

Figure 3-11 shows this assembly as finally developed. Details of this assembly are described below:

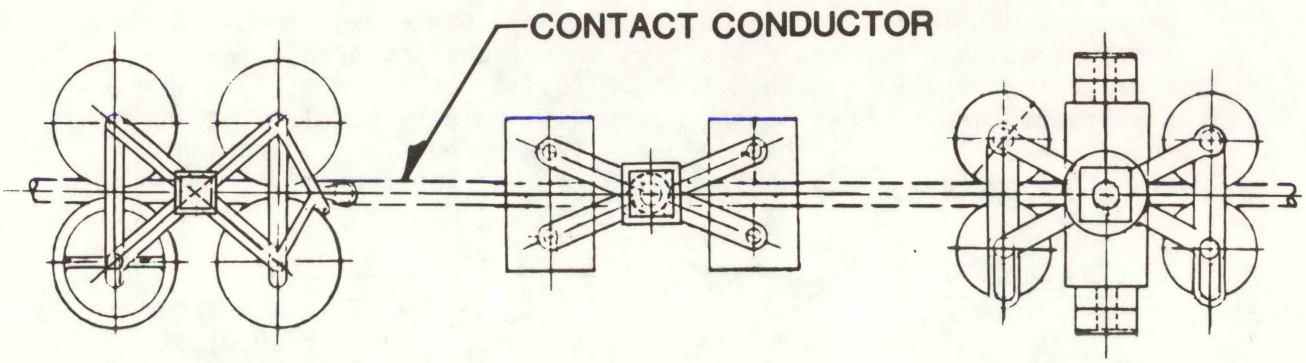

TYPE	CURRENT COLLECTION	FOLLOWING ABILITY	MASS	REACTIVE FORCES	MAINTENANCE
A	MODERATE	LOW	HIGH	HIGH	INTERMEDIATE
B	GOOD	LOW	LOW	LOW	HIGH
C	GOOD	HIGH	INTER-MEDIATE	INTER-MEDIATE	LOW

FIGURE 3-10. COMPARISON OF VARIOUS TRAVELLER WHEEL ASSEMBLY DESIGNS.

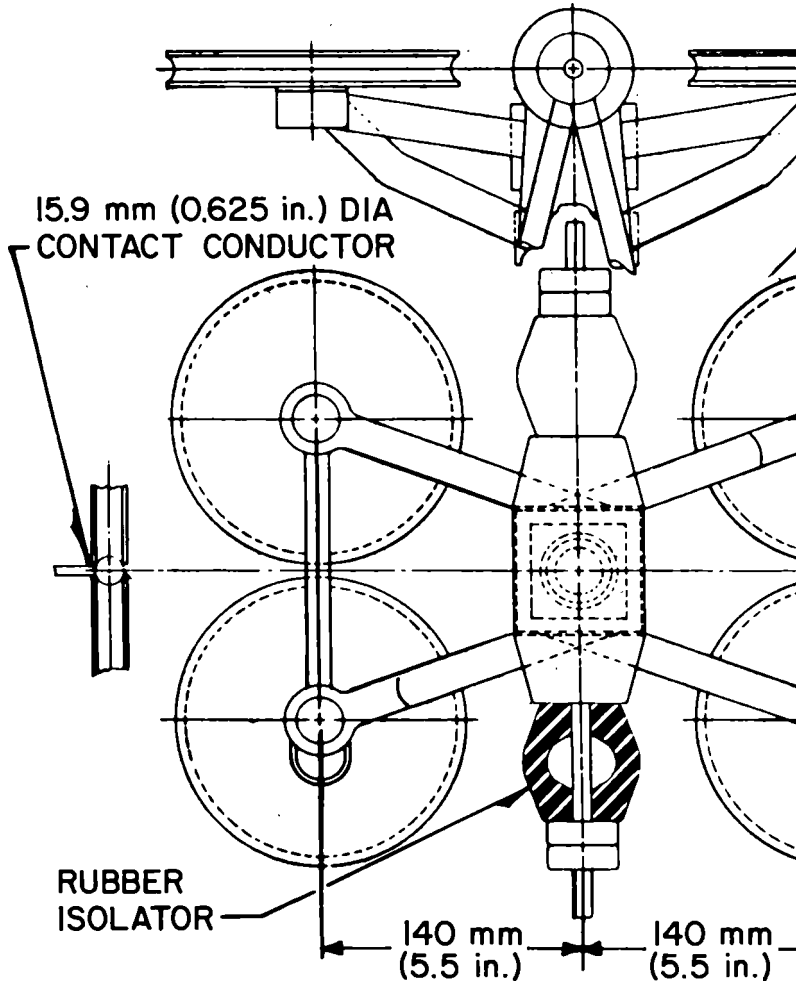

FIGURE 3-11. TRAVELLER WHEEL ASSEMBLY.

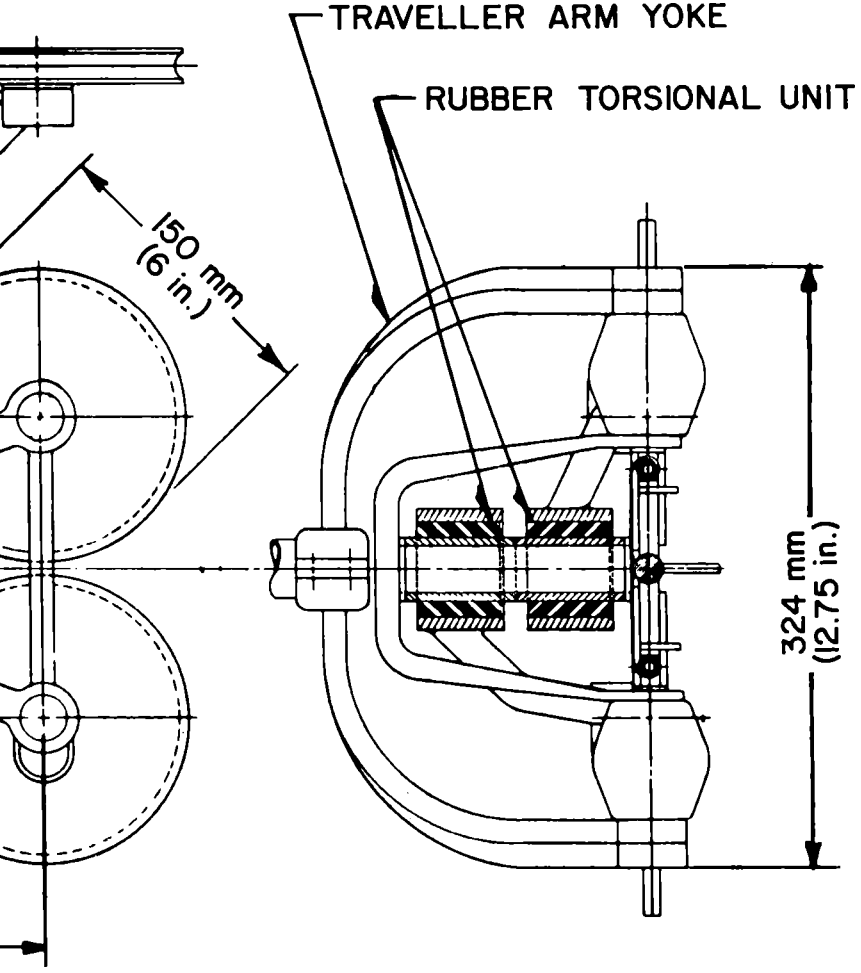
TRAVELLER ARM YOKE
RUBBER TORSIONAL UNIT
150 mm
(6 in.)
324 mm
(12.75 in.)

1. Shoe Collectors. These are an opposing pair of shoes resiliently mounted midway between the two pairs of guide wheels. Holders are designed to guide shoes, of a standard carbon compound, uniformly against opposite sides of the contact conductor. Constant force springs are used so that pressure against the conductor is unchanged as the carbon shoes wear. Since the shoes are relieved of the mechanical guidance function, the shoe size is based on meeting an assembly current carrying rating of 500 amp for short durations and 200 amp continuously. The brush life depends on many factors including the actual current demand, conductor and weather conditions, pressure on the conductor and occurances of loss of contact. Life well in excess of one thousand miles operation is reasonable.

2. Guide Wheels. Drawing layouts were made showing the fit of the wheels on 15.9 mm (0.625 in.) diameter wire at support points. Judgment suggested that wheels smaller than 150 mm (6 in.) diameter may have difficulty in providing guidance. The value of light weight in reducing reaction forces suggest the use of polymer materials. The most attractive material is polyether urethane with a hardness of 90-95 Shore A durometer. It has the desirable characteristics of stability, abrasion and wear resistance, and may be reinforced with fibers. Although data sheets suggest as much as one order of improvement in abrasion resistance over other polymers, performance comparisons will require actual tests. This design will permit the use of a replaceable rim if desirable. Various types of rolling and sleeve bearings were reviewed. For the best life expectance ball bearings are recommended.

3. Rubber Torsional Bushings. Rubber torsional units are employed to press the wheels against the contact conductor. This arrangement gives fast response to wheel/conductor dynamics with the advantages of light weight and damping. The physical size shown will provide about 169 N-m (1500 lb-in.) torque on each set of wheels. Design testing of scissors action vs. clamping action is recommended.

4. Metal Components. The arms and yokes are shown in sections suitable for aluminum alloys similar to 6061-T6 or 356.0-T6. Pins and studs may be of plated medium carbon steel or stainless steel.

5. Rubber Isolator. The wheel assembly is mounted on the yoke of the traveller arm assembly through a pair of rubber isolators to reduce the mechanical forces which occur when the wheel assembly travels past the conductor support. The design shown will have a spring constant of about 17.5 N/mm (100 lb/in.).

Traveller Arm Assembly Design

Many alternate arrangements for the traveller arm assembly were considered. An extensible arm was given primary consideration to connect the traveller wheel assembly on the contact conductor to the rail vehicle. A flexible, leash-like connection was not seriously reviewed because of electrical clearance and current carrying requirements and

because of the limited amount of mechanical restraint which could be placed on the wheel assembly.

A study was made to determine a reasonable length requirement for the arm. The minimum requirement is 914 mm (36 in.). The maximum is set by the extreme location expected for the contact conductor. Appendix C tabulates the variables which determine the conductor location for both tangent track and three degree curve track. With an added allowance, the maximum separation of the contact conductor from the top of the insulator support assembly is 4270 mm (14 ft). The design study is based on this range of arm length.

Two possible assemblies are shown in Figure 3-12 - the single arm and double parallelogram arm. Both of these designs will follow the contact conductor when being pulled by the rail vehicle. When reversing direction the arms must be reset. As conductor/vehicle spacing changes, the arm angle to the vehicle axis changes and the wheel assembly accelerates on the contact conductor relative to the vehicle. The single arm assembly must have a joint yoke at the wheel assembly, that is free to move plus or minus 90 degrees. Because of the parallelogram action with the double arm, this joint for the double arm assembly requires only limited movement, perhaps plus or minus 15 degrees.

A third assembly is shown in Figure 3-13, a diamond pantograph. For this design, no special action is required to reverse direction. As conductor/vehicle spacing changes, the velocity of the wheel assembly remains the same as the vehicle and only limited movement is required of the yoke to wheel assembly joint.

Possible materials include fiberglass-reinforced plastic rod or tube, aluminum alloy tube and steel tube. Careful consideration was given to each. The fact that an additional electrical conductor must be added to the fiberglass reinforced material and that mechanical joints became somewhat more complex led to the rejection of this material. The light weight of the aluminum alloy tube and its good electrical conductivity resulted in its choice for preliminary design of the traveller arm.

Table 3-3 summarizes characteristics of the possible traveller arm configurations with aluminum tube. From these comparisons it was decided to proceed with use of the diamond pantograph Figure 3-13 for further system dynamic analysis.

For the pantograph design the arms are required to move uniformly as the pantograph extends. This is obtained by a pivot and equalizer assembly at the base of the pantograph. The equalizer controls uniform extension of both arms, and the pivot permits a full 180 degree periphery movement as the contact conductor changes from one side of the vehicle to the other. Bearing joints require special attention to meet the deflection characteristics in Table 3-3 and shunts are required to provide the electrical continuity around the joints.

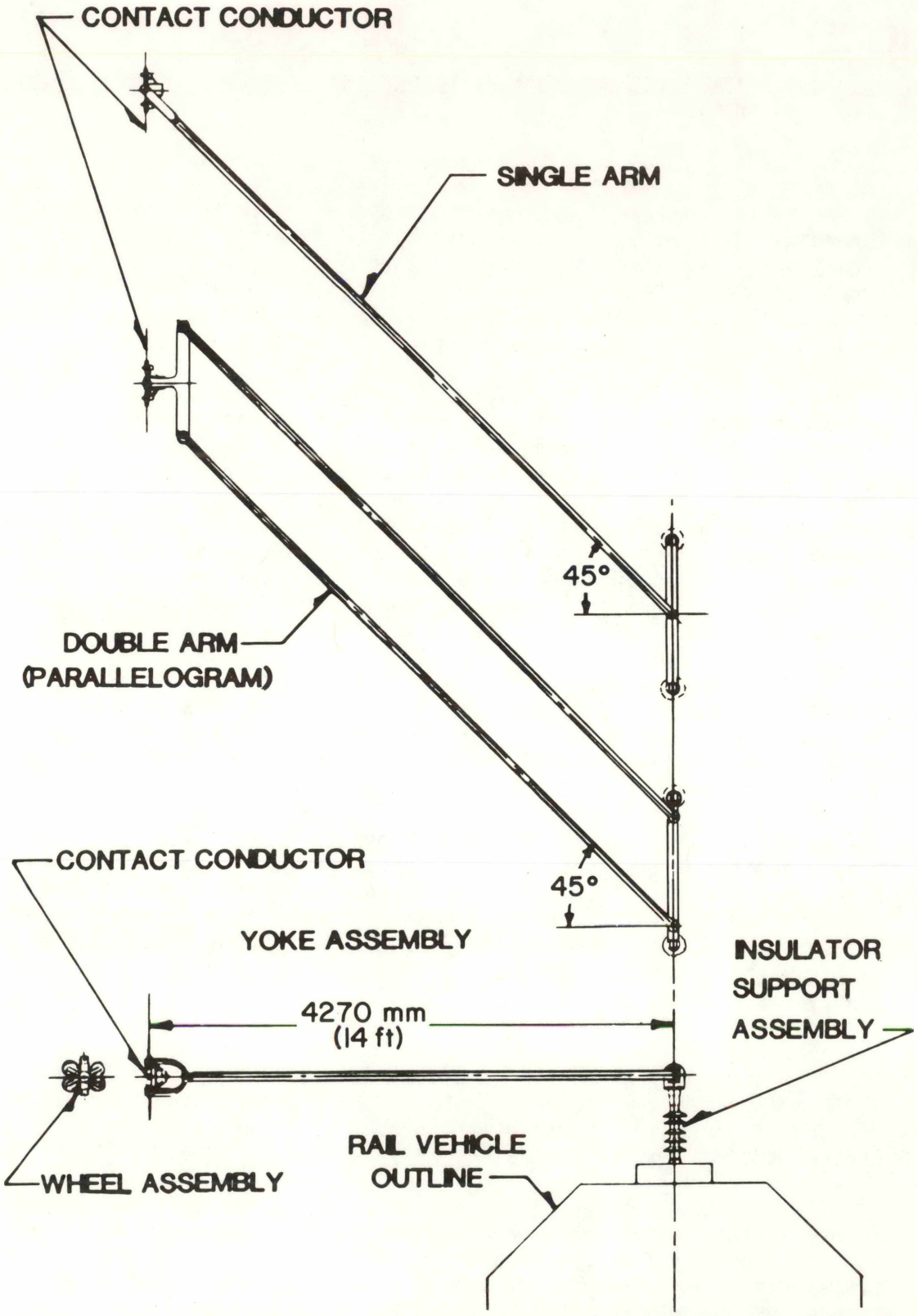

FIGURE 3-12. POSSIBLE ARM ARRANGEMENTS FOR THE TRAVELLER ASSEMBLY.

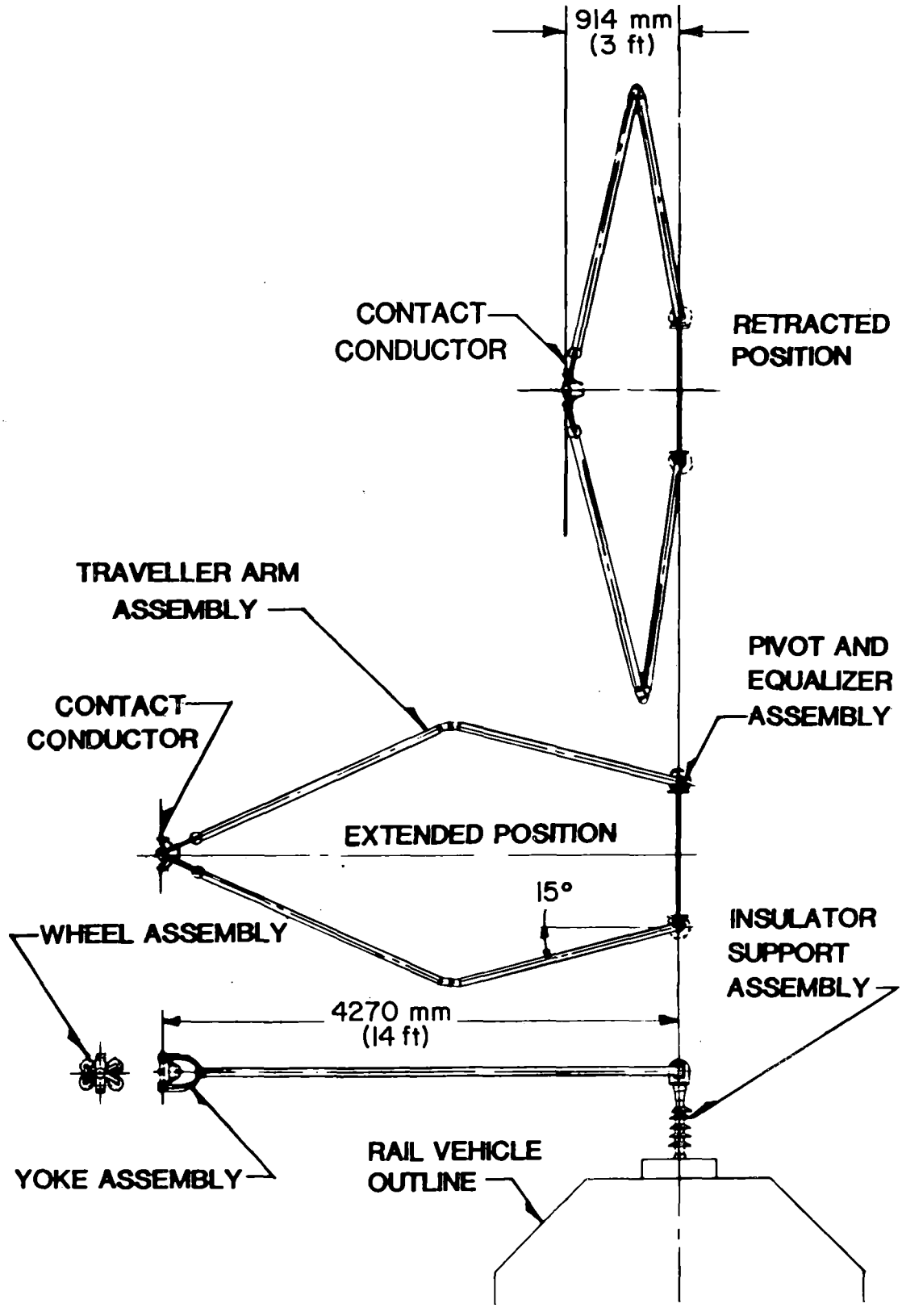

FIGURE 3-13. POSSIBLE ARM ARRANGEMENT FOR THE TRAVELLER ASSEMBLY (DIAMOND PANTOGRAPH).

TABLE 3-3. COMPARISON OF CHARACTERISTICS OF TRAVELLER ARM ASSEMBLIES

	Single Arm	Double Arm	Diamond Pantograph
Vehicle direction reversal	Must be reset	Must be reset	No attention needed
Traveller wheel assembly velocity compared to vehicle velocity when conductor/vehicle spacing changes.	changes	changes	same
Joint design - Arm yoke to the traveller wheel assembly	Must be free nearly ± 90 deg.	Needs limited movement ± 15 deg.	Needs limited movement ± 15 deg.
Mass of Aluminum Tubular Arms Alone			
31.75 mm (1-1/4 in.) OD x 1.65 mm (0.065 in.) thk			3.8 kg (8.3 lb)
5.08 mm (2 in.) OD x 1.65 mm (0.065 in.) thk	4.05 kg (8.95 lb)	8.1 kg 17.9 lb)	
Deflection			
Arm horizontal supported at each end	22.4 mm (0.88 in.)	22.4 mm (0.88 in.)	16.8 mm (0.66 in.)
Cantilever Stress			
44.5 N (10 lb) force at contact conductor	64710 kPa (9385 psi)	32358 kPa (4693 psi)	84305 kPa (12227 psi)

Summary - Preliminary Design

The traveller assembly system has been studied and requirements have been enumerated. Assemblies have been reviewed in detail and suitable materials have been identified. Possible designs have been described and areas requiring further development have been identified. Characteristics of these designs have been estimated and these data have been used in making dynamic analysis of the system. Further refinement of the proposed designs was made possible by the results of the dynamic analysis.

4. DYNAMIC ANALYSIS

Analysis Models

Single Degree of Freedom Simulation

The traveller system consisted of a wheel assembly with two sets of flanged wheels riding on the conductor, Figure 4-1. The wheel assembly was attached to a yoke assembly through two yoke bushings. It was recognized that the greatest potential dynamic problem would occur at the pole insulator where the traveller motion changed from its maximum upward velocity to its maximum downward velocity, Figure 4-2. The shorter the time interval over which this velocity change was required, the greater would be the force between the traveller system and the conductor. Therefore, a worst case scenario was assumed, i.e., the traveller system experienced a step input in velocity equal to the conductor's vertical velocity change at the insulator.

For this analysis it was assumed that the conductor was pin-attached at the insulator. The change in vertical velocity at the insulator can be derived from the equation of a catenary (see Appendix D, Section 1). It was next assumed that a single degree of freedom (1-DOF), base-mounted, mass/spring/damper system, Figure 4-3, was

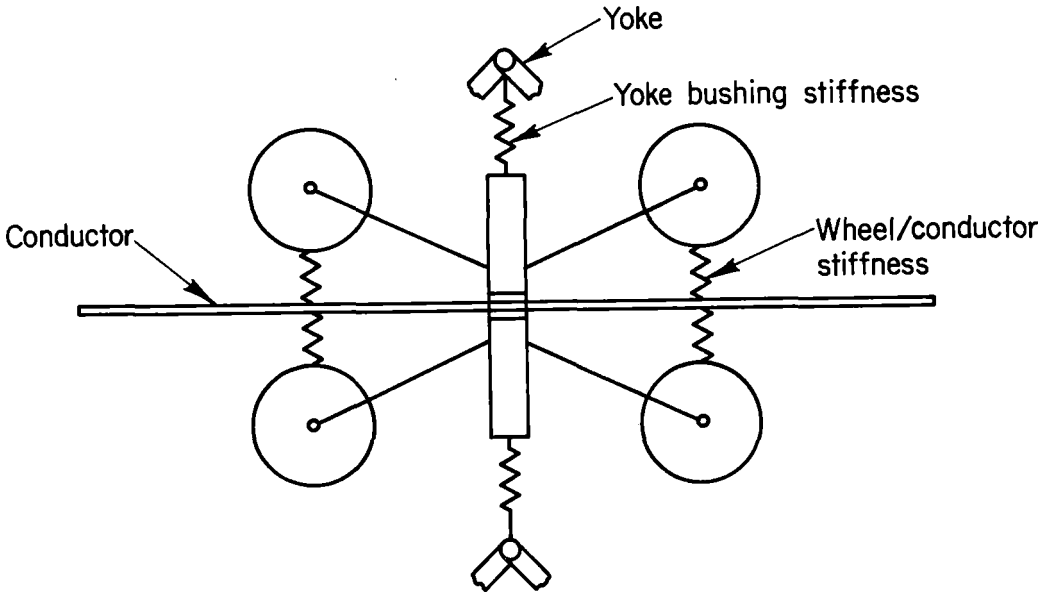

FIGURE 4-1. TRAVELLER/CONDUCTOR CONFIGURATION

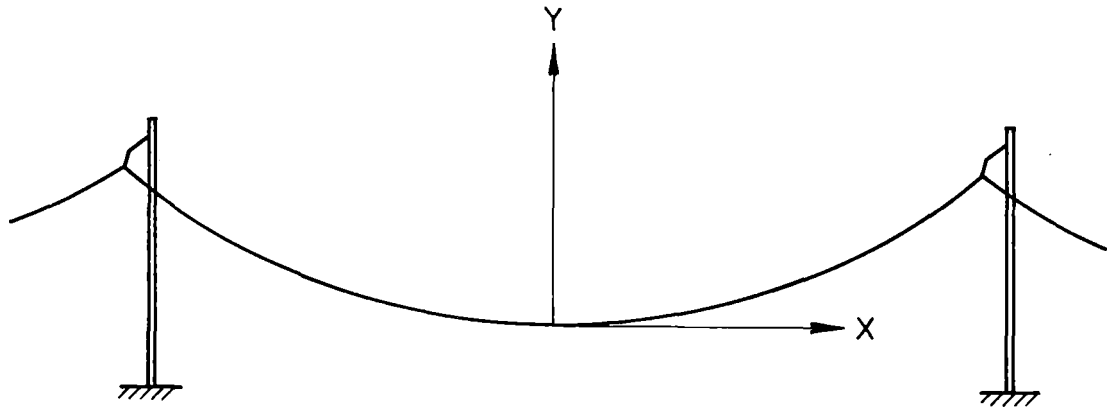

FIGURE 4-2. GEOMETRY OF SIMPLE CATENARY

excited by an initial change in base velocity (the conductor to which the traveller was attached). The displacement solution to the initial condition problem is derived in Appendix D, Section 2. The maximum force between the traveller and conductor will occur at the first peak displacement, and was assumed equal to the product of the displacement and stiffness of the traveller. This force is given by

$$F_o = \frac{\rho \pi d^2 SV}{4T} \left[\frac{KW}{g}\right]^{\frac{1}{2}} \qquad (4\text{-}1)$$

where

ρ = weight density of conductor material, 87,400 N/m^3 (0.322 lb/in.^{3}) for copper
d = diameter of conductor, m (in.)
S = pole span, m (in.)
V = forward velocity of traveller (rail vehicle), m/s (in./s)
T = tension in conductor, N (lb)
K = effective stiffness between conductor and traveller, N/m (lb/in.)
W = effective weight of traveller, N (lb)
g = acceleration of gravity, 9.80 m/s^2 (386 in./s^2)

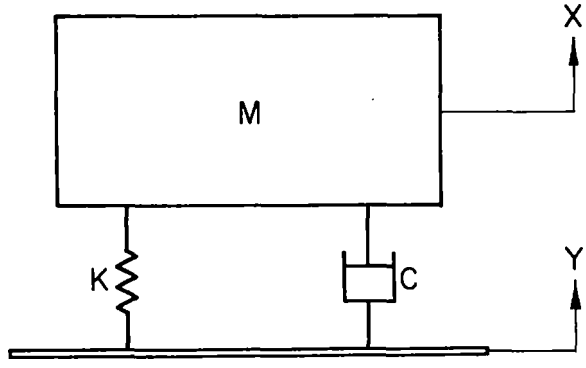

FIGURE 4-3. BASE-EXCITED 1-DOF MASS/SPRING/DASHPOT MODEL

It can be seen from Equation (4-1) that for a worst case situation (step change in velocity) the maximum force between the conductor and traveller system can depend on seven independent variables. Actually, the conductor tension and diameter would probably be dependent, i.e., maintain the greatest possible tension in the conductor without overstressing it. If a larger diameter conductor were used, the conductor tension would increase in proportion to the area to maintain a constant prestress. Density is another variable that is not entirely independent of conductor diameter and tension. If aluminum conductor were used because it has a lower density than copper, the tension may have to be decreased so as to not overstress the conductor, or the diameter increased, to provide sufficient electrical conductivity. Pole span depends on the maximum sag allowed between poles, and that value depends on the conductor density, diameter, and tension (Equation D-2 of Appendix D). Therefore, although the force derived in Equation (4-1) considered the variables ρ, d, T, and S to be independent, "real world" constraints would dictate changes in one or more of these variables if any other one was changed.

The real significance of Equation (4-1) is that the term $\rho\pi d^2S/4T$ defines the total change in slope of a simple catenary at its support, see Appendix, Equation D-3. Therefore, to reduce forces the slope of the conductor should be minimized.

The other three variables in Equation (4-1), V, K, W, are independent and not a function of the conductor. They indicate that for a specified maximum speed of the rail vehicle: (1) the weight of the traveller system should be as light as possible, and (2) the stiffness in the traveller system should be as low as possible.

In the design of the traveller system two stiffnesses were defined. The first one was between the yoke assembly and the wheel assembly; the second was between the wheel and conductor, Figure 4-1. The yoke bushing stiffness was initially designed based on Equation (4-1). But to keep the forces low between the wheel and conductor would require a low wheel radial stiffness, which would mean unacceptable wear, and wheel flanges that could not sustain a lateral load in curves. Therefore, Equation (4-1) could not be used to design wheel stiffness.

Although Equation (4-1) was useful for indicating general trends of several parameters of the traveller/conductor system, it could not account for the effects of multi-degree of freedom response, wheel spacing, nonlinearities in the insulator/conductor stiffness and a more gradual change in vertical velocity at the insulator.

Six Degree of Freedom Simulation

The six degree of freedom simulation (6-DOF) provided a detailed model of the traveller's vertical dynamics, and a reasonable approximation of the insulator/conductor's vertical dynamics. The

degrees of freedom were the vertical and pitch motion of both the yoke and wheel assemblies, and the vertical motions of the effective insulator/conductor mass under each wheel (Figure 4-4). Simple calculations were used to approximate the mass and inertia of the yoke and wheel assemblies, and the mass of the insulator, but the effective mass of the conductor depended on how it was excited. The effective mass of the insulator/conductor was assumed to be one half the mass of the insulator plus top hardware, plus 508 mm (20 in.) of the conductor. This value was varied in the parametric study, to determine its sensitivity.

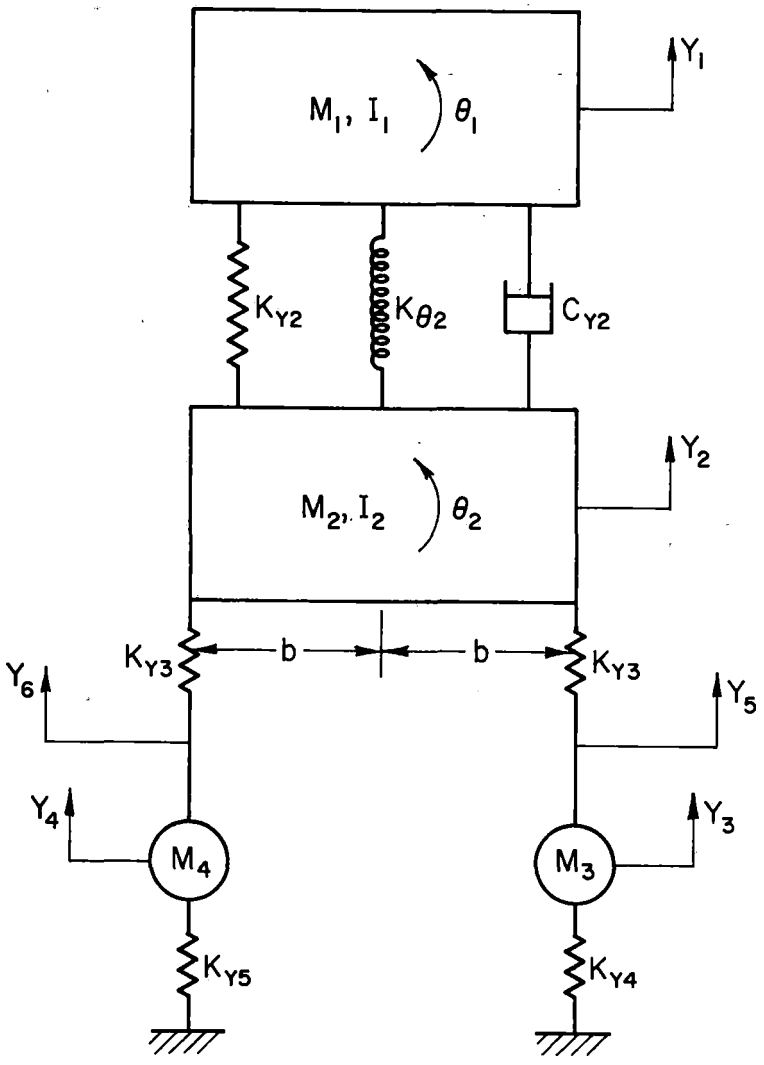

FIGURE 4-4. 6-DOF MODEL FOR TRAVELLER/CONDUCTOR

The effective stiffness of the insulator/conductor was a second parameter that was difficult to establish. As explained in the Appendix D, Section 3, the stiffness of the conductor was determined by assuming it was a tensioned beam, pin-attached at the insulators. The conductor stiffness was then added in series to the actual stiffness of the insulator to provide an effective stiffness of the insulator/conductor. This stiffness varied with the distance of each wheel from the insulator.

The solution of the six differential equations of motion (given in Appendix D, Section 3) was accomplished by a computer program using 4th order Runge Kutta numerical integration techniques. Each solution was a time history of the motions and forces generated in the traveller/conductor system. The maximum forces were automatically determined by the computer program along with the time at which they occurred. The excitation was the changing displacement of the conductor, which was modeled as a catenary with a circular transition at the insulator (see Appendix D, Section 3 for details). The length of the transition was the most critical parameter in the system, and must be maintained to insure reasonably low forces between the wheels and conductor.

Finite Element Simulation

The 1- and 6-DOF models discussed previously, required several simplifying assumptions which did not represent the actual physical hardward, especially the 1-DOF model. It was not known previously that the results from the simple models would be adequate in their approximation of the dynamics of the system. In addition, even the 6-DOF model did not model the total conductor length between poles or the traveller arms, so that effect was unknown. To verify the results of the simplifying assumptions in the 6-DOF model, and to determine bending stresses in the conductor, a finite element approach was used.

In general, finite element techniques are specifically useful for systems that contain a large number of degrees of freedom. The unique aspect of finite element methods is that it is not necessary for the user to develop any equations; only the geometry, the element properties, and the loading conditions must be defined.

The finite element code, which can be simply defined as a transformation between the loading conditions on the system and the resulting dynamic motion, establishes the equations of motion. The actual continuous structure, in this case the conductor and traveller arm, is replaced by an equivalent mathematical model made up of discrete elements having known stiffness, damping, and mass properties which are expressible in matrix form. The elements are considered as building blocks which, when fitted together in accordance with a set of rules derived from the theories of solid mechanics, provide the properties of the actual system under the assumptions utilized in the generation of the discrete elements.

The first step in a finite element analysis is to discretize the continuous system into a finite number of elements. The geometry of the conductor, including the transition, was modeled by pretensioned trusses (no bending stiffness) and with weightless beams (with bending stiffness) in the vicinity of the transition. The pole, insulators, clamp, and arms of the traveller were also modeled with beam elements. Spring and damping elements were used to model the yoke bushing, while a special follower element was used to model the wheels that followed the conductor. The model was three-dimensional.

The advantage of the finite element code is its capability to model details of the system. On the other hand, the finite element model has the disadvantage of being very costly to execute, especially for a high frequency, transient problem. The particular model used in this analysis had 303 degrees of freedom.

Single Degree of Freedom Simulation for Curved Track

Although the primary objective of this study was a dynamic analysis of the traveller/conductor system on tangent track, a preliminary analysis was made to investigate the forces exerted on the traveller/conductor system for curved track. The objective of this analysis was to determine the magnitude of the lateral flange forces at the pole. Assuming that the traveller system can be modeled as a 1-DOF model experiencing an instantaneous change in lateral velocity at the pole, the lateral force (see Appendix D, Section 4) is given by

$$\overline{F}_o = \frac{V\theta S}{57.3d}\left[\frac{KW}{g}\right]^{1/2} \qquad (4\text{-}2)$$

where

V = forward velocity of traveller (or rail vehicle), m/s (in./s)
θ = degree of curvature [based on 30.48-m (100-ft) chord], deg
S = pole span, m (in.)
K = effective stiffness between conductor and traveller, N/m (lb/in.)
W = effective weight of system, N (lb)
g = acceleration of gravity, 9.80 m/s^2 (386 in./s^2)
d = chord length, 30.48 m (1200 in.)

Equation (4-2) assumed a worst case condition, i.e., an instantaneous change in lateral velocity at the pole (no transition). Similar to Equation (4-1) for the maximum vertical force, Equation (4-2) can be used to give the maximum lateral force as a function of five independent variables. It will give the maximum lateral force in the yoke bushing or at the wheel flange.

Analysis Results

Parameter Definition

The major results of the dynamic analysis were provided by a parametric study using the six degree of freedom, time domain model. After several iterations of the design, as suggested by the analysis, a nominal set of traveller/conductor parameters was established. It is expected that these values will closely approximate the initial fabrication of the system. However, changes will undoubtedly occur during testing and development. To provide information on changes in force levels, caused by changes in design, each parameter was varied. In several cases the lowest or highest value of a particular parameter may be somewhat beyond realistic values, but in these cases the results of the parametric study established a limit.

The nominal parameters and their variations are listed in Table 4-1. The nominal value given for conductor tension is not the actual tension that would be expected under normal temperature conditions, but it is the lowest tension expected under extremely high temperature conditions. As shown by Equation (4-1) the maximum forces developed in the system are inversely proportional to conductor tension. Since the designer has no control on atmospheric conditions, the worst-case tension was taken as nominal. The parametric study did, however, consider lower and higher values.

Parametric Study

Based on the variable limits given in Table 4-1, a series of time domain computer runs were made with the six degree of freedom (6-DOF) model. Each run computed the maximum forces in the yoke bushing, at each wheel/conductor interface, and in the insulator for each wheel passing through the transition and beyond. The results of those maximum values were plotted for each parametric variation. As mentioned previously, it is unlikely that some of the parameters could be changed without changes in other parameters, which would result in a cancelling effect. Nevertheless, each parameter was varied independently to indicate trends.

Where appropriate, the results in the following figures were compared to the results obtained from the 1-DOF model, Equation (4-1). Since Equation (4-1) assumed a zero wheel spacing and transition length and a rigid insulator, the comparison will show that Equation (4-1) gave conservative force magnitudes and predicted some of the trends quite well for the yoke bushing force. Because of the transition length in the conductor, however, Equation (4-1) cannot be used to predict wheel/conductor forces.

TABLE 4-1. VARIABLES FOR 6-DOF PARAMETRIC STUDY

Variable	Nominal	Minimum	Maximum
Yoke assembly weight, N*(lb)	40.0 (9.00)	22.2 (5.00)	133 (30.0)
Wheel assembly weight, N (lb)	53.4 (12.0)	22.2 (5.00)	133 (30.0)
Insulator/conductor weight, N (lb)	66.7 (15.0)	22.2 (5.00)	133 (30.0)
Yoke bushing stiffness, N/mm (lb/in.)	17.5 (100)	8.75 (50.0)	70.0 (400)
Wheel/conductor stiffness, N/mm (lb/in.)	875 (5000)	175 (1000)	5250 (30,000)
Insulator stiffness, N/mm (lb/in.)	52.5 (300)	17.5 (100)	280 (1600)
Conductor diameter, mm (in.)	15.9 (0.625)	12.7 (0.50)	25.4 (1.00)
Conductor tension, N (lb)	8900 (2000)**	4450 (1000)	44,500 (10,000)
Pole Span, m (ft)	61.0 (200)	15.2 (50)	122 (400)
Wheel spacing, mm (in.)	280 (11.0)	150 (6.00)	610 (24.0)
Transition length, mm (in.)	510 (20.0)	0.00 (0.00)	1520 (60.0)
Vehicle speed, kph (mph)	81 (50.0)	16 (10.0)	145 (90.0)
Conductor density, N/m^3 ($lb/in.^3$)	8.74×10^4 (0.322)	--not varied--	

* N = Newtons (1.0 lb = 4.448 N).
** Assumes 54 C (130 F) temperature.

Effect of Yoke Assembly Weight

The effect of varying the yoke assembly weight is illustrated in Figure 4-5. As the yoke assembly weight increased, the maximum force in the yoke bushing increased rapidly at a slightly decreasing rate. The maximum forces at the wheel/conductor interface and at the insulator increased somewhat, but the effect was not significant. The yoke bushing force, based on the 1-DOF model, indicated greater magnitudes, but a similar trend to the 6-DOF model.

Effect of Wheel Assembly Weight

When the wheel assembly weight was increased, Figure 4-6, the maximum wheel/conductor interface forces increased rapidly, but the yoke bushing force actually decreased. The maximum forces on the insulator also increased with wheel asembly weight but not as rapidly as the wheel/conductor forces. The 1-DOF model of Equation (4-1) predicted a wheel/conductor force of 4090 N (920 lb) for the nominal conditions, clearly much higher than forces predicted by the 6-DOF model. The reasons for the high force value given by Equation (4-1) were the high wheel/conductor stiffness, and the lack of a smooth transition in the conductor at the insulator. Equation (4-1) is not a good expression for determining wheel/conductor forces for the real system with a finite slope transition and flexibility at the pole suspension point.

Effect of Insulator/Conductor Weight

A variation in the effective weight of the insulator and conductor section did not have a significant effect on the maximum forces in the yoke bushing or at the wheel/conductor interface, Figure 4-7. However, increasing the insulator/conductor weight did decrease the force in the insulator (greater inertia to move). The 1-DOF model can not be used to predict the effect of insulator/conductor weight.

Effect of Yoke Bushing Stiffness

Figure 4-8 illustrates the maximum force changes with variations in the yoke bushing stiffness. Although there was a generally increasing trend in force with stiffness, the yoke bushing stiffness did not have a great effect unless the stiffness value was very low. Again, the 1-DOF model gave conservative results, but in this case it was overly conservative and could not be used as a good indication of trends. The poor comparison was due to the nonzero transition length in the 6-DOF model. The results in Figure 4-8 indicate that the yoke bushing stiffness can be increased without adversely affecting force levels.

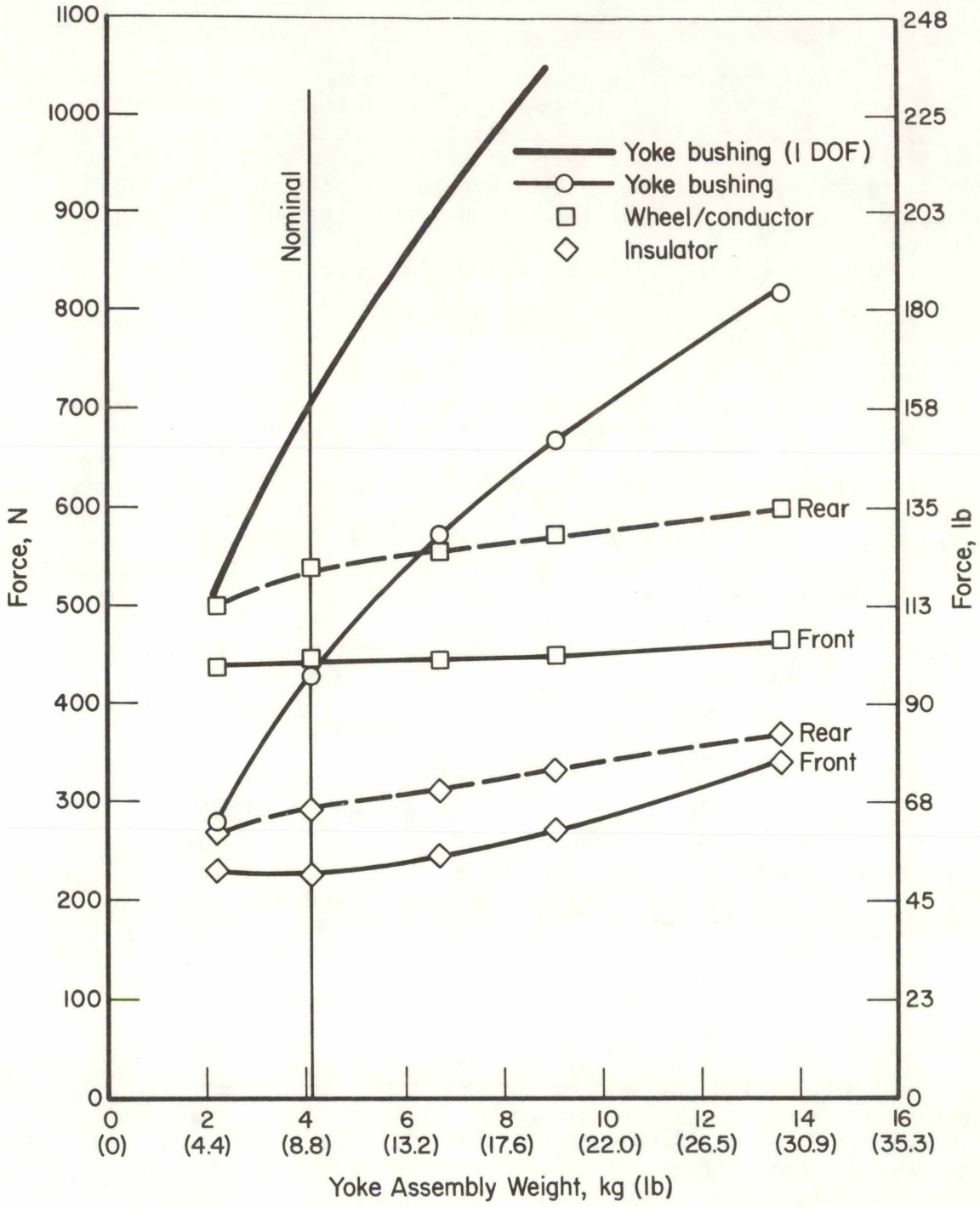

FIGURE 4-5. EFFECT OF YOKE ASSEMBLY WEIGHT ON YOKE BUSHING, WHEEL/ CONDUCTOR, AND INSULATOR FORCES, 1Kg = 9.8 N

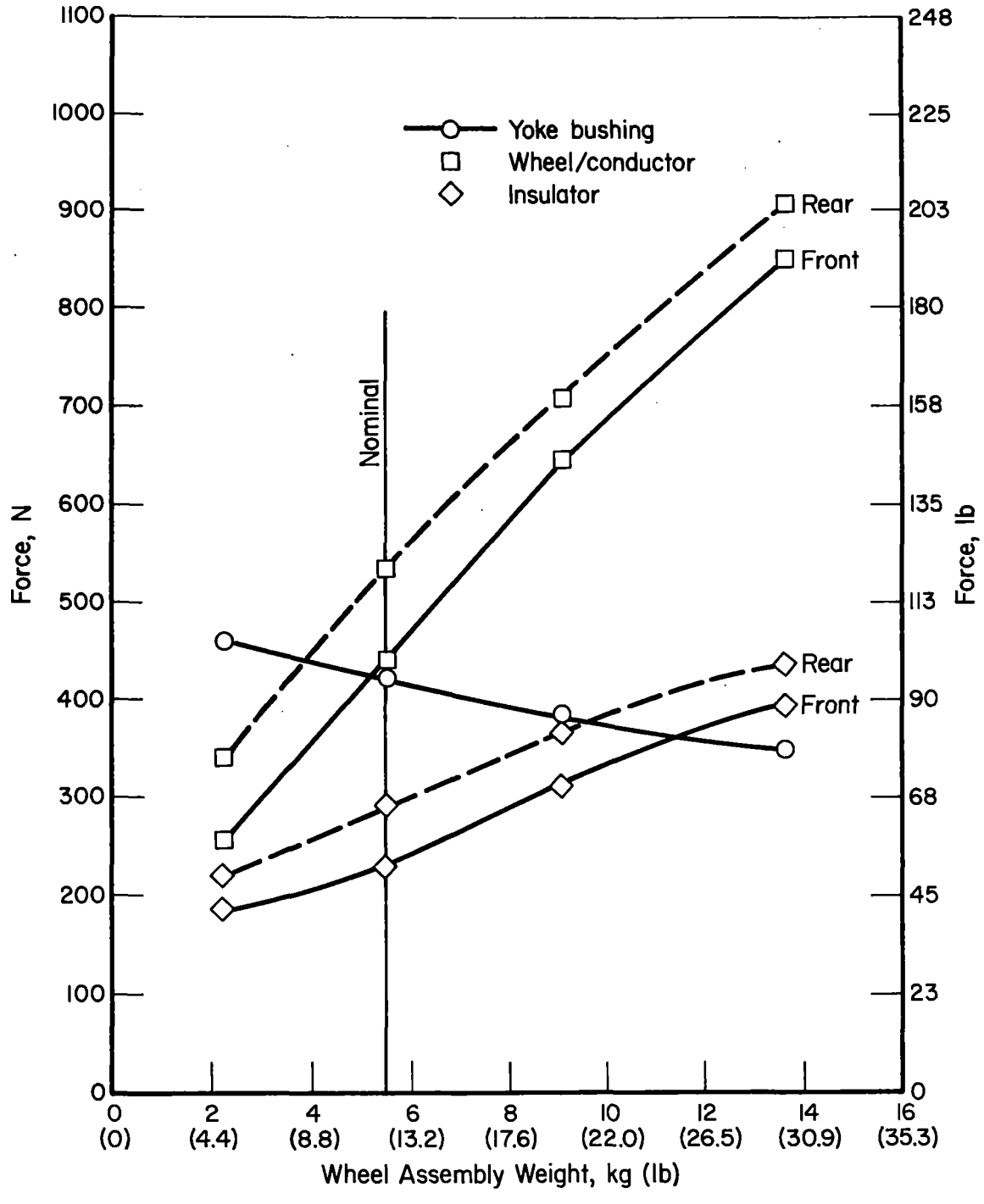

FIGURE 4-6. EFFECT OF WHEEL ASSEMBLY WEIGHT ON YOKE BUSHING, WHEEL/ CONDUCTOR, AND INSULATOR FORCES, 1Kg = 9.8 N

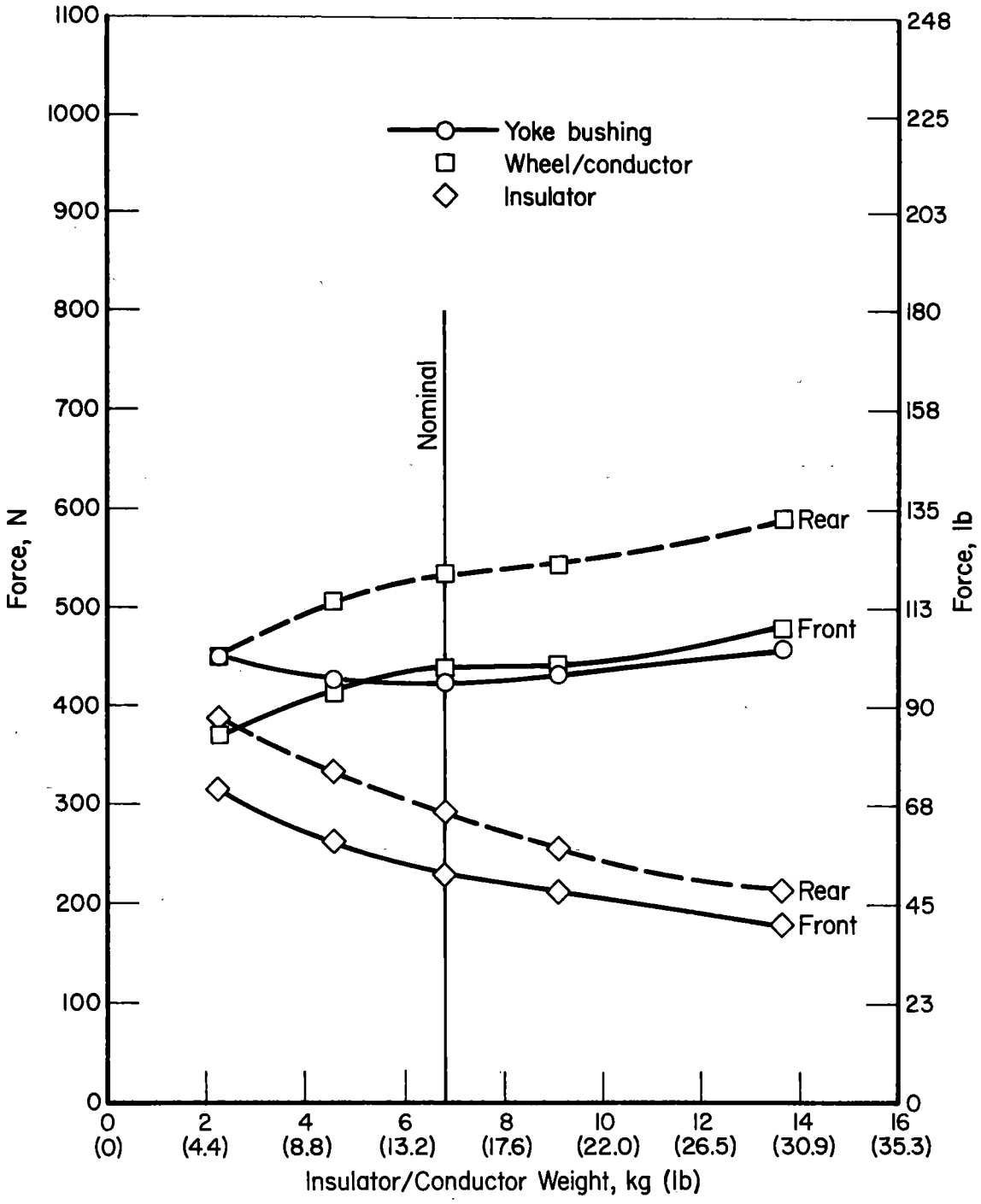

FIGURE 4-7. EFFECT OF INSULATOR/CONDUCTOR WEIGHT ON YOKE BUSHING, WHEEL/CONDUCTOR, AND INSULATOR FORCES, 1Kg = 9.8 N

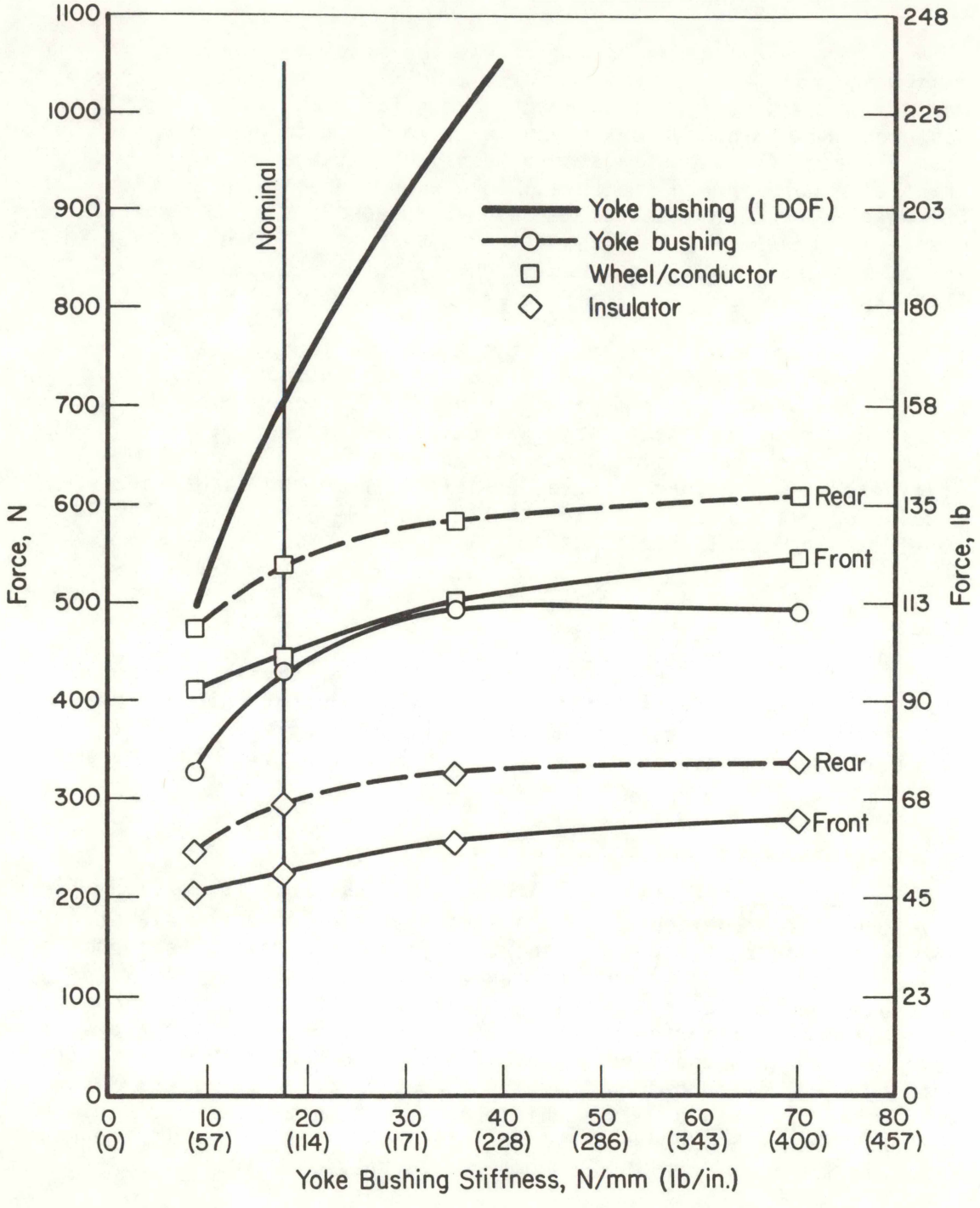

FIGURE 4-8. EFFECT OF YOKE BUSHING STIFFNESS ON YOKE BUSHING, WHEEL/CONDUCTOR, AND INSULATOR FORCES

Effect of Wheel/Conductor Stiffness

The wheel/conductor stiffness was a major problem during the design and analysis iterations. The 1-DOF model indicated that the maximum force at the wheel/conductor interface was 4090 N (920 lb), based on the nominal values given in Table 4-1. It was this high value that dictated the use of a smooth transition at the insulator. If the transition were indeed smooth and long enough, the force developed at the wheel/conductor interface should be independent of the wheel stiffness. The reason for this assertion is that if the transition time was large, the system would respond gradually rather than undergo a large transient.

Figure 4-9 does show that the maximum forces developed were nearly independent of the wheel/conductor stiffness. The value of 875 N/mm (5000 lb/in.) was chosen as the nominal value because the maximum wheel/conductor interface force was developed at that stiffness. The important conclusion to be drawn from Figure 4-9 is that the wheel stiffness can be a very high value without producing large forces. This conclusion was not consistent with Equation (4-1) because the 1-DOF model did not model the transition.

Effect of Insulator Stiffness

Figure 4-10 shows that the stiffness of the insulator has a small effect on the yoke bushing and wheel/conductor forces and a moderate effect on the force generated in the insulator. The 1-DOF model assumed a rigid insulator, so it did not apply to this parameter.

Effect of Conductor Diameter

Based on Equation (4-1) it can be seen that the maximum forces developed are proportional to the square of the conductor diameter because the conductor weight, and therefore, the transition approach angle (Equation D-3) are proportional to the diameter squared. As mentioned above, it is probably not reasonable to change the conductor size without a proportional change in tension. However, Figure 4-11 was developed to show the independent effect of conductor diameter. If nothing else, it does show that the conductor diameter (transition approach angle) has a very significant effect on maximum forces in the yoke bushing, wheel/conductor interface, and insulator--note the change in scale for the force levels compared to previous figures.

The 1-DOF model overestimated the yoke bushing force levels by 50 to 70 percent, which provided a good conservative value that followed approximately the same trend as the 6-DOF model.

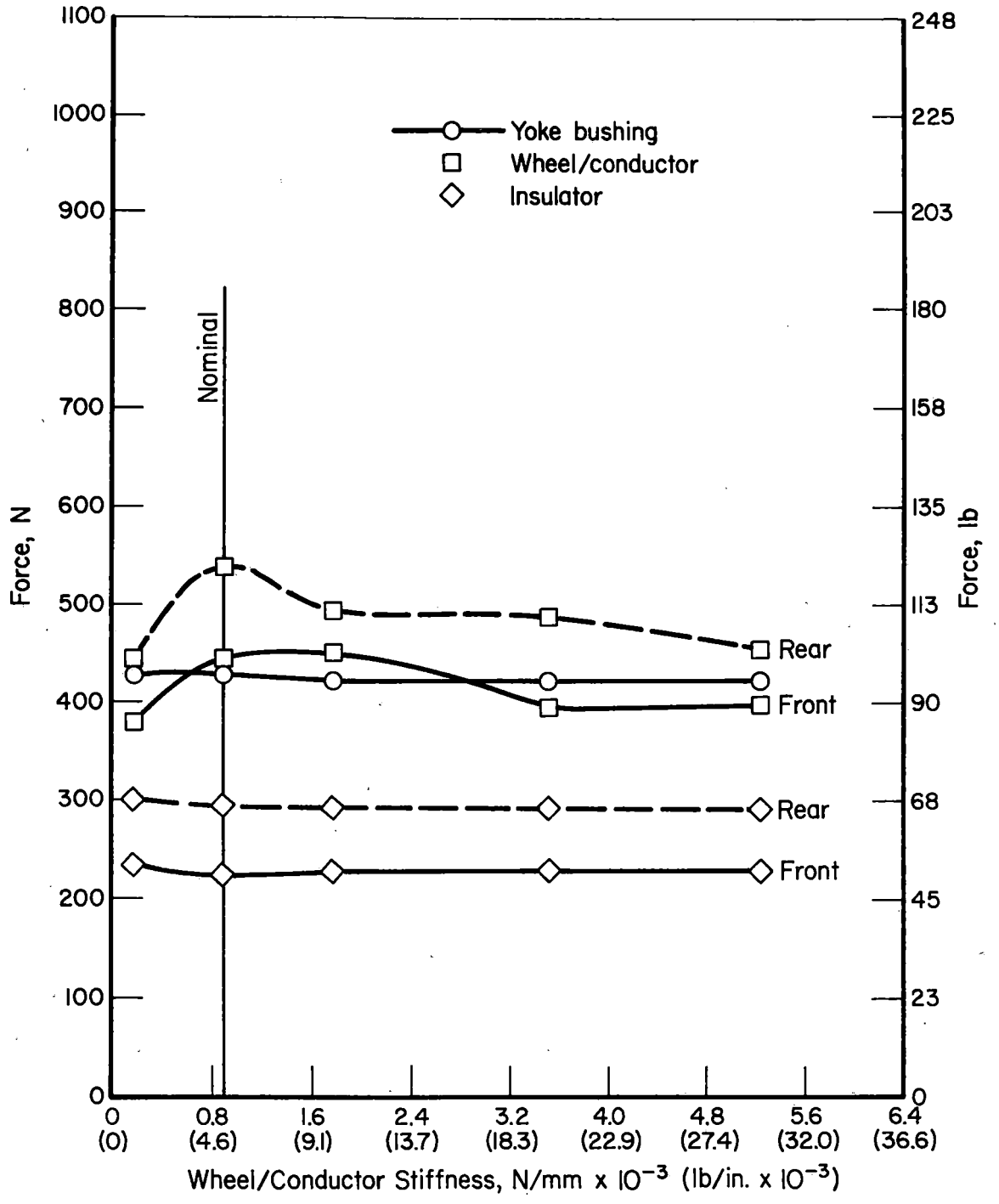

FIGURE 4-9. EFFECT OF WHEEL/CONDUCTOR STIFFNESS ON YOKE BUSHING, WHEEL/CONDUCTOR, AND INSULATOR FORCES

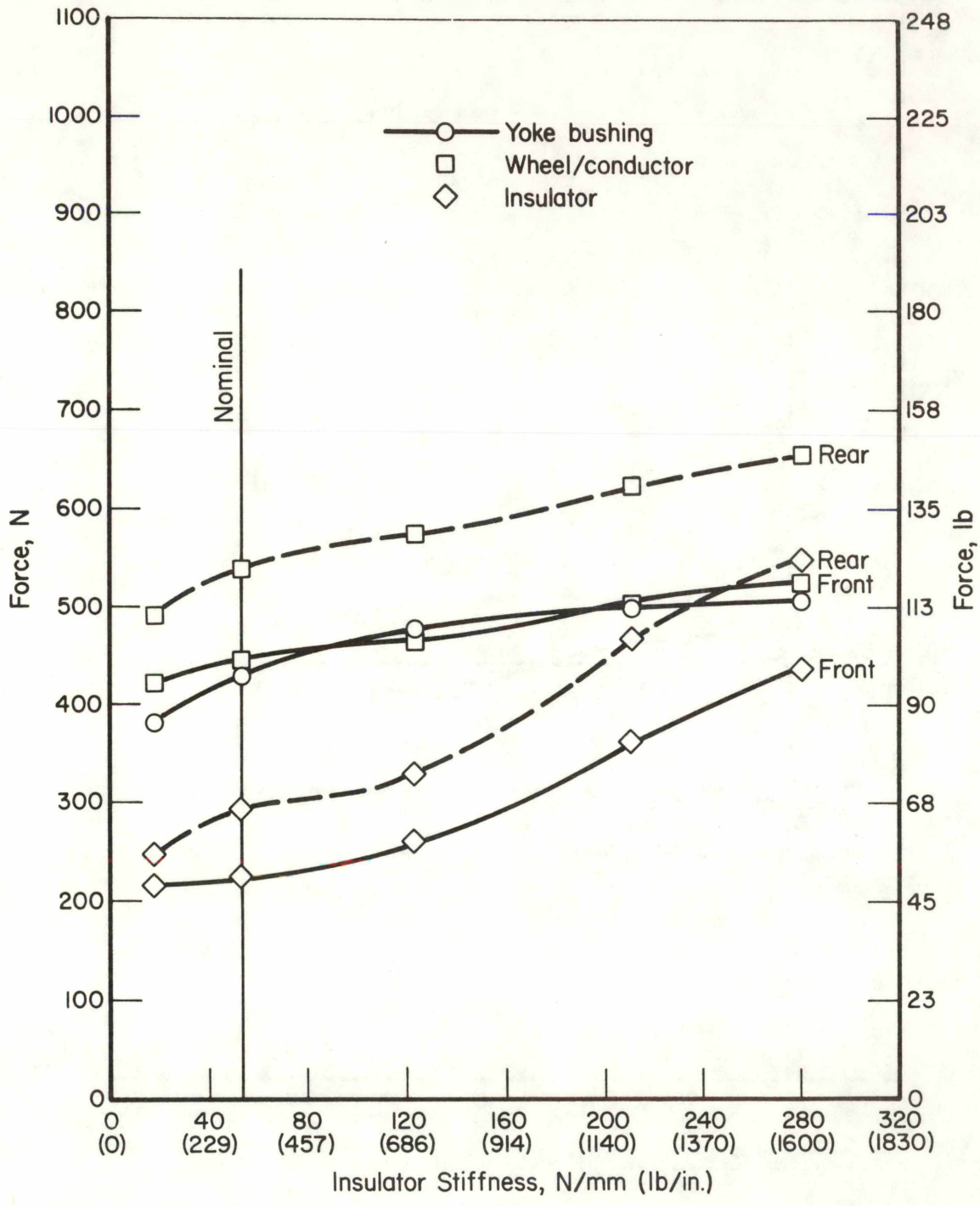

FIGURE 4-10. EFFECT OF INSULATOR STIFFNESS ON YOKE BUSHING, WHEEL/CONDUCTOR, AND INSULATOR FORCES

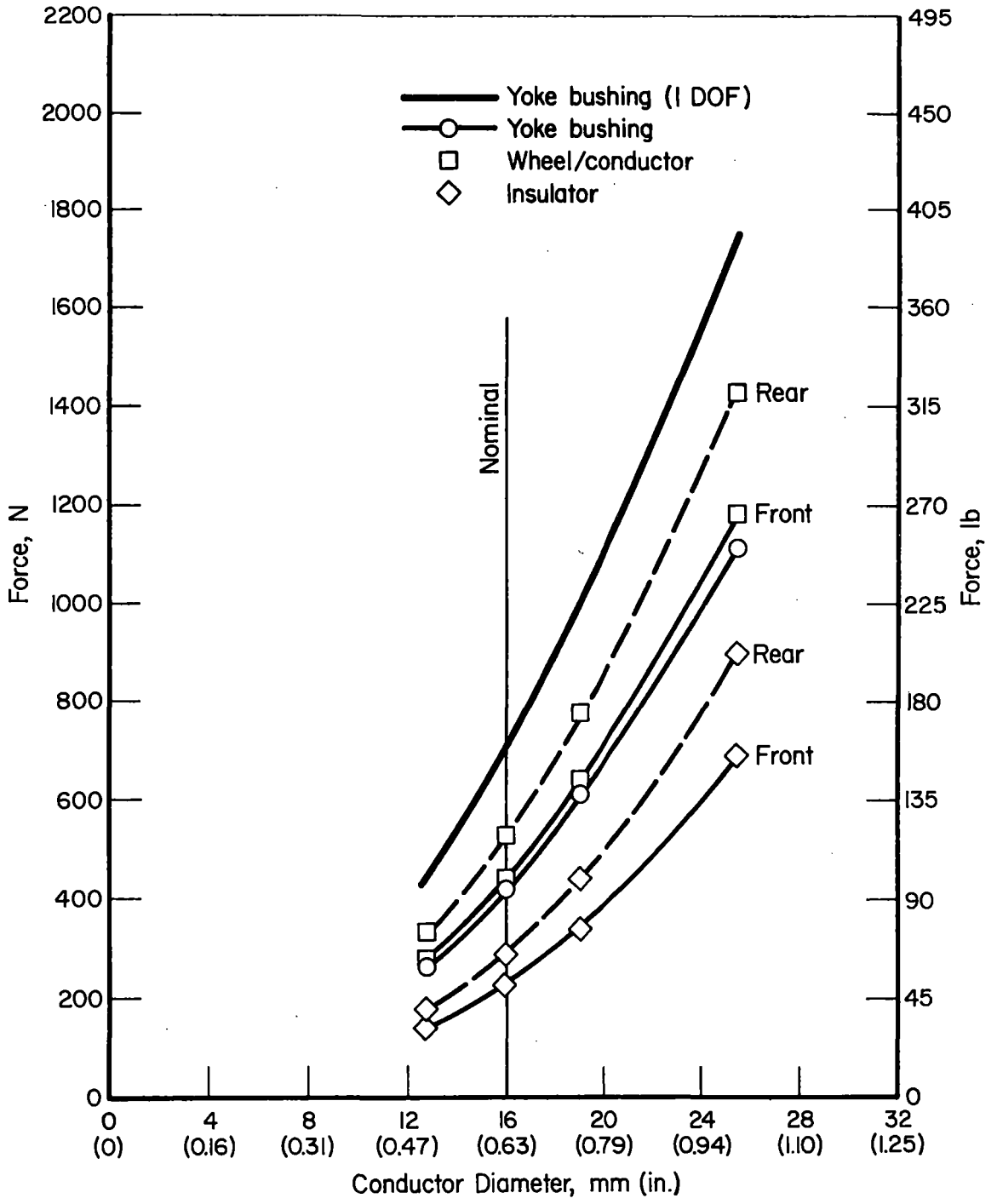

FIGURE 4-11. EFFECT OF CONDUCTOR DIAMETER ON YOKE BUSHING, WHEEL/CONDUCTOR, AND INSULATOR FORCES

Effect of Conductor Tension

The effect of changing the conductor tension independent of the conductor diameter is shown in Figure 4-12. As indicated in Equation (4-1) the force was inversely proportional to the tension. Increasing tension decreases the conductor slope, Equation D-3. Again the 1-DOF model provided a conservative approximation to the yoke bushing force.

Effect of Constant Prestress

It has been mentioned several times that larger diameter conductors would carry a greater tension to maintain a constant prestress. According to Equation (4-1), if the ratio of conductor tension to cross-sectional area was held constant, there would be no change in force level. Because the 1-DOF model did not consider several of the parameters included in the 6-DOF model, the 6-DOF model was run to determine the effect of increasing conductor diameter while maintaining constant prestress. The results are shown in Table 4-2. As predicted by the 1-DOF model, the yoke bushing forces remained nearly constant, as did the wheel/conductor forces. The small increase in these forces with increased diameter can be attributed to the increased stiffness of the conductor (bending stiffness is proportional to the fourth power of diameter). The effect was similar to the increase in insulator stiffness shown in Figure 4-10.

On the other hand, the insulator force increased significantly when the conductor diameter increased at constant prestress. Again, the effect was similar to an increase in insulator stiffness, see Figure 4-10; i.e., a stiffer system will exert a greater force because it cannot move out of the way.

One factor that was not included in the constant prestress study was the variation in effective insulator/conductor weight due to the change in conductor diameter. As shown in Figure 4-7, increasing the effective weight of the insulator/conductor at constant line tension and diameter, will cause a small increase in wheel/conductor force, little change in yoke bushing force, and a significant decrease in insulator force. The increase in insulator force due to increased conductor diameter would be partially offset by the decrease due to increased conductor weight.

Effect of Pole Span

Equation (4-1) indicates that the yoke bushing force is linearly proportional to pole span (slope at conductor). As seen in Figure 4-13, the 6-DOF model predicted yoke bushing force to be a linear function of pole span. The wheel/conductor and insulator forces were also linear functions of pole span.

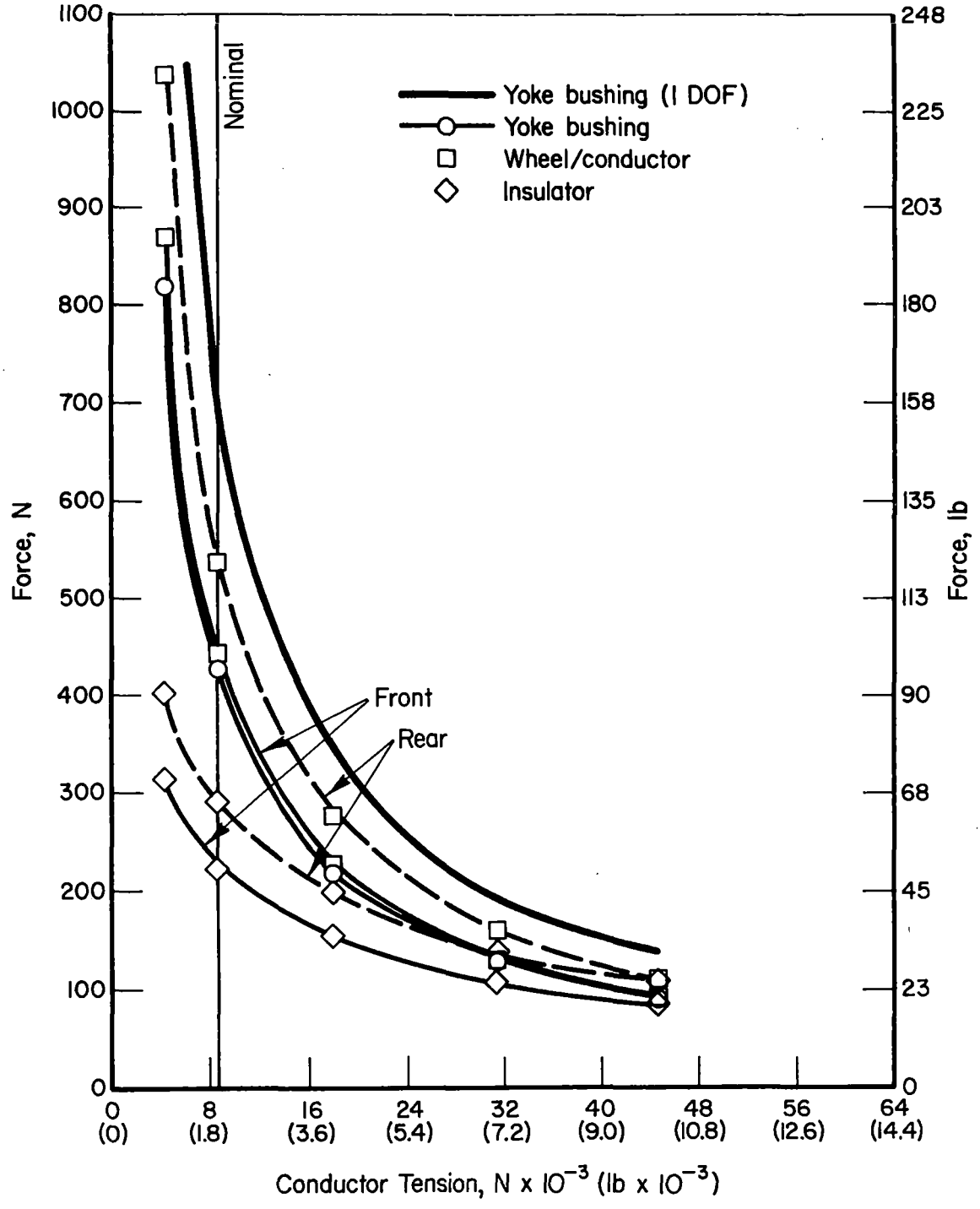

FIGURE 4-12. EFFECT OF CONDUCTOR TENSION ON YOKE BUSHING, WHEEL/ CONDUCTOR, AND INSULATOR FORCES

TABLE 4-2. FORCE COMPARISON WITH CONSTANT CONDUCTOR PRESTRESS

Tension N (lb)	Diameter mm (in.)	T/d^2 N/mm^2 ($lb/in.^2$)	Yoke Bushing Force N (lb)	Wheel/Conductor Force N (lb)	Insulator Force N (lb)
5693 (1280)	12.7 (0.50)	35.3 (5120)	411 (92)	431,516 (97, 116)	180, 218 (41, 49)
8896 (2000)	15.9 (0.625)	35.3 (5120)	425 (95)	443, 534 (100, 120)	231, 294 (52, 66)
12810 (2880)	19.1 (0.75)	35.3 (5120)	436 (98)	454, 552 (102, 124)	281, 364 (63, 83)
22774 (5120)	25.4 (1.0)	35.3 (5120)	455 (102)	467, 574 (105, 129)	367, 476 (83, 107)

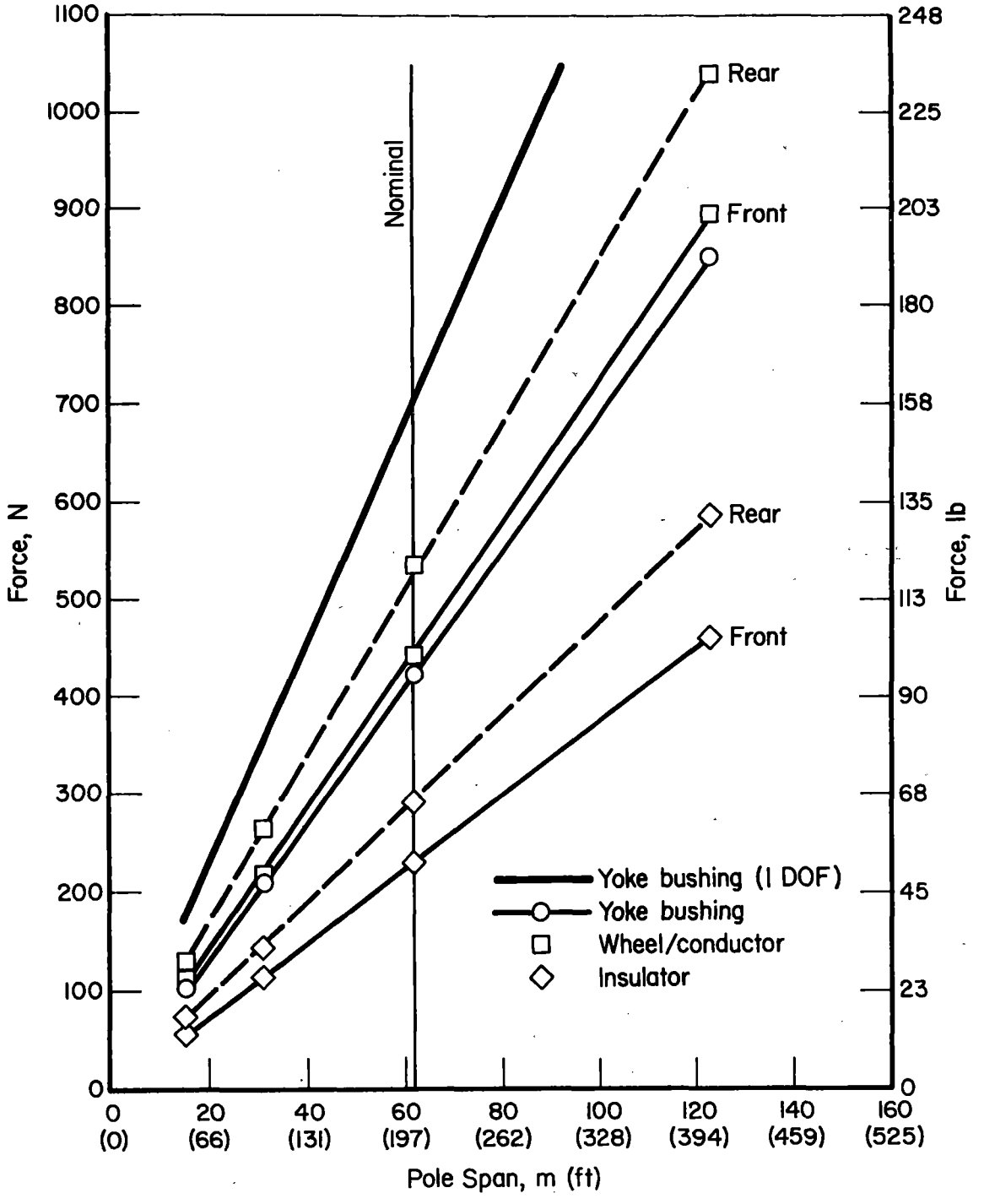

FIGURE 4-13. EFFECT OF POLE SPAN ON YOKE BUSHING, WHEEL/CONDUCTOR, AND INSULATOR FORCES

Effect of Wheel Spacing

Wheel spacing could not be analyzed by the 1-DOF model, but its effect was investigated by the 6-DOF model as illustrated in Figure 4-14. As might be expected, an increase in wheel spacing did decrease the yoke bushing force somewhat. But the wheel/conductor and insulator forces did not show any strong trend with wheel spacing, except that the wheel/conductor force increased substantially at small wheel spacing. The nominal wheel spacing used appeared to be close to optimal for reducing wheel/conductor forces.

Effect of Conductor Transition Length

Conductor transition length was defined as the total length of the conductor on both sides of the pole that did not follow a catenary shape. For simplicity the transition length was specified as a circular arc. The reason that a transition length was deemed necessary was to reduce the large transient forces generated at the wheel when the conductor made an instantaneous change in slope at the insulator connection. Although it was intuitive that the conductor should have a smooth transition at the insulator, it was not known how long the transition should be or how significant the effect would be.

Figure 4-15 illustrates the effect of transition length on the forces generated in the system. The effect on the wheel/conductor force was dramatic. A 1000-mm (39.4-in.) transition reduced the force level by an order of magnitude. However, most of the gain was produced by a 508-mm (20-in.) transition. For ease of fabrication, that value was chosen as nominal. It is of particular interest to note that the yoke bushing and insulator forces had only a slightly decreasing trend with increasing transition length.

Equation (4-1) can be used to compare the 1-DOF model results with that shown in Figure 4-15 at zero transition length. For the force in the yoke bushing the 1-DOF model predicted 707 N (154 lb), approximately 50 percent greater than the 6-DOF model at zero transition length. The 1-DOF model predicted 4090 N (920 lb) for the wheel/-conductor force, approximately 25 percent greater than the 6-DOF model. In this particular case the 1-DOF model results gave a moderately conservative force level for zero transition length, and the 6-DOF model demonstrated its own necessity and the necessity of a transition length.

Effect of Vehicle Speed

Vehicle speed was the one parameter of the system over which there was no control, except to set a limit. Based on Equation (4-1) the yoke bushing force should increase as a linear function of vehicle speed, and as shown in Figure 4-16, it did. However, the forces at the wheel/conductor interface increased more rapidly while the force at the insulator increased less rapidly.

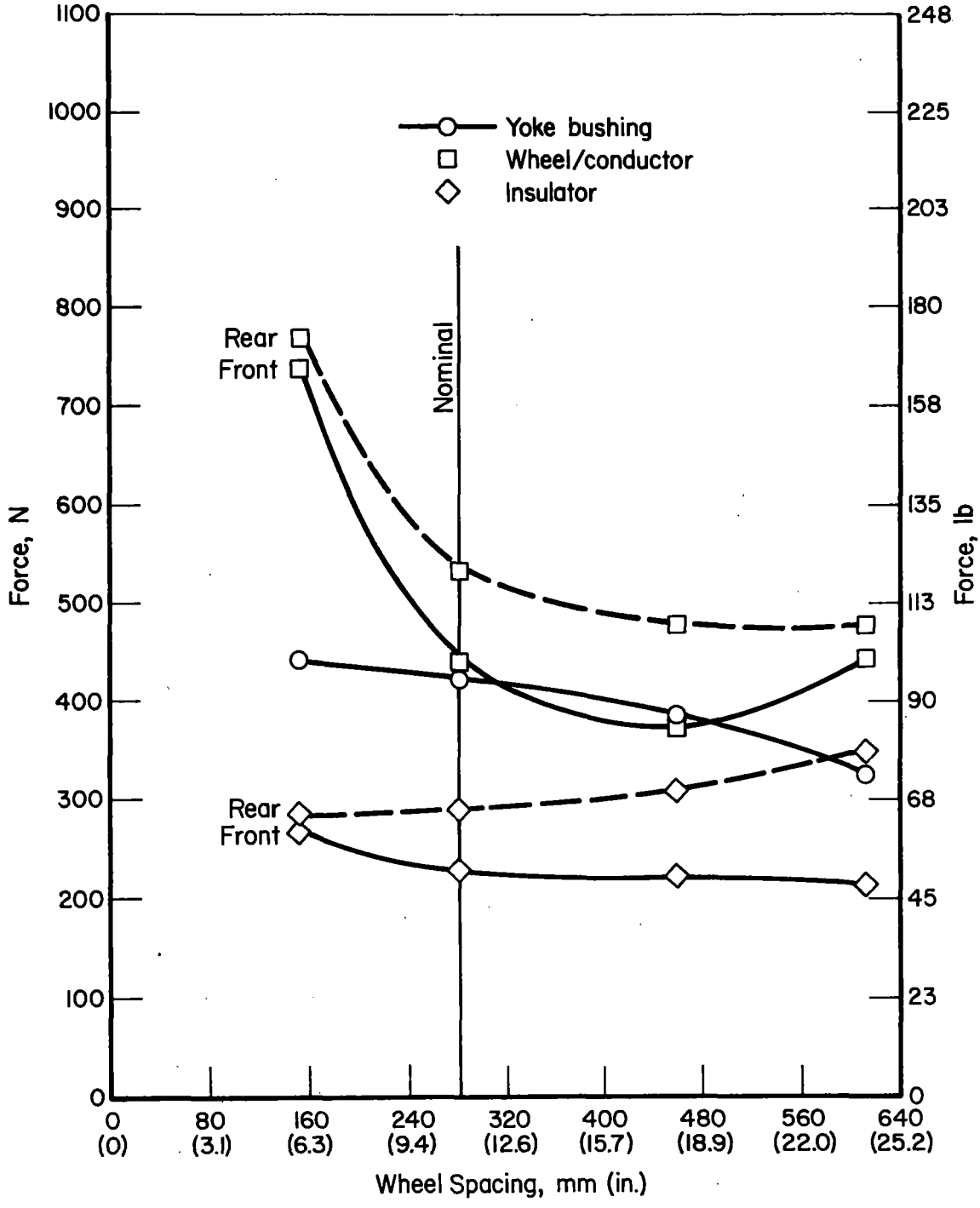

FIGURE 4-14. EFFECT OF WHEEL SPACING ON YOKE BUSHING, WHEEL/CONDUCTOR, AND INSULATOR FORCES

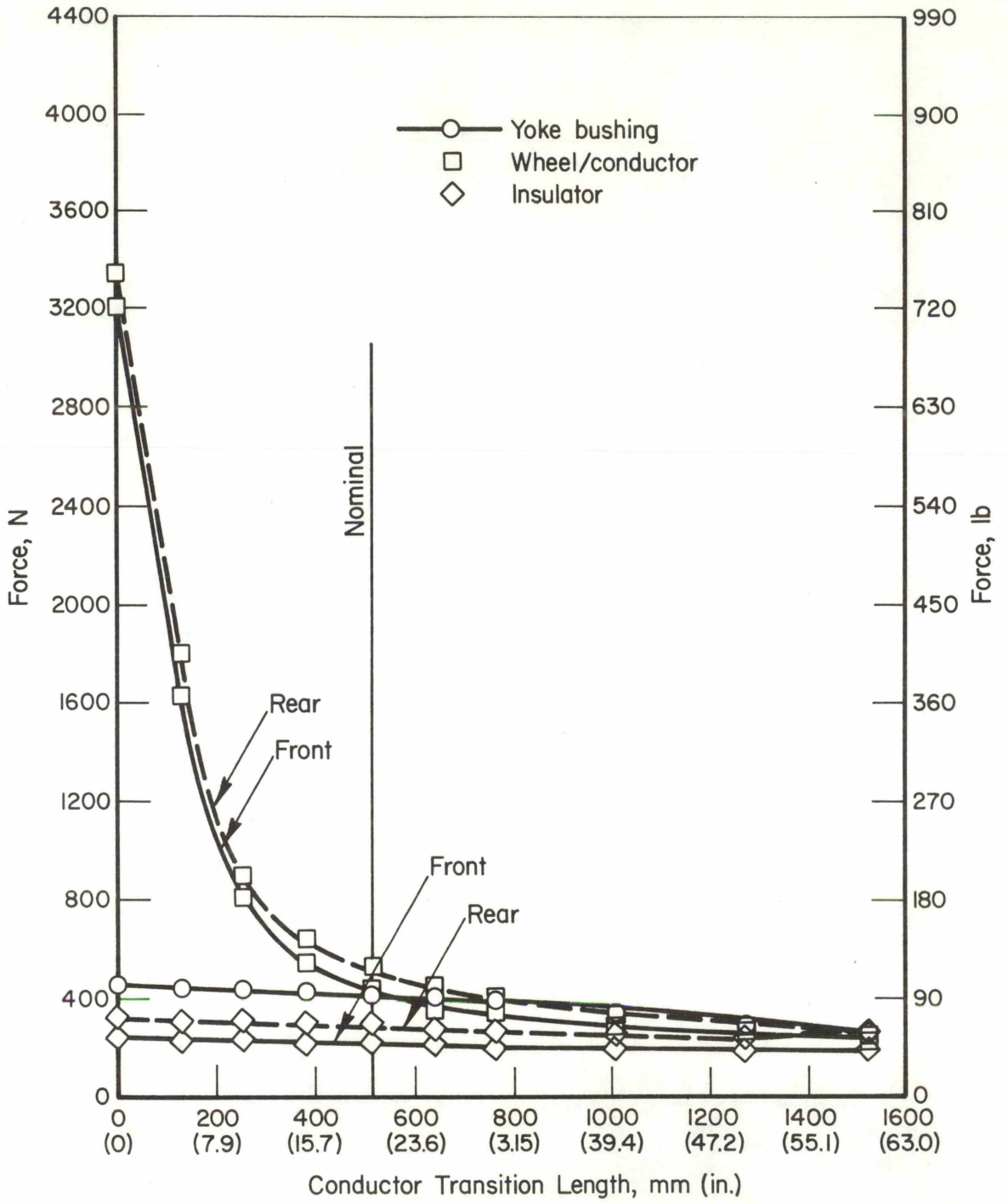

FIGURE 4-15. EFFECT OF CONDUCTOR TRANSITION LENGTH ON YOKE BUSHING, WHEEL/CONDUCTOR, AND INSULATOR FORCES

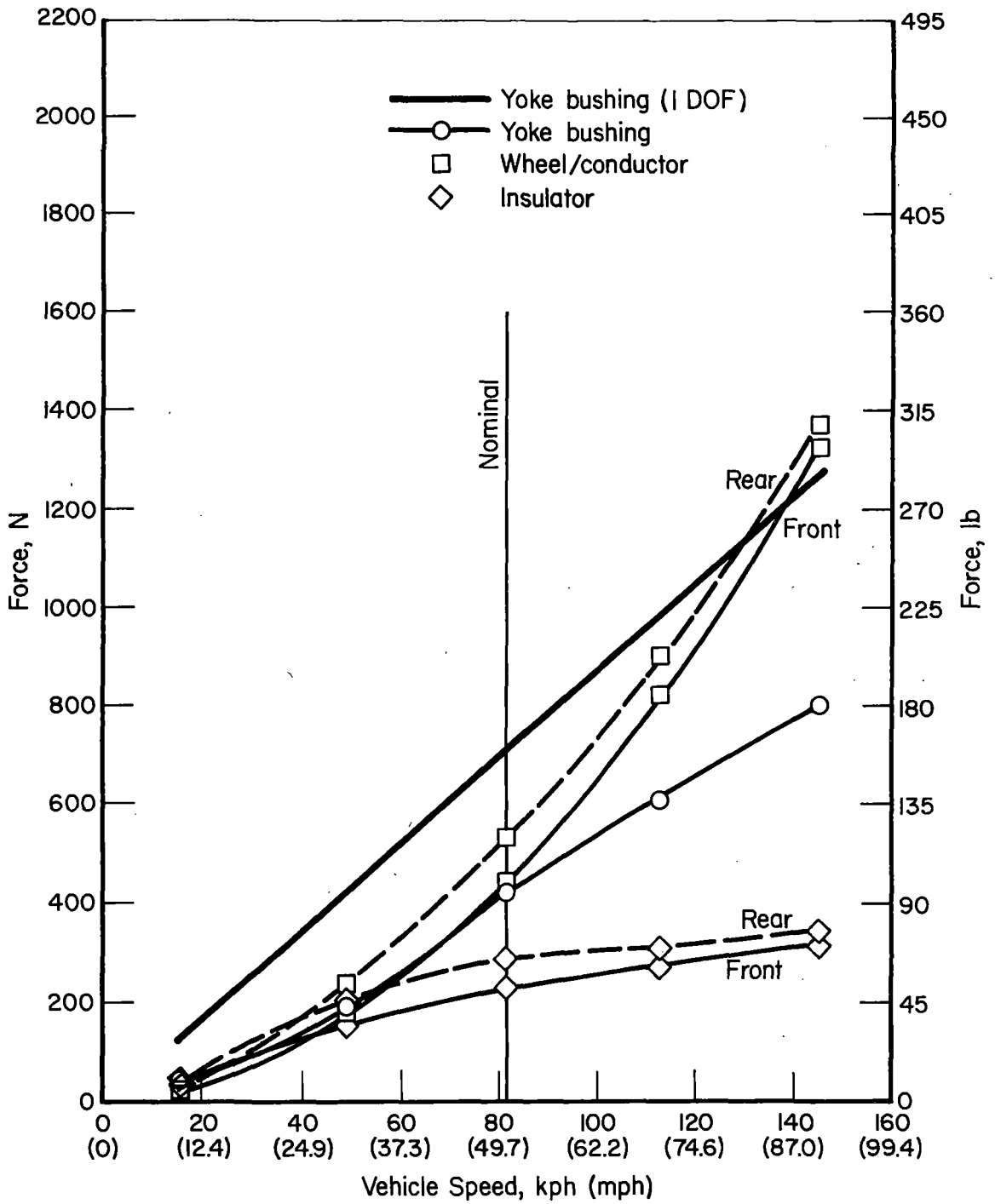

FIGURE 4-16. EFFECT OF VEHICLE SPEED ON YOKE BUSHING, WHEEL/CONDUCTOR, AND INSULATOR FORCES

Curved Track

A worst-case, preliminary analysis of the lateral forces in curves is given by Equation (4-2). Using the nominal values given in Table 4-1 and a curvature of 1.0 degree, the maximum yoke bushing force was 210 N (47 lb), and the maximum wheel/conductor interface force was 1200 N (270 lb).

While the yoke bushing force was not unreasonably high, the wheel/conductor interface force was excessive, because it would have to be resisted by the wheel flanges. These results dictated that the wheel would have to be constructed of a relatively rigid material so that the flanges could take the lateral forces in the curves, and that the circular transition of the conductor at the insulator would be necessary in the lateral direction as well as in the vertical direction. Even with the incorporation of these two suggestions into the design, there is a possibility that the wheel flanges will not take the lateral load without an unrealistic vertical preload on the wheels. If this situation occurs, it may be necessary to consider a three-wheel arrangement at each end of the wheel assembly.

A sketch of the three-wheel concept is compared to the two-wheel concept in Figure 4-17. If a three-wheel arrangement is used, the lateral force at the insulator will be reacted in the radial direction of the wheels, rather than against the flanges of the wheels.

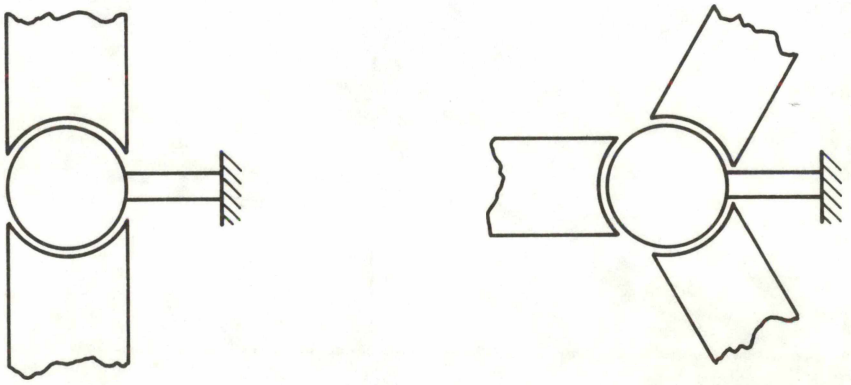

FIGURE 4-17. COMPARISON OF 2-WHEEL AND 3-WHEEL CONCEPTS

Finite Element

Three principal results were obtained from the finite element simulation: the time histories of the yoke bushing forces, the wheel/conductor forces, and the bending stress in the conductor. The first two results are compared to the 6-DOF model and are presented as a verification that the 6-DOF model gave reasonably accurate results. The third result, bending stress in the conductor, was not available from the 6-DOF model. The results of the finite element simulation are based on the nominal parameters listed in Table 4-1, and the design of the diamond pantograph described in Section 3.

Yoke Bushing Force. Figure 4-18 shows the time histories of the forces developed in the top and bottom yoke bushing, respectively. Since the bushings were modeled symmetrically on each side of the wheel assembly, a vertical force into the wheel assembly will be resisted equally by the two yoke bushings. Because of the modeling technique, Figure 4-1, one bushing must be in tension while the other is in compression when a force is applied in the plane of the wheels. In Figure 4-19 the total yoke bushing force is plotted as a comparison to the 6-DOF model. It is apparent that the two responses are identical in the first mode frequency (12 Hz), and are reasonably close in the maximum amplitude--the 6-DOF model might be judged to be somewhat conservative since it gave a 30-percent higher maximum force. Extending the force time history further than shown in Figure 4-19 showed a slowly damped oscillation.

Wheel/Conductor Force. The wheel on the conductor will respond with a much higher frequency because the wheels were much stiffer than the yoke bushing. Figure 4-20 compares the finite element and 6-DOF model time histories for the force at the wheel/conductor interface. As can be seen the response frequency (110 Hz) was much higher than for the yoke bushing, Figure 4-19, and the comparison was not very good at any particular time in the simulation. However, the frequency content of the two simulations was similar; and more important, the force magnitudes were similar.

It should be noted that the finite element simulation modeled the conductor as a series of truss and beam elements. This type of model introduced a discontinuity at the end of each beam or truss element. Through the 508-mm (20-in.) transition there were eleven discontinuities (10 beam elements); and each discontinuity introduced a transient into the dynamics of the system. On the other hand, the 6-DOF model assumed a continuous transition. The finite element model, with its discontinuities, would probably be closer to "real world" conditions. Nevertheless, the 25-percent difference in maximum force magnitude between the two models was well within acceptable accuracy.

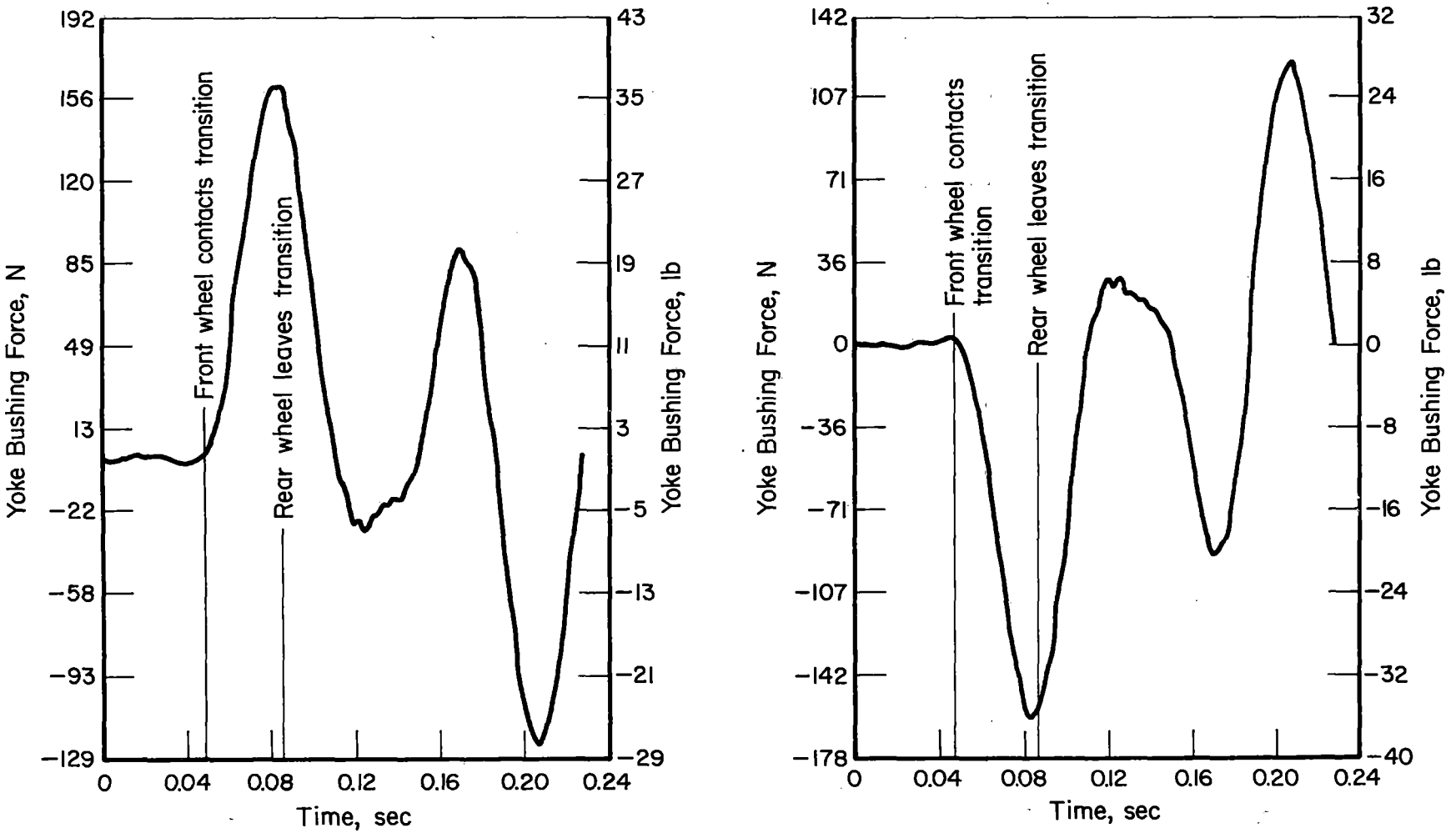

a. Top yoke bushing

b. Bottom yoke bushing

FIGURE 4-18. FORCE TIME HISTORY OF YOKE BUSHINGS TRAVERSING 508 mm (20 in.) CONDUCTOR TRANSITION

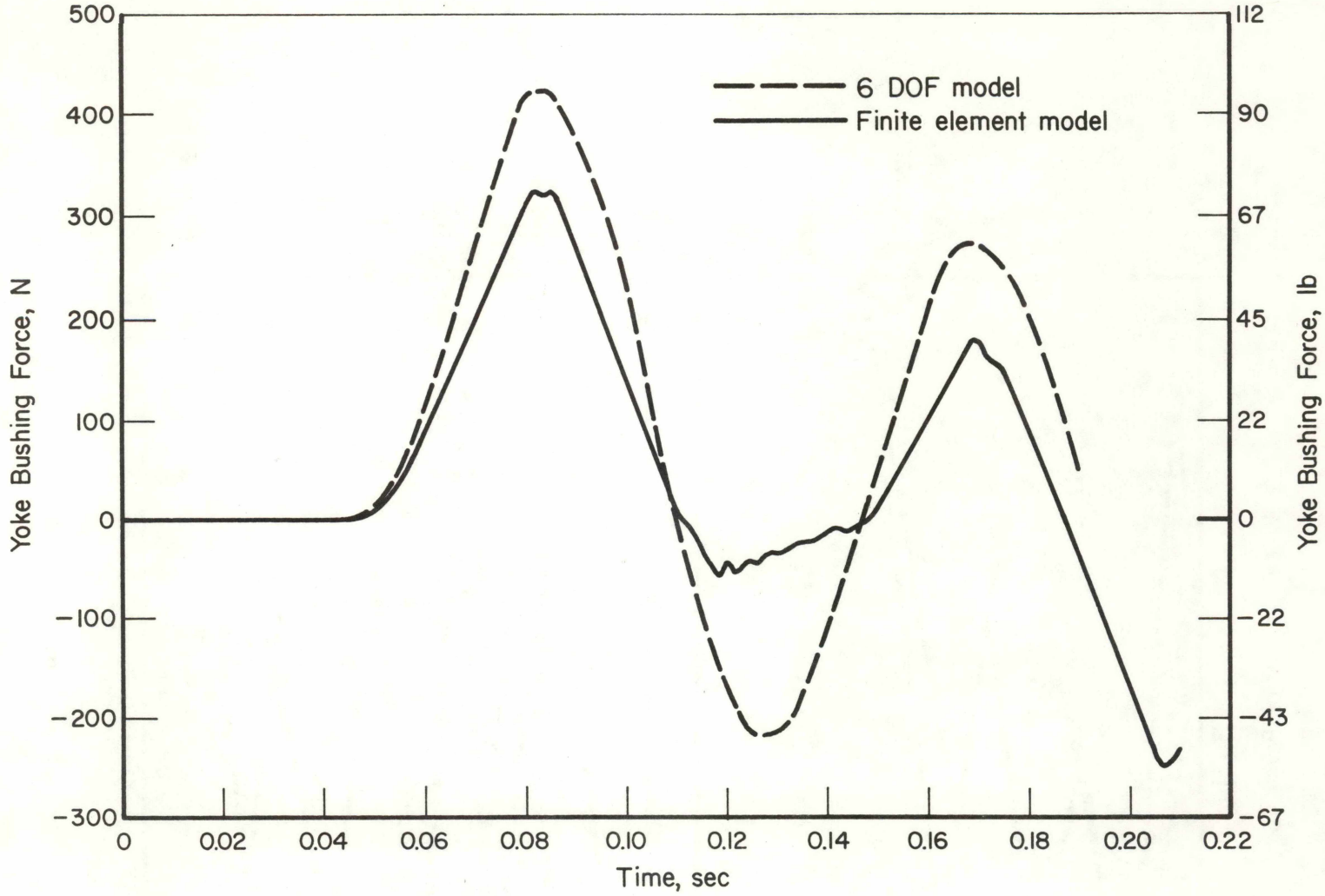

FIGURE 4-19. COMPARISON OF YOKE BUSHING FORCE TIME HISTORY OVER CONDUCTOR TRANSITION FOR FINITE ELEMENT AND 6-DOF MODEL

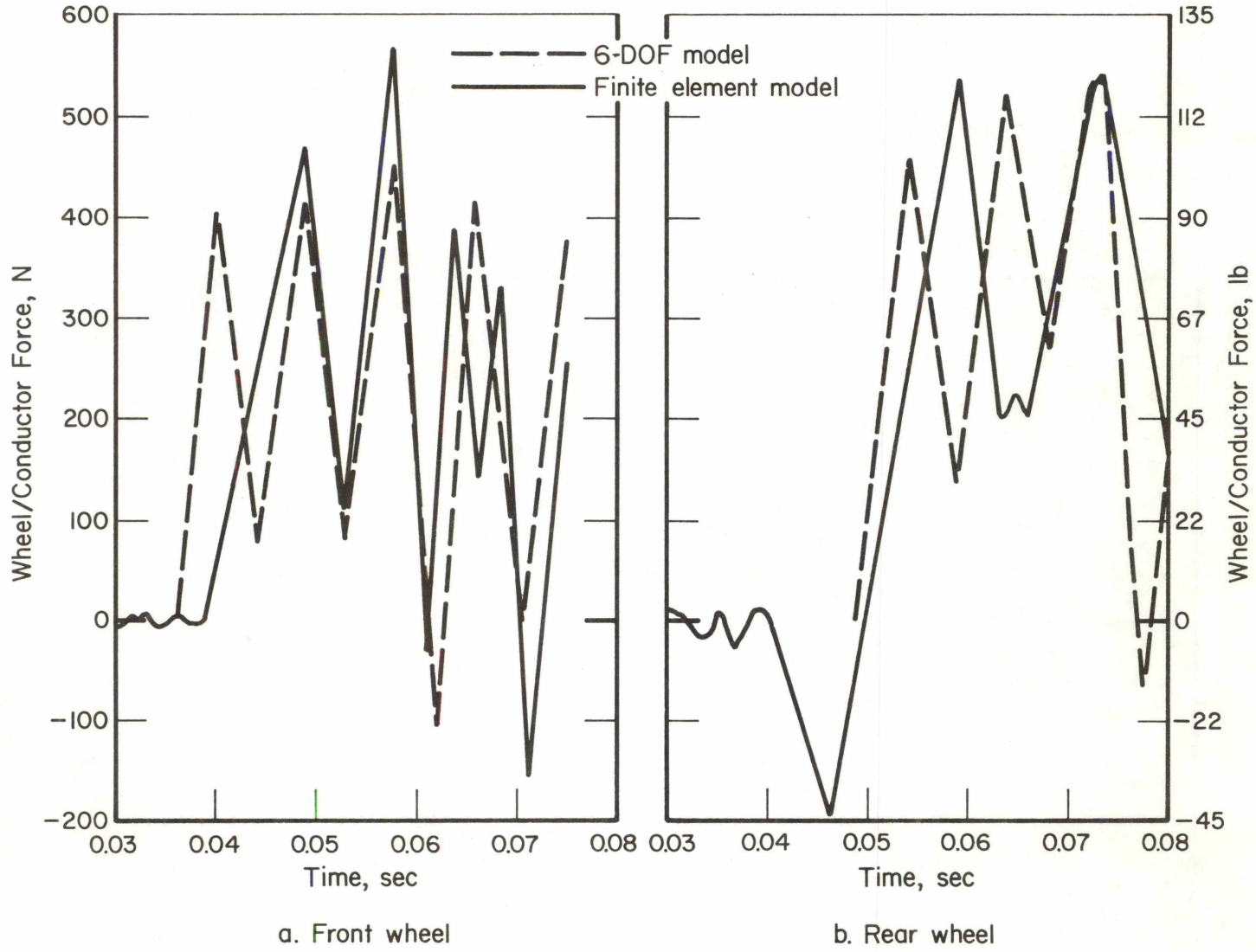

a. Front wheel

b. Rear wheel

FIGURE 4-20. COMPARISON OF WHEEL/CONDUCTOR FORCE TIME HISTORY OVER TRANSITION FOR FINITE ELEMENT AND 6-DOF MODELS

Conductor Bending Stress. Figure 4-21 shows a time history of the dynamic bending stress in the conductor at the end of the transition, the point of highest predicted bending stress. A maximum dynamic bending stress of approximately 100 N/mm^2 (14,500 psi) occurred after the first wheel had departed the 508-mm (20-in.) transition, but before the second wheel departed. An increase in conductor tension would increase the static stress, but decrease the dynamic bending stress.

The high-frequency, slowly-damped response after the peak stress was due to numerical stability problems associated with this simulation. Although the initial response should be accurate, subsequent response may be masked by numerical noise.

Summary - Dynamic Analysis

Four mathematical simulations were used to investigate the dynamics of an electrical pickup, traveller system riding on a tensioned conductor. Two of the simulations were 1-DOF models that resulted in closed-form solutions, one for the vertical dynamics of the traveller as it traversed the catenary cusp at the insulator, and one for the lateral curving dynamics of the traveller as it traversed the conductor at the insulator. The third simulation was a 6-DOF model of the vertical dynamics of a two-wheeled traveller traversing the conductor near the insulator. In particular, a circular transition arc was modeled into the catenary geometry. The fourth simulation was a finite element model that included the full details of the conductor and traveller hardware.

The two, 1-DOF models showed that under worst-case, nominal conditions, the forces at the wheel/conductor interface would be 4090 N (920 lb) vertical and 1200 N (270 lb) lateral for a 1.0 degree curve. These forces were determined by assuming that there was no geometric transition in the conductor at the pole insulator. Also using the 1-DOF vertical simulator, the yoke bushing force was predicted to be 707 N (154 lb).

The results of the 6-DOF simulation, which modeled the transition in the vertical plane, lowered the maximum wheel/conductor interface force to 530 N (120 lb) and the maximum yoke bushing force to 420 N (94 lb).

The finite element model was run for the nominal case, and its results were comparable to the 6-DOF model. In addition the finite element model predicted a maximum dynamic bending stress in the conductor of 100 N/mm^2 (14,500 psi).

The results of the 6-DOF model parametric study are summarized qualitatively in Table 4-3. The force trends are indicated for increases in the specified parameter. Large increases in the yoke bushing force can be expected from increases in yoke assembly weight,

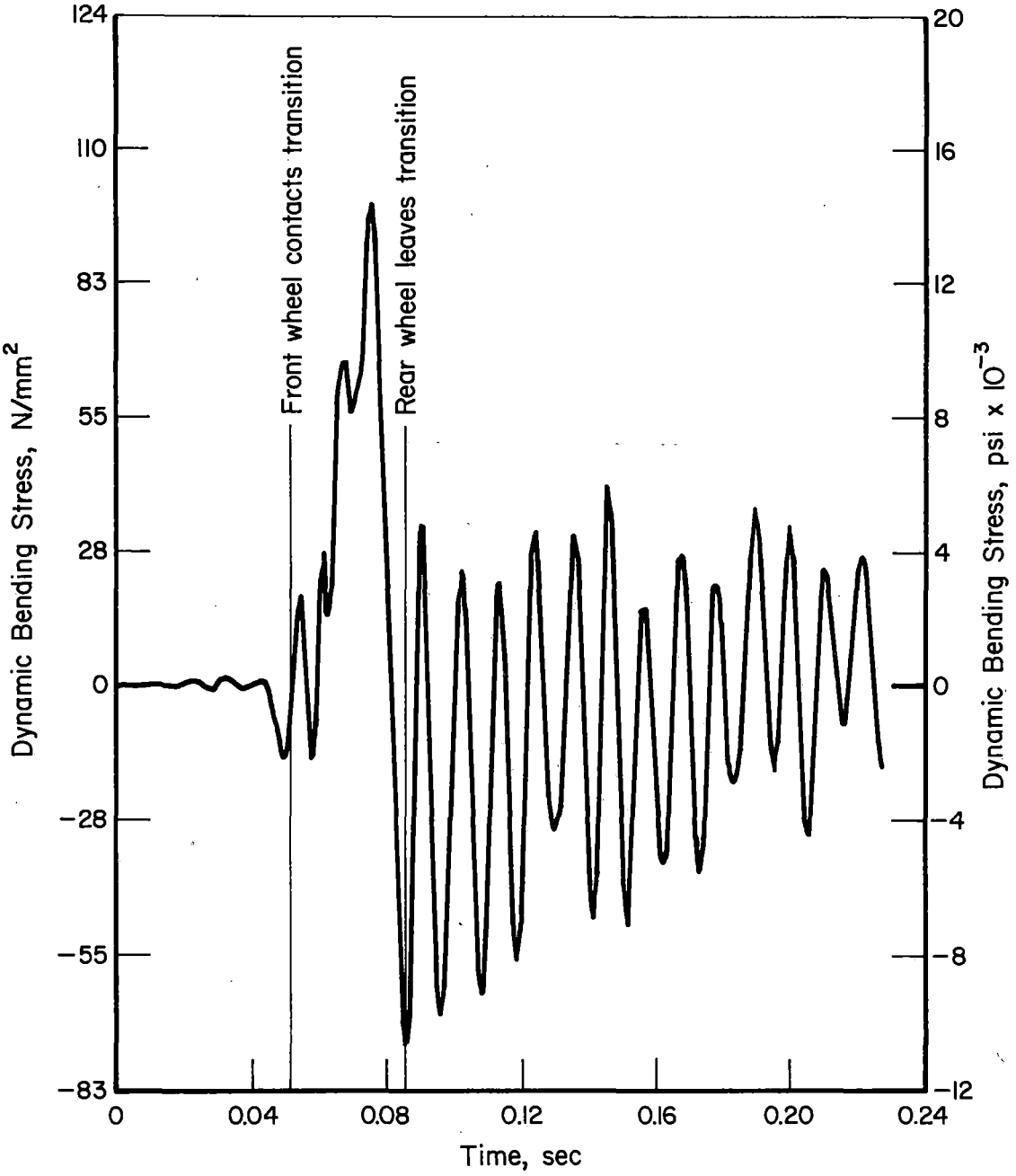

FIGURE 4-21. TIME HISTORY OF DYNAMIC BENDING STRESS IN CONDUCTOR AT END OF TRANSITION, 254 mm (10 in.) FROM INSULATOR

TABLE 4-3. QUALITATIVE SUMMARY OF 6-DOF MODEL PARAMETRIC STUDY

Increasing Parameter	Yoke Bushing Force	Wheel/Conductor Force	Insulator Force
Yoke Assembly Weight	Increase rapidly	Increase slightly	Increase slightly
Wheel Assembly Weight	Decrease slightly	Increase rapidly	Increase moderately
Insulator Weight	Small change	Increase slightly	Decrease moderately
Yoke Bushing Stiffness	Increase slightly	Increase slightly	Increase slightly
Wheel/Conductor Stiffness	Small change	Small change	Small change
Insulator Stiffness	Increase slightly	Increase slightly	Increase moderately
Conductor Diameter	Increase rapidly	Increase rapidly	Increase rapidly
Conductor Tension	Decrease rapidly	Decrease rapidly	Decrease moderately
Pole Span	Increase rapidly	Increase rapidly	Increase rapidly
Wheel Spacing	Decrease slightly	Small change*	Increase slightly
Transition Length	Decrease slightly	Decrease slightly*	Small change
Vehicle Speed	Increase rapidly	Increase rapidly	Increase slightly

* A decrease in the parameter will result in a rapid increase in force.

conductor diameter, pole span, and vehicle speed. Large increases in the wheel/conductor interface forces can be expected for increases in wheel assembly weight, conductor diameter, pole span, and vehicle speed. Large increases in wheel/conductor forces can also be expected from a decrease in wheel spacing, and especially from decreased transition length. Large increases in the insulator force can be expected from increases in conductor diameter, and pole span. Decreasing tension increases all force levels. For practical situations the increasing force due to conductor diameter can be effectively negated by increasing the conductor tension. The pole span and vehicle speed place an upper limit on the system. The weight of the traveller system is critical, and should be minimized.

The single most important parameter that must be controlled to insure an operational system is to provide a smooth transition at the insulator, i.e., reduce the sudden change in conductor slope. This requirement was shown to be necessary for the vertical dynamics, and was strongly implied for the lateral dynamics involved at track curves. The use of a smooth transition also allows the use of less flexible wheels to withstand the vertical and lateral loads.

Recommendations - Dynamic Analysis

Based on the preliminary analytical studies, the following recommendations are made:

- A 805-mm (20-in.) circular transition should be built into the conductor at each pole attachment. The transition was shown to be necessary in the vertical plane, and probable will also be necessary in the lateral plane at track curves.

- A preload of at least half of the maximum wheel/conductor force should be built into the wheel assembly to prevent wheel/conductor separation. The preload should not be excessively high to minimize wheel/conductor wear and to prevent fatigue failure. The recommended preload between each wheel and the conductor should be 270 to 445 N (60 to 100 lb).

- The traveller system weight should be minimized.

- The slope of the conductor should be minimized by: decreasing density, diameter, and pole span, and increasing conductor tension.

5. PRELIMINARY CONCEPT FEASIBILITY AND COST COMPARISONS

The preliminary design was prepared utilizing existing design techniques and mechanisms. The design was tested iteratively by the theoretical dynamic analysis to establish the best choice of materials, mechanisms and dimensions. A final theoretical analysis was made utilizing the six degree of freedom model confirmed by the finite element model.

It is believed a low cost catenary system as described in this report can be designed within the constraints of existing technology for railroad electrification systems and for electric power utility distribution lines. The design as presently prepared is believed to be a viable design and generally indicates the concept of the low cost catenary system is feasible.

A cost comparison was made for the low cost catenary system and the conventional catenary system. See Table 5-1. This cost comparison was made for a hypothetical 50 mile railroad section consisting of 40 miles of straight track and 10 miles of curved track. It includes those items necessary to support the contact conductor in the appropriate position and, of course, includes the cost of the contact conductor itself. The cost of the power supply system and locomotives is common to both systems and was excluded for purposes of simplification. Further, the cost of the current collection devices - the pantograph and the traveller - is assumed the same for both systems. Also for simplification, rail switching arrangements such as turnouts and crossovers were excluded, since their assumed higher cost for the low cost catenary system would be offset by the omission of the special tensioning structures required for the conventional system. No special tensioning structures are required for the low cost system.

For the conventional catenary system a simple catenary configuration was assumed such as used for the Muskingum Railroad in Ohio. This catenary has a 4/0 copper contact conductor, a 4/0 copperweld messenger, and is designed for 25kV, 60 Hertz operation. The specifications for this design were used for the 50 mile hypothetical railroad section.

For the low cost catenary design 25kV, 60 Hertz operation also was assumed and a 400 mcm copper contact conductor was assumed since it has the equivalent current carrying capability as the 2-4/0 conductors of the conventional catenary. Further, 200 foot spans between supports were assumed throughout for the low cost catenary whereas for the conventional system the spans for the curved track sections were shortened to 100 feet for centering the contact conductor over the rails.

The material and labor costs for the two systems were estimated "side-by-side" to preserve as much as possible the comparison function. The material costs for the Muskingum Railroad design were updated and 1981 material costs likewise were used for the low cost catenary design.

TABLE 5-1. ESTIMATED COST OF CONVENTIONAL VS. LOW COST CATENARY SYSTEM FOR 50-MILE RAILROAD SECTION

(40 Miles Straight, 10 Miles Curved)

	Material			Installation		
CONVENTIONAL CATENARY SYSTEM						
1000 Tangent Structures:	ea	$558.35	$ 558,350	ea	$245.00	$245,000
500 Curve Structures:	ea	515.49	257,745	ea	325.00	162,500
50 Miles of Catenary:						
50 mi 4/0 CW Messenger	mi	7,809.63	390,482)			
50 mi 4/0 CU Conductor	mi	5,472.56	273,628)			
1000 - 200' Span Hangers	ea	151.10	151,100)	mi	11,200.00	560,000
500 - 100' Span Hangers	ea	49.74	24,870)			
			$1,656,175			$967,500
Stores Expense 10%			165,618			-
			$1,821,793			$967,500
						$2,789,293
Services, Contingencies and Overheads 46%						1,283,075
Total Estimate Conventional Catenary System						$4,072,368
LOW COST CATENARY SYSTEM						
1000 Tangent Structures:	ea	$169.37	$169,370	ea	$180.00	$180,000
250 Curve Structures:	ea	195.28	48,820	ea	260.00	65,000
50 Miles of 400-MCM CU Conductor:	mi	10,050.60	525,080	mi	1,400.00	70,000
			$743,270			$315,000
Stores Expense 10%			74,327			-
			$817,597			$315,000
						$1,132,597
Services, Contingencies and Overheads 46%						520,995
Total Estimate Low Cost Catenary System						$1,653,592

A power line construction contractor was provided with the specifications and designs for both systems and again labor costs were estimated side-by-side as for the material costs. Various precentile charges were assumed for stores expense, contingencies and overheads, but, since these are applied as multipliers, they do not affect the overall comparison.

As can be seen by Table 5-1, the overall installed cost of the low cost catenary system is less than one-half the cost of the conventional system. Significant items contributing to this reduction are:

1. Material cost of the tangent structures - $169,370 for the low cost system versus $558,350 for the conventional system. The low cost system requires a shorter pole with a single post insulator. The conventional system requires a taller pole with insulator/arm system centering the contact conductor over the rails plus a guy wire and anchor to maintain the pole alignment hence the elevation of the contact conductor.

2. Material cost of the curve structures - $48,820 versus $257,745. This reduction results from the lower per unit cost of the structures as described above plus the reduced number of structures required for the curved track sections.

3. Material cost of the conductor - $525,080 versus $840,080 (the total of the four conductor items for the conventional system). The cost of the single conductor for the low cost system is much less than the combined cost of the messenger, the contact conductor and the many span hangers required for the conventional system.

4. Installation cost of the conductor - $70,000 versus $560,000. Installation cost of installing a single conductor for the low cost system is considerably less than installing the conventional catenary.

No provision was included in the low cost catenary estimate for attaching the contact conductor to the support insulator. As mentioned in Section 3, Contact Conductor Support Design, "Further study and design testing is recommended to develop both . . . conductor support methods described . . ." At this time we do not have a knwon, workable support method. Nevertheless, referring to Table 5-1, the installation cost of any support method should be much less than the cost of installing the contact conductor - or $70,000. If the installation cost were to equal this value, the total cost of the low cost system will continue to be less than one-half the cost of the conventional system.

6. CONCLUSIONS

As a result of the preliminary design studies, the dynamic analyses, and the cost comparison, the following was concluded:

1. The mechanical loads determined by the dynamic analysis are within the limits of reasonable design practice. These loads are not in thousands of pounds but in the order of hundreds of pounds.

2. As expected, to minimize these loads the weight of the assembly and the sag angle of the conductor must be low. Sag angle is minimized by conductor tension and low conductor weight.

3. Further reduction of these mechanical loads can be effected by providing a transition curve in the conductor at the supports. The arc radius and length of the transition are within the limits of reasonable design practice.

4. Velocities above 81 kph (50 mi/h) and lateral deflections of the conductor for curved track sections were briefly investigated. These conditions increase the mechanical loads, but is is believed a properly designed conductor support and transition curve will offset their effect.

5. The cost comparison indicates the installed cost of the low cost catenary system is less than one-half that of the conventional catenary system.

6. The preliminary design and the results of the dynamic analysis and cost comparison justify proceeding with the physical testing of the system. Testing should include initial design testing of the contact conductor support and of the traveller wheel assembly. Following this an outdoor full-scale laboratory test with rail vehicle speeds up to 81 kph (50 mi/h) is required to confirm concept feasibility.

7. BIBLIOGRAPHY

1. National Electric Safety Code ANSI C2-1981

   Institute of Electrical and Electronic Engineers, Inc.
   345 East 47th St. New York, NY 10017

2. Manual for Railway Engineering

   Chapter 33
   Electrical Energy Utilization
   Americal Railway Engineering Association (AREA)

3. William D. Middleton - When The Steam Railroads Electrified.

   Kalmbach Publishing Co. 1974

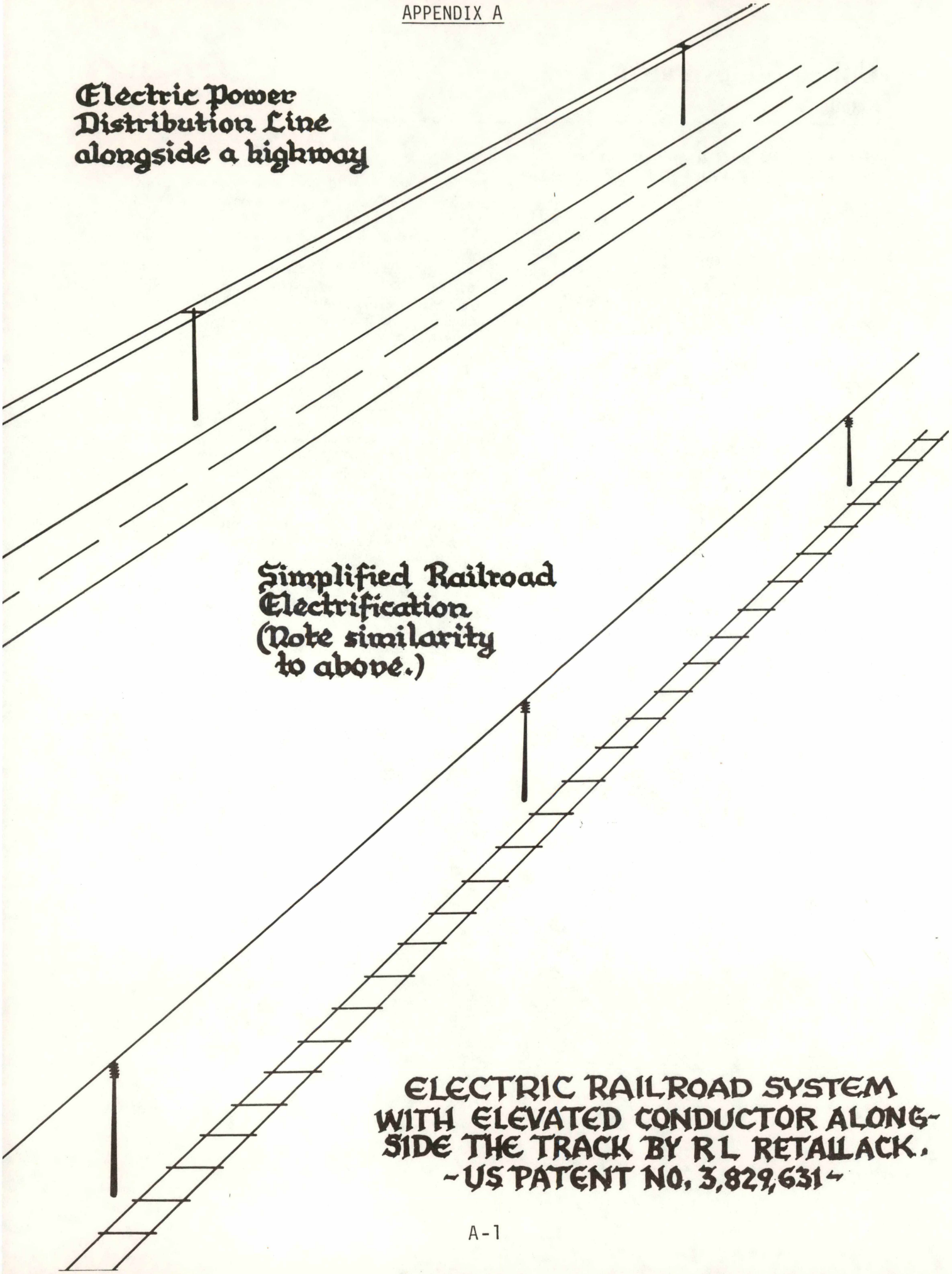

ELECTRIC RAILROAD SYSTEM WITH ELEVATED CONDUCTOR ALONGSIDE THE TRACK BY R L RETALLACK. ~US PATENT NO. 3,829,631~

United States Patent [19]

Retallack

[11] **3,829,631**

[45] **Aug. 13, 1974**

[54] **ELECTRIC RAILROAD SYSTEM WITH ELEVATED CONDUCTOR ALONGSIDE THE TRACK**

[76] Inventor: **Robert L. Retallack,** 510 Fairfield Ave., Ridgewood, N.J. 07450

[22] Filed: **May 18, 1972**

[21] Appl. No.: **254,616**

[52] **U.S. Cl.** **191/66,** 191/32, 191/40

[51] **Int. Cl.** **B60l 5/12**

[58] **Field of Search** 191/22, 29, 32, 33, 45, 191/47, 48, 49, 50, 53, 57, 59, 59.1, 60.2, 60.3, 60.5, 64–70

[56] **References Cited**

UNITED STATES PATENTS

574,632	1/1897	Schlesinger	191/53
590,527	9/1897	Kenway	191/53
749,042	1/1904	Eader	191/49
1,747,489	2/1930	Schaake	191/70
2,935,576	5/1960	Faiveley	191/68
3,712,430	1/1973	Charamel	191/49
3,730,311	5/1973	Maison	191/49

Primary Examiner—M. Henson Wood, Jr.
Assistant Examiner—D. W. Keen
Attorney, Agent, or Firm—Pennie & Edmonds

[57] **ABSTRACT**

In this electric railroad system, the elevated contact conductor is mounted primarily alongside the track, with sections extending over the track and then back alongside the track at grade crossings, railraod crossings, switch locations, transition locations where the conductor is transferred to the opposite side of the track, etc. The electrically-powered vehicle has an overhead traveler mounted on an extensible arm for obtaining power from the contact conductor. The arm is pivotally mounted on top of the vehicle for movement about an axis of rotation extending longitudinally of the vehicle, and also allows the traveler to move toward and away from the axis of rotation so that the traveler can follow changes in position of the contact conductor while remaining in engagement therewith. In the specific embodiments, the traveler has pairs of grooved wheels engaging opposite sides of the conductor and the arm is articulated to maintain substantially the same orientation of the traveler with respect to a radius to the axis of rotation of the arm as the traveler follows changes in position of the contact conductor. Sections of the conductor over the track may rise to a higher level than alongside sections. At a switching location a fixed conductor frog mounted beyond the track switching point and having angled guide channels for the traveler may be employed.

12 Claims, 24 Drawing Figures

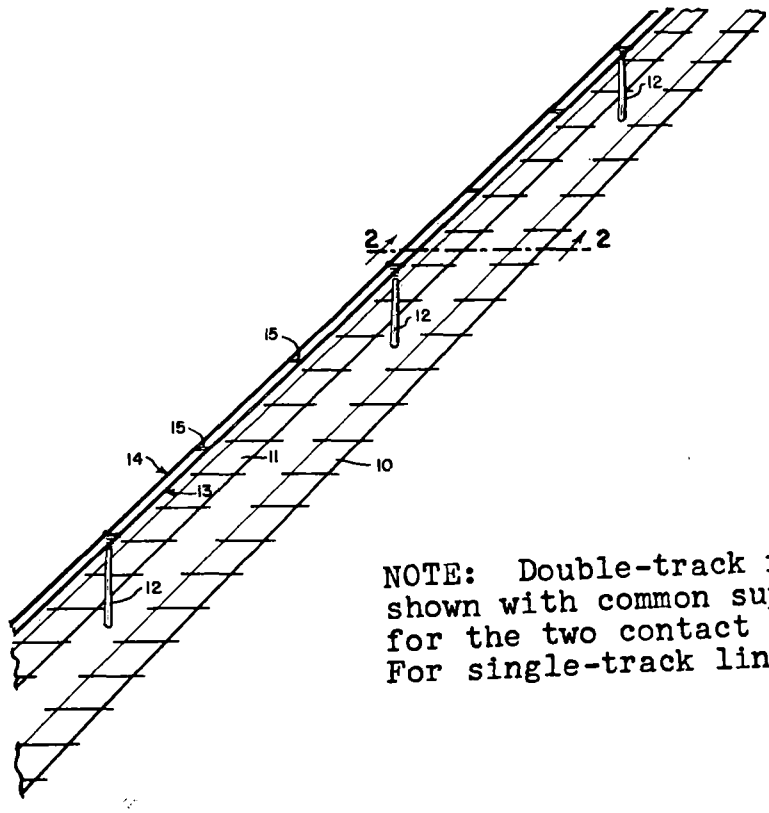

NOTE: Double-track railroad shown with common supports for the two contact conductors. For single-track line, see cover.

NOTE: Double-track railroad shown with common supports for the two contact conductors. For single-track line, see cover.

FIG. 1

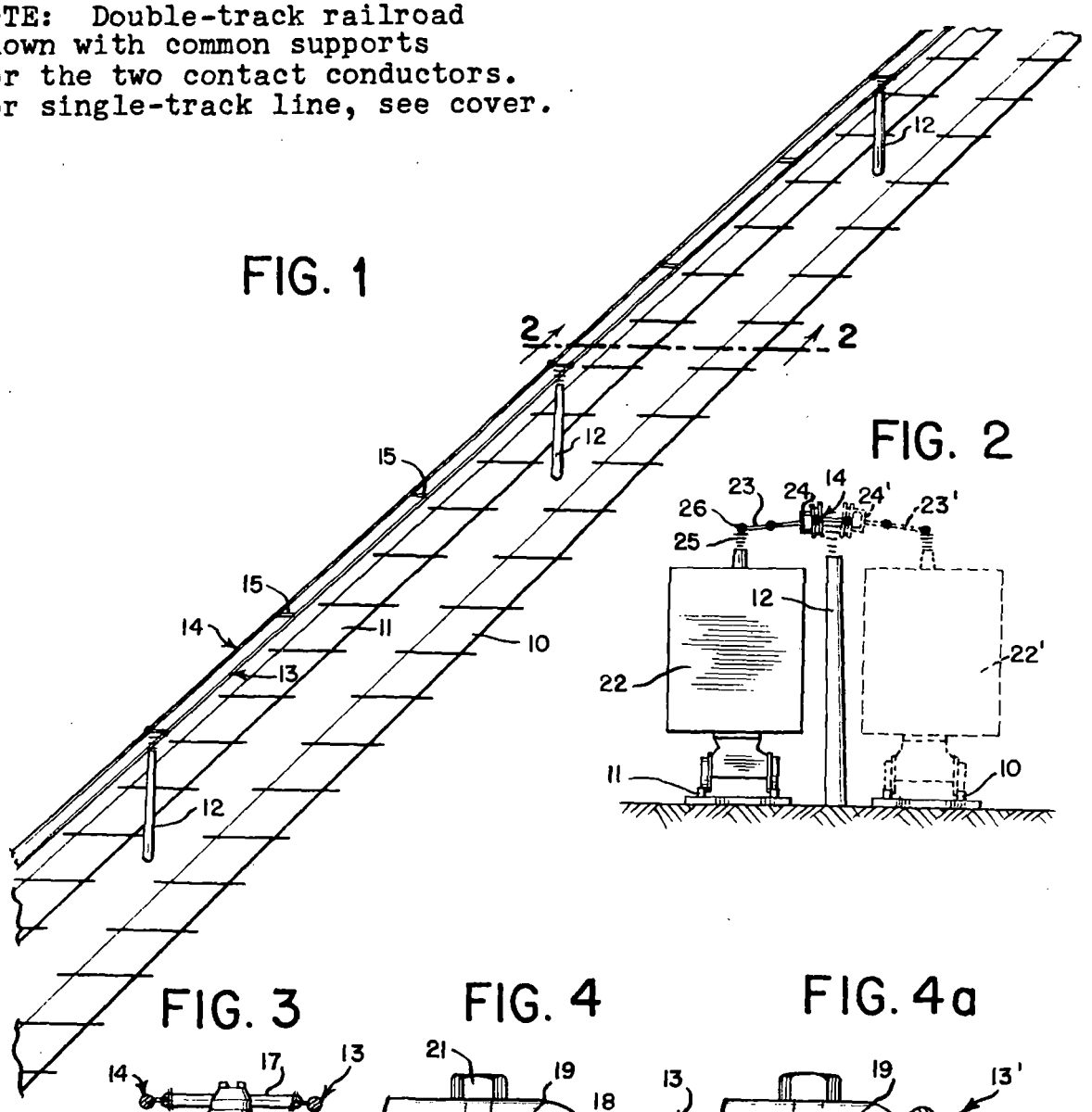

FIG. 2

FIG. 3

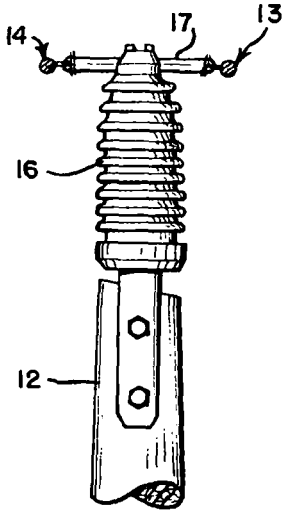

FIG. 4

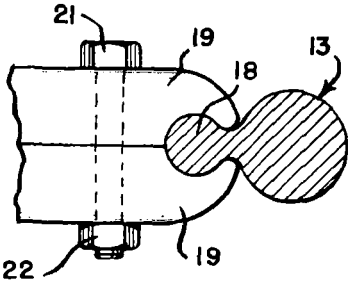

FIG. 4a

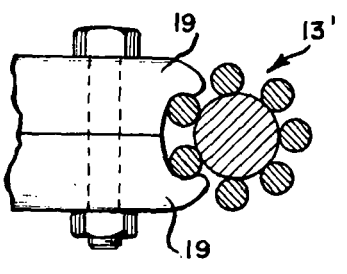

NOTE: Double-track railroad shown with common supports for the two contact conductors. For single-track line, see cover.

FIG. 5

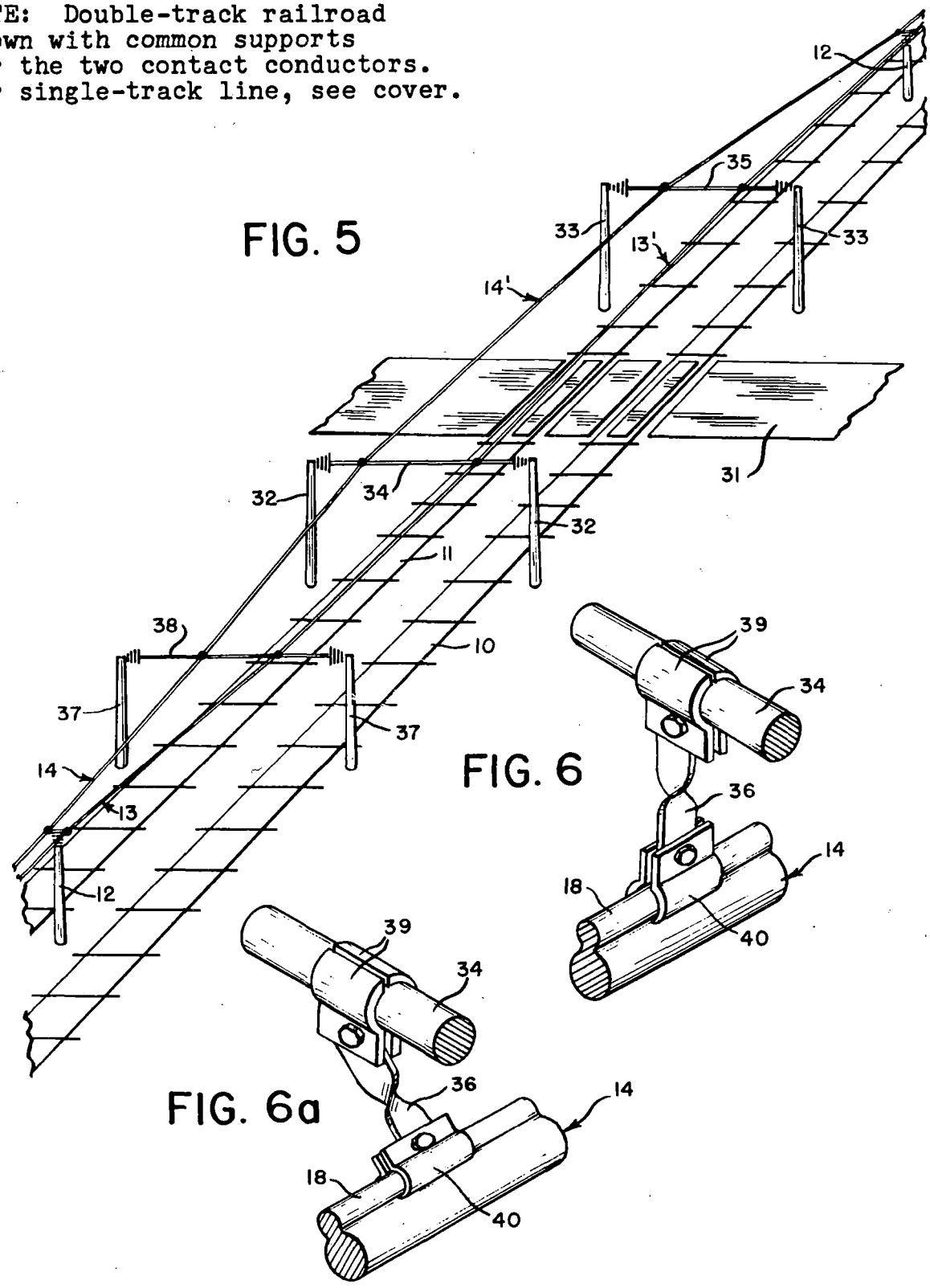

FIG. 6

FIG. 6a

FIG. 7

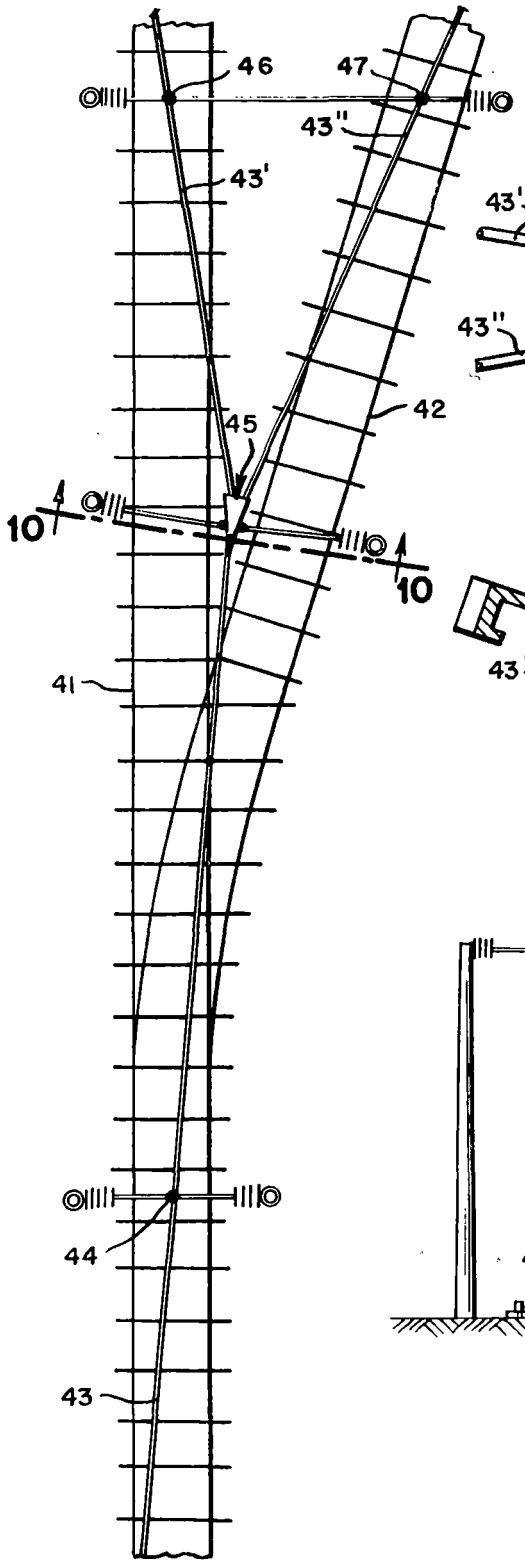

FIG. 8

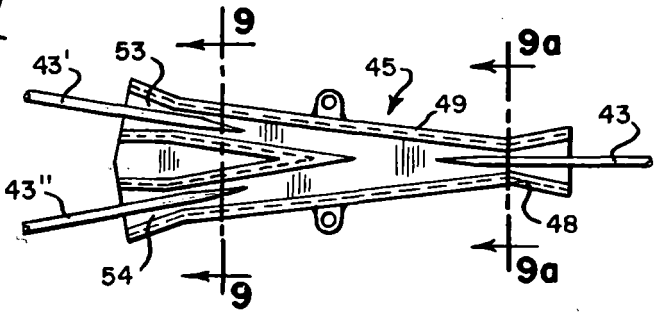

FIG. 9

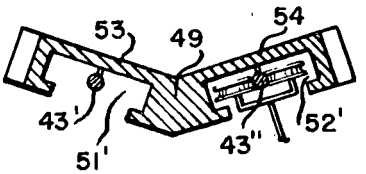

FIG. 9a

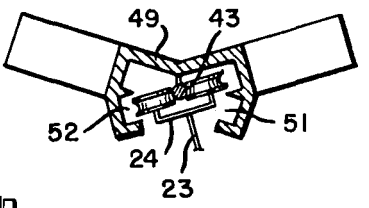

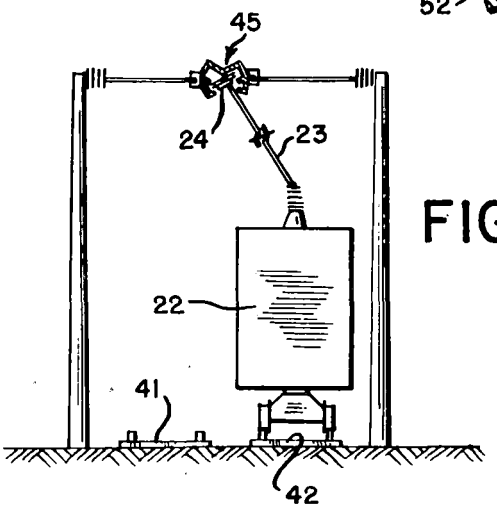

FIG. 10

FIG. 11

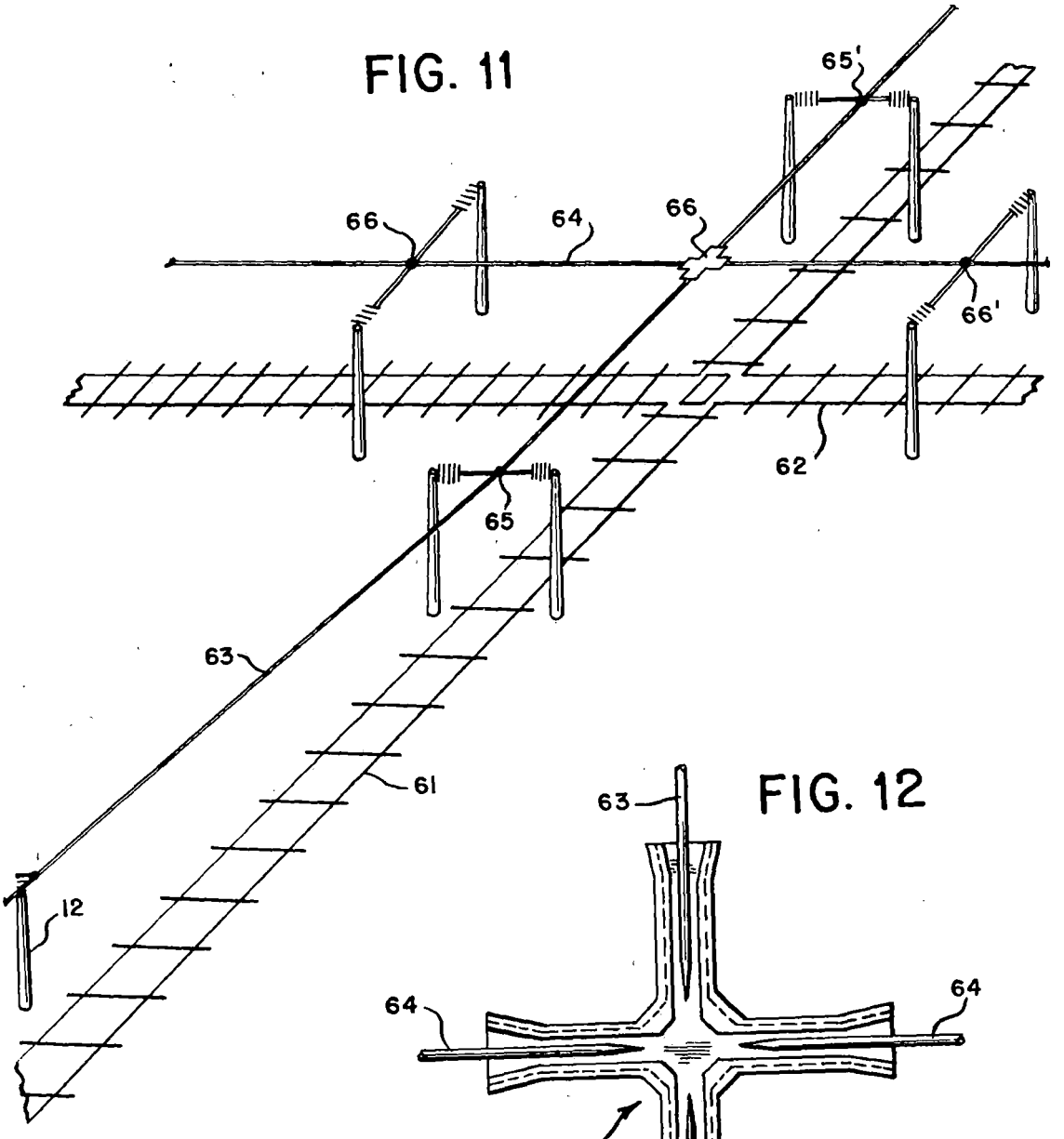

FIG. 12

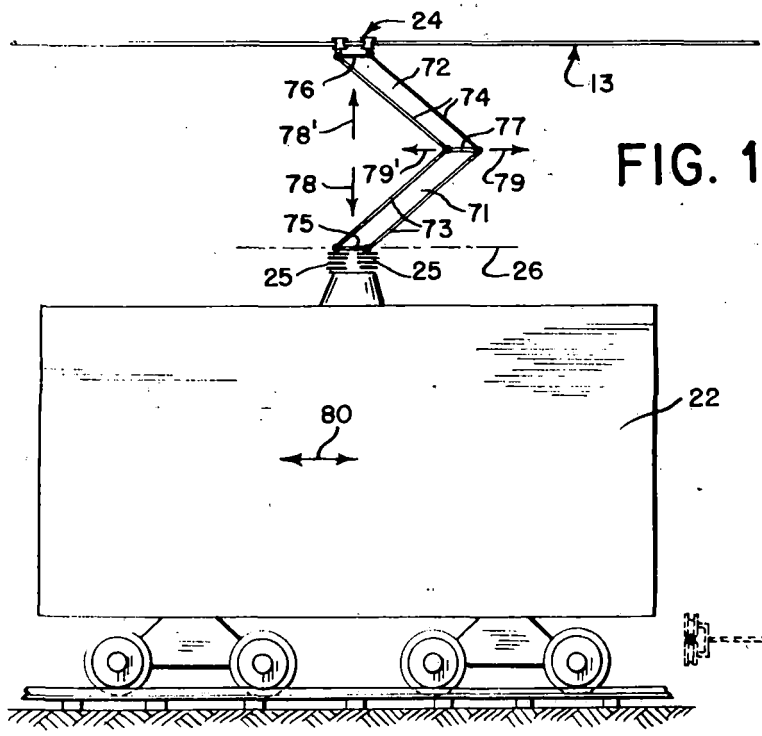

FIG. 13

FIG. 15

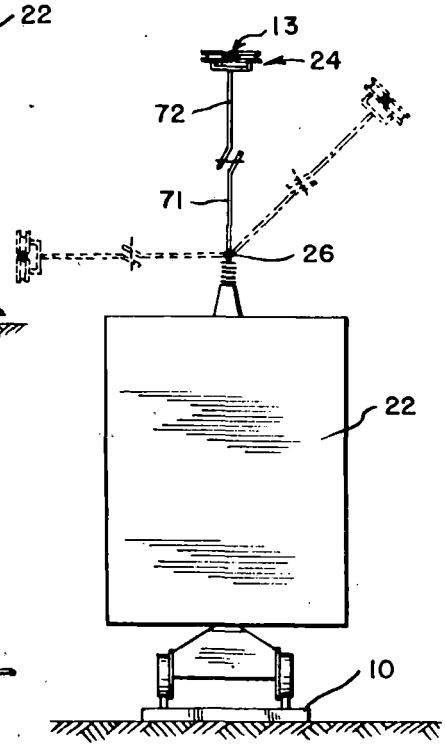

FIG. 14

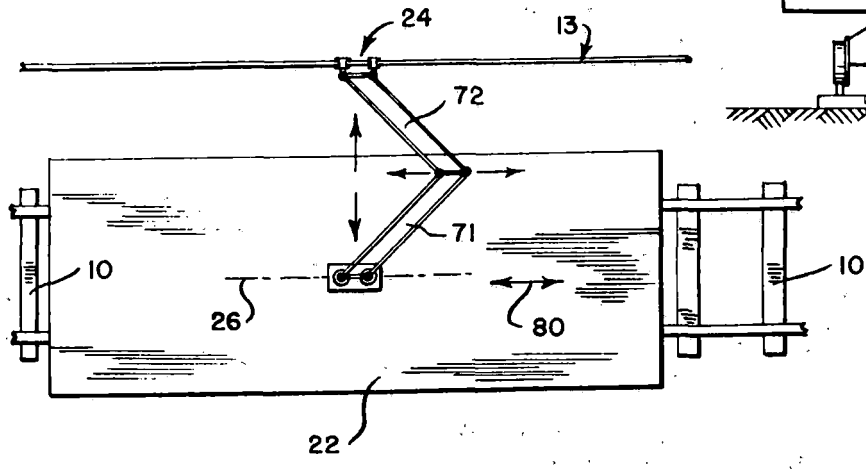

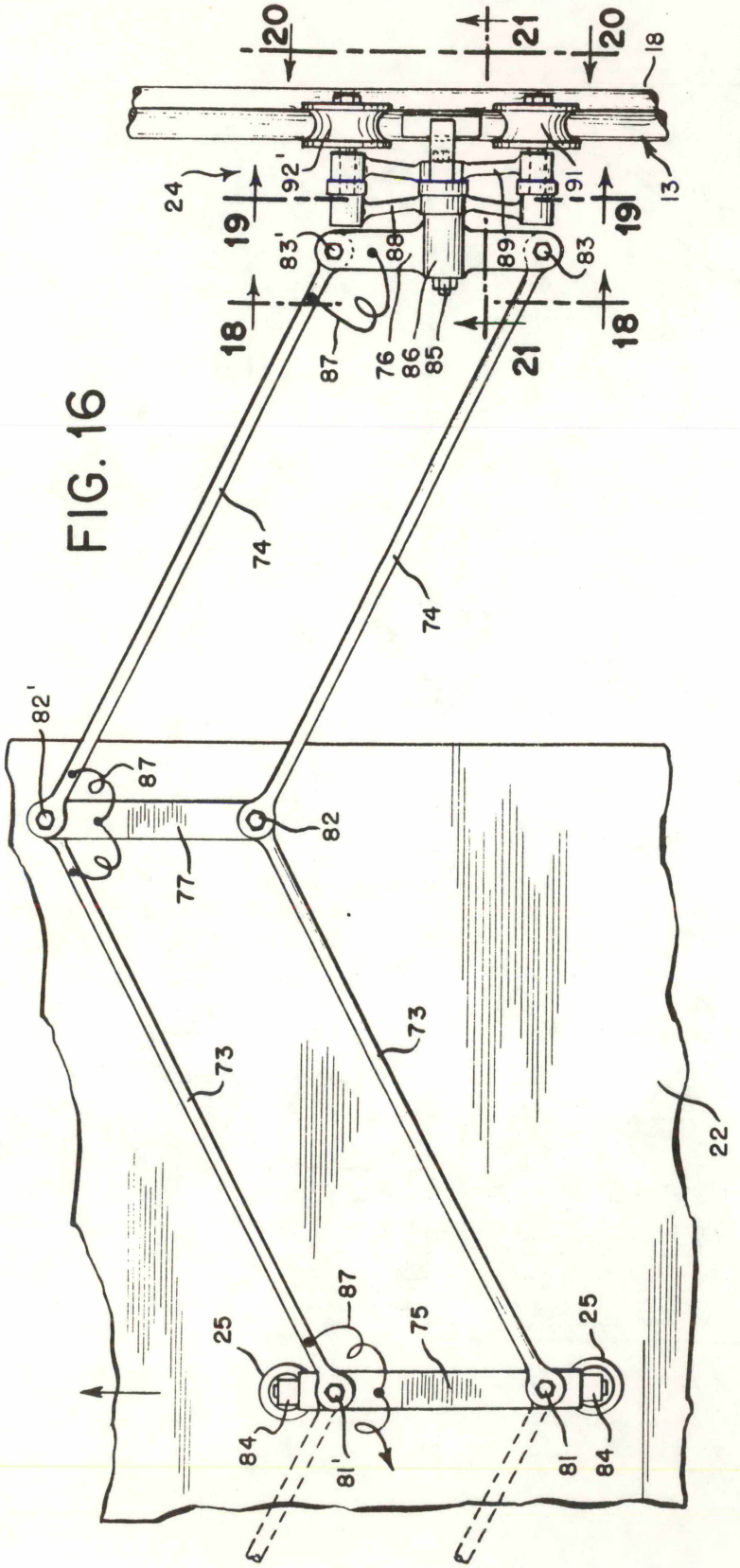
20
21
20
18
24
92'
91
13
19
19
83'
88
89
83
18
18
87
76
86
85
21
74
74
82'
87
82
77
73
73
22
25
87
75
25
84
81'
81
84

FIG. 16

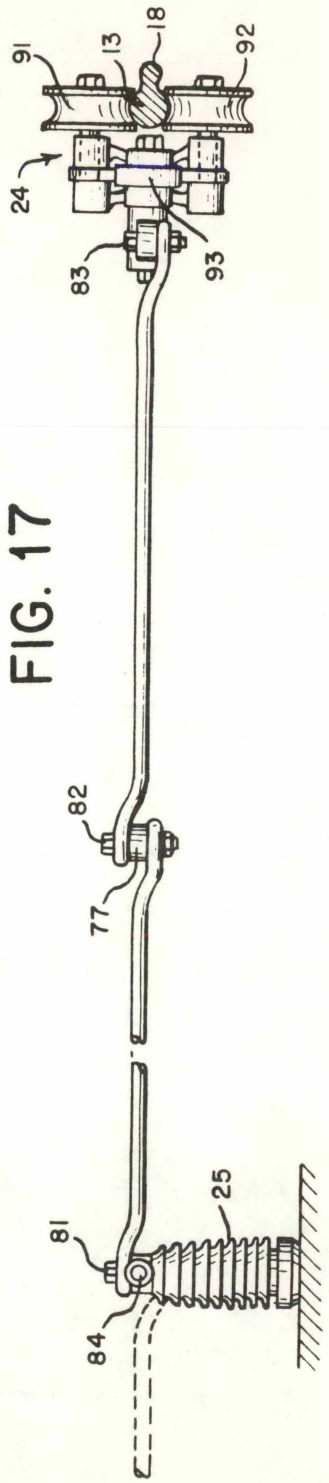
91
13
18
92
24
83
93
82
77
81
25
84

FIG. 17

FIG. 18

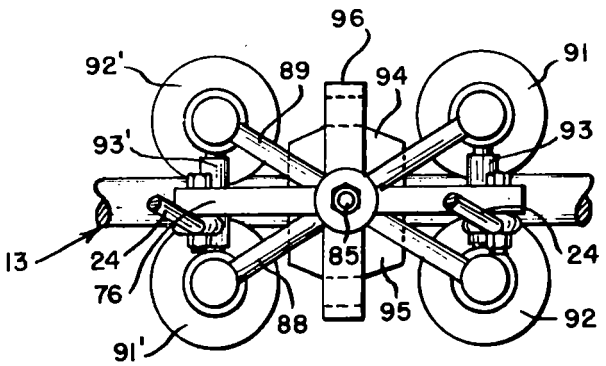

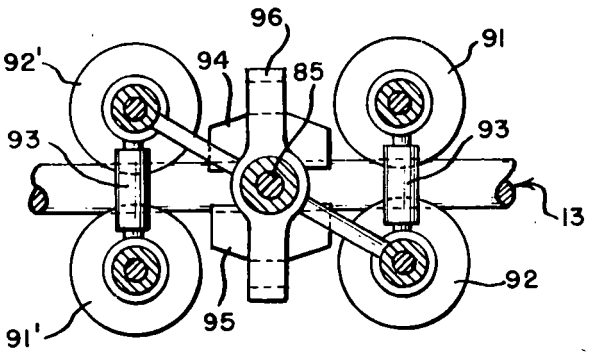

FIG. 19

FIG. 20

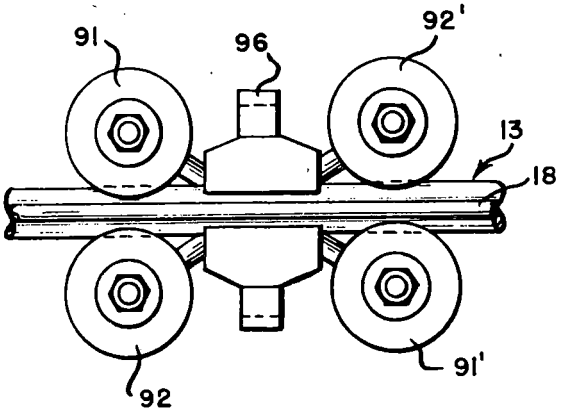

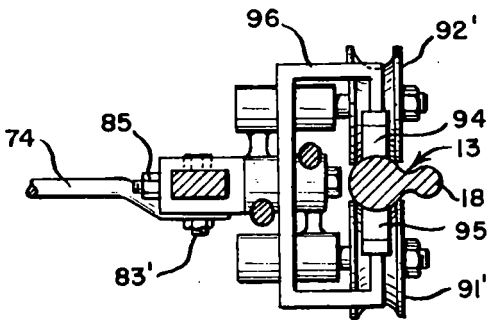

FIG. 21

ELECTRIC RAILROAD SYSTEM WITH ELEVATED CONDUCTOR ALONGSIDE THE TRACK

BACKGROUND OF THE INVENTION

Electric railroad systems with overhead power conductors engaged by trolley wheels or by pantograph mounted lateral conductor shoes have been known for many years. For high speed systems, the overhead contact conductor is commonly under high mechanical tension, and supported at a uniform height centrally over the track by a catenary suspension system and frequent supporting structures extending over the track. A major cost in electrifying a railroad is the cost of the overhead catenary system and associated support structures.

Third rails at the side of the track near ground level are also in use in protected locations and at relatively low voltages, but are inherently more dangerous than overhead systems.

There also have been proposals for mounting an elevated contact conductor alongside a track, but in general the vehicle trolley or other current collecting arrangements do not provide for track switching points or for transfer of the conductor from one side of the track to the other, and to positions over the track, as may be required in practical railroad systems, while still maintaining delivery of power to the vehicle.

It is a principal object of the present invention to provide an elevated contact conductor system and vehicle power collecting arrangement which will substantially reduce the cost of electrifying a railroad, while providing for switching, cross-overs, grade crossings, etc. as required in a given system.

SUMMARY OF THE INVENTION

In accordance with the invention, an elevated contact conductor is mounted primarily alongside the track, with sections as required extending over the track and then back alongside the track. Sections of contact conductor over the track may be used, for example, at grade crossings to allow clearance for highway traffic, at railroad crossings if such exist, at transition locations where necessary to transfer the contact conductor from one side of the track to the other, at switch locations, etc.

Electrically-powered vehicles such as locomotives and self-powered cars are provided with an overhead traveler mounted on an extensible arm for obtaining power from the contact conductor. The extensible arm is pivotally mounted on top of the vehicle for movement about an axis of rotation extending longitudinally of the vehicle, and the traveler includes means for engaging the conductor and holding the traveler in guided relationship therewith. The extensible arm is adapted for movement of the traveler toward and away from the axis of rotation of the arm. Thus the traveler can move to either side of the vehicle and to a central position over the vehicle, and also in and out, to follow changes in position of the contact conductor while remaining in engagment therewith.

With this arrangement it is believed that some sag in the conductor between support poles will be allowable, so that high mechanical tension in the conductor and lengthwise supporting cables will be unnecessary. Such support may be employed if desired, but in general may be less elaborate and expensive than for centrally located overhead conductors of the presently known systems.

It is particularly contemplated that the height of the conductor when alongside the track will be such that the traveler arm will be generally horizontal or at a small angle above the horizontal, thus allowing the traveler to rise and fall to accommodate sag in the conductor. At grade crossings, transitions to the opposite side of the track, etc., the height of the conductor may be increased and the conductor brought over the track, the traveler arm swinging over the vehicle and extending as required so as to maintain the traveler in engagement with the conductor.

At switching locations, the conductor may be brought to a position centrally over the track and a conductor switching frog employed to switch fron one position to the other. Or, as described in the specific embodiments, a fixed conductor frog may be located overhead beyond the track switching point and intermediate the centers of the tracks, so that the traveler and arm will swing to positions on opposite sides of the vehicle depending on which track it is following. Thus the pull on the traveler will guide it to the proper outlet leg of the frog. Advantageously the frog is provided with a pair of guide channels at respective angles corresponding to the traveler angles of vehicles traveling down respective tracks.

Preferably the traveler and arm are designed to maintain the same orientation of the traveler with respect to a radius to the axis of rotation of the arm as the traveler moves between side and central positions of the vehicle and toward and away from the axis of rotation. An articulated arm is described hereinafter which accomplishes this result. Preferably the traveler includes grooved means for engaging the conductor on opposite sides thereof and resiliently biased against the conductor, and pairs of grooved wheels longitudinally spaced along the conductor are particularly described hereinafter. The plane of the wheels is advantageously perpendicular to a radius to the axis of rotation of the arm so that the traveler can readily follow changes in position of the elevated conductor in either direction of movement of the vehicle.

BRIEF DESCRIPTION OF THE DRAWINGS

FIG. **1** illustrates a double track railroad with elevated contact conductors mounted alongside respective tracks on a single set of poles;

FIG. **2** is an end view of a pair of vehicles having travelers engaging respective elevated conductors and supported on extensible swinging arms;

FIGS. **3**, **4** and **4***a* illustrate means for mounting the conductors alongside the tracks;

FIG. **5** illustrates a highway grade crossing wherein the conductors are raised to a higher level and positioned centrally of the tracks;

FIG. **6** illustrates means for mounting the conductor centrally of a track, and FIG. **6***a* illustrates angular mounting between alongside and central positions;

FIG. **7** illustrates a conductor arrangement at a switching location;

FIG. **8** is a bottom view of the frog used in FIG. **7**;

FIGS. **9** and **9***a* are cross-sections of the frog taken along the lines **9—9** and **9***a*—**9***a* of FIG. **8**;

FIG. **10** illustrates a vehicle passing the switch at **10—10** in FIG. **7**;

FIG. 11 illustrates a conductor arrangement suitable for a railroad crossing;

FIG. 12 is a bottom view of the frog used in FIG. 11;

FIG. 13 is a side view of a vehicle with an articulated arm and traveler engaging a conductor centrally located over the track;

FIG. 14 is a top view of a vehicle with the traveler engaging a conductor alongside the track;

FIG. 15 is an end view of the vehicle illustrating various positions of the articulated arm and traveler;

FIG. 16 is a plan view of the articulated arm and traveler with the arm extending horizontally;

FIG. 17 is an elevation view of the arm and traveler of FIG. 16; and

FIGS. 18–21, inclusive, are views of the traveler taken along the lines 18—18 through 21—21 of FIG. 16, respectively.

DESCRIPTION OF THE SPECIFIC EMBODIMENTS

Referring to FIG. 1, a pair of railroad tracks 10, 11 of conventional construction are shown diagrammatically. Between the tracks is a set of poles 12 insulatedly supporting a pair of conductors 13, 14 alongside the tracks for delivering electric power to a vehicle. The conductors may be connected together at intervals by spacers 15 if desired.

FIG. 3 is a detail showing an insulator 16 mounted on top of a pole 12, with a cross bar 17 to which conductors 13, 14 are attached in suitable manner.

FIG. 4 shows one way of clamping a conductor in place. Here conductor 13 is a solid conductor with a ridge 18 formed along one side which is held between jaws 19 by a bolt and nut 21, 22. FIG. 4*a* is similar except here a stranded conductor 13′ is shown, and the jaws 19 are shaped to firmly engage a pair of the strands. Conductors of various cross-sectional configuration may be employed as desired, with suitably conforming clamps.

FIG. 2 shows two electrically-powered vehicles 22,22′ traveling in the same or opposite directions on tracks 10,11. The vehicles may be locomotives, self-powered individual cars, etc. and are shown only diagrammatically since their construction is well-known. Vehicle 22 runs on track 11 and conductor 14 is on the right side of the track. An extensible arm 23 has a traveler 24 mounted thereon for obtaining power from the conductor. Arm 23 is mounted on top of the vehicle on standoff insulators 25, only one of which appears in this view, and is pivotally mounted for movement about an axis 26 extending longitudinally of the vehicle. Thus the arm 23 and traveler 24 can swing angularly over the vehicle to the opposite side thereof. This is indicated for vehicle 22′ on track 10 in FIG. 2. Further details will be described later.

In FIG. 1 it is assumed that the spacing of tracks 10 and 11 is sufficient to allow the erection of poles 12 therebetween. If not, two lines of poles could be erected on the outside of the tracks, each line supporting an individual conductor alongside the respective track. Due to the alongside location, relatively simple support means suffices, as will be apparent from FIG. 3, rather than the elaborate support structure commonly employed when the conductor is positioned centrally over the track.

Inasmuch as the arm 23 can move angularly about axis 26, and is extensible, the traveler can move up and down, and in and out, while maintaining engagement with the conductor. Some sagging of the conductor between successive support poles 12 is believed allowable, so that high mechanical tension in the conductor and lengthwise supporting cables between poles are believed to be unnecessary. However, additional support between poles may be employed if desired, but in general may be less elaborate and expensive than for centrally located overhead conductors.

The height of the poles 12 may be selected as desired, taking into account public safety, etc. A height such that the extensible arm 23 is generally horizontal is preferred, but greater heights may be employed if desired. In FIG. 2 the arms 23, 23′ are shown somewhat above the horizontal at pole 12, so that they will be approximately horizontal midway between poles at the low point of conductor sag. Accordingly, clamps such as shown in FIGS. 4 and 4*a* are angled slightly downward in FIG. 3 so that the conductor is supported radially outward of the arm and traveler. For greater pole heights, greater clamp angles may be employed.

Depending on the normal height of the alongside conductor, at road crossings it may be necessary to increase the height to allow adequate clearance for road vehicles. Although this may be accomplished while preserving the alongside location and supporting the conductor at an angle as described above, it may require undue extension of the arm or an arm of greater length. These disadvantages may be avoided by bringing the conductor to a central position over the track so that the arm swings upward to a vertical position over the vehicle.

Referring to FIG. 5, highway 31 is shown crossing the tracks 10, 11. Poles 12 support conductors 13, 14 alongside the tracks as in FIG. 1. As the tracks approach highway 31, overhead conductors 13, 14 gradually move outward and upward so that they move across respective tracks to positions centrally of the tracks and at a higher level to provide the desired clearance. Pairs of poles 32, 33 taller than poles 12, have respective insulated supporting cables 34, 35 extending across the tracks and conductor sections 13′, 14′ are supported therefrom by suitable clamps.

FIG. 6 shows one form of clamp which may be used. A twisted bar 36 has jaws 39 gripping support cable 34, and jaws 40 gripping the ridge 18 of conductor 14. It will be noted that, with the conductor over the middle of the track, ridge 18 is on top rather than on the side as in FIG. 4 for the alongside location, so that the support means does not interfere with passage of the traveler thereby.

If the conductors need support between a pole 12 and poles 32, one or more additional sets of poles may be employed. Thus in FIG. 5 poles 37 are midway between a pole 12 and poles 32, and have an intermediate height. Supporting cable 38 has clamps supporting the overhead conductors laterally intermediate their alongside location at pole 12 and their central location at poles 32. At poles 37, the clamps are arranged at an angle so as to support the conductor on the side thereof away from the traveler and extensible arm of the vehicle. Thus clamp 40 is turned as shown in FIG. 6*a* so that conductor 14 is supported on the outside at approximately 45°. For conductor 13 at poles 37, the clamp

would be turned to approximately 45° in the opposite direction.

In operation, as a vehicle approaches pole **12** its arm and traveler will extend laterally to engage the alongside conductor, as shown in FIG. **2.** Between pole **12** and poles **37** the traveler will gradually move upwards and inwards of the vehicle until the arm **23** is about 45° above the horizontal. Between poles **37** and **32** the traveler will continue to rise and move over to the center of the vehicle, so that the arm **23** will be vertical. After passing poles **33** the arm and traveler will move gradually back to their original position. Intermediate poles and supports **37, 38** may be used between poles **33** and the following pole **12** if required.

Referring to FIG. **7,** a switching location is shown. Here track **41** is assumed to continue straight ahead while track **42** turns off to a branch line or siding, etc. Conventional track switches are employed, but are not shown in detail to avoid unnecessary complexity. Elevated conductor **43** is initially supported alongside the track **41,** and starts moving upwards and across the track as it approaches the switch point until, at point **44,** it is centrally located over the track. The conductor is supported at this point as indicated in FIG. **6.** Conductor **43** continues across track **41** until it reaches a conductor frog **45.** Advantageously conductor frog **45** is located somewhat beyond the track switching point and intermediate the centers of the tracks, so as to accentuate the pull on the traveler and traveler arm and guide the traveler to the proper outlet leg of the frog depending on whether the vehicle continues on main line **41** or turns onto branch line **42.**

At the outlet legs of frog **45,** conductor **43** branches to two conductors **43'** and **43''.** The conductors may be led to either side of the respective tracks as desired. As here shown, conductor **43'** moves back across main track **41** to a central position at **46,** and thereafter to an alongside position at the left of the track corresponding to its initial alongside position. Conductor **43''** is led back to a central position **47** over the branch track **42,** and thence downward and alongside the right side of the track.

FIG. **8** illustrates a suitable construction for frog **45.** At the entering leg or throat **48,** the conductor **43** is supported from the top, as indicated in FIG. **9***a*, and the frame **49** of the frog has two angled guide channels **51,52** corresponding to the angles of the traveler **24** when the vehicle is moving down respective tracks. FIG. **9***a* and FIG. **10** show the traveler being on the left side of the vehicle and at a raised level, hence entering guide channel **52.** For a vehicle continuing down the main track **41,** the traveler will be on its right side and inclined oppositely to that shown, thus entering guide channel **51.**

In outlet legs **53** and **54,** conductors **43'** and **43''** are mounted from overhead positions, and the angled guide channels **51,52** of FIG. **9***a* separate into correspondingly angled channels **51'** and **52'** as shown in FIG. **9.** For a vehicle traveling down the branch line **42,** the traveler will leave the frog along outlet channel **52'** as shown in FIG. **9.** If the vehicle continues on the main line **41,** with its traveler on the right side when it reaches frog **45,** it will leave through channel **51'** in the outlet leg **53.**

If desired, conductor switching frogs can be employed in which runners are mechanically switched from one position to the other automatically as the track is switched, in a manner known in the art. In such case the conductor switching frog may be located overhead at a suitable position with respect to the track switch.

FIG. **11** illustrates a railroad crossing which, although not common, may sometimes occur. Here tracks **61** and **62** cross each other with suitable crossing construction, not shown in detail to avoid unnecessary complexity. At locations remote from the crossing, conductors **63, 64** are supported alongside the respective tracks as previously described. At the crossing the conductors are raised and suspended centrally over the respective tracks at points **65, 65'** and **66, 66'** in a manner similar to that described for FIG. **5,** with clamps as shown in FIG. **6.** Additional support poles between alongside and central positions may be employed if desired, as previously described. At the junction a four-legged frog **66** is employed, and a bottom view thereof is shown in FIG. **12.** Conductors **63** and **64** are supported from the top by the frame of the frog and each leg is provided with a guide channel similar to one of the channels in FIG. **9,** except horizontally disposed.

FIGS. **13–15,** inclusive, illustrate an articulated arm suitable for mounting the traveler on the vehicle, and FIGS. **16–21** illustrate details thereof.

Referring to FIG. **13,** the articulated arm comprises two jointed sections **71,72,** each comprising a pair of spaced parallel rods **73,74** with respective end joining members **75,76** and a common mid joining member **77,** forming two parallelogram sections. The ends of the rods are pivoted for movement in the plane of the parallelogram sections, thus allowing movement of the end joining member **76** toward and away from member **75,** as indicated by arrows **78, 78'.** Such movement will be accompanied by movement of the mid joining member **77** longitudinally of vehicle **22** as indicated by arrows **79, 79'.** Joining member **75** is mounted on standoff insulators **25,** and is pivoted for movement about axis **26** extending longitudinally of the vehicle. The traveler **24** is mounted on the outer joining member **76,** which remains parallel to axis **26** as it moves toward or away from the axis or swings thereabout.

In FIG. **13** the traveler **24** and articulated arm are shown in an overhead central position with respect to the vehicle **22,** and it will be apparent that the traveler can move up and down to accommodate different vertical heights of the power conductor **13,** while remaining in engagement therewith.

FIG. **14** shows conductor **13** mounted alongside the track, with the articulated arm extending laterally of the vehicle. Due to the articulation described above, traveler **24** can follow lateral and vertical excursions of conductor **13** while remaining in engagement therewith.

FIG. **15** shows several positions of the traveler and articulated arm as viewed from the end of the vehicle. As will be apparent, the traveler **24** can move from one side of the vehicle through a central position to the other side of the vehicle, the articulated arm bending as required to allow the traveler to maintain engagement with the power conductor **13.** It will also be noted that the orientation of the traveler with respect to a radius to the axis of rotation **26** of the arm remains the same as the traveler and arm move to various angular positions about axis **26.**

In FIGS. **13** and **14,** the arm sections are shown in a bent knee configuration, and it is particularly contem-

plated that the vehicle will be moving toward the right, with the knee pointing of the direction of movement. However, movement of the vehicle in the opposite direction is possible, as indicated by the double-headed arrow **80.** It is preferred to select the length of the arm sections and the spacing of the conductor **13** from the axis of rotation **26** so that the bent knee configuration is maintained during normal operation.

Referring to FIGS. **16** and **17,** parallel rods **73** are pivoted to the inner joining member **75** at **81, 81'** and to the mid joining member **77** at **82, 82'.** Rods **74** also are pivoted to the mid joining member **77** at **82, 82'** and to the outer joining member **76** at **83, 83'.** Inner joining member **75** is pivoted on a longitudinally extending bearing **84** mounted on standoff insulators **25.** A shaft **85** is mounted in a central enlargement **86** of the outer joining member **76,** and supports the traveler **24.** Bonding wires **87** may be used to assure good electrical conductivity from the traveler to the inner joining member **75,** and power may be delivered from member **75** to the vehicle in any suitable manner.

Referring to FIGS. **16–21,** inclusive, details of the traveler **24** are shown. Pivotally mounted on shaft **85** are a pair of crossed arms **88** and **89,** each carrying a pair of grooved wheels **91, 91'** and **92, 92'** rotatably mounted at the ends thereof. Tension devices **93, 93'** attached to the ends of arms **88, 89** bias the wheels against power conductor **13** so as to produce a contact pressure which serves to hold the traveler in engagement with the conductor and establish good electrical contact. Tension devices **93, 93'** may be spring or hydraulic operated, etc.

With the pairs of wheels **91, 92** and **91', 92'** spaced longitudinally of the conductor, the traveler will be guided longitudinally by the conductor, so that it will follow lateral and vertical changes in the position of the conductor, as described in previous figures. Also, with the plane of the wheels perpendicular to the plane of the arm assembly, and hence perpendicular to the radius to the axis of rotation **26,** the traveler can follow changes in position of the conductor in either direction of movement of the vehicle along the track.

If greater electrical contact area is required, sliding contact shoes **94, 95** may be employed. These are mounted on a frame **96** attached to shaft **85** and spring-pressed against conductor **13** by suitable means (not shown).

With the power conductor supported in the simple manner described hereinbefore, without high mechanical tension, the traveler may force or "milk" the slack in the conductor toward the forward end of a span, particularly at high speeds. If this becomes troublesome, one or more small motors may be used to drive one or more of the contact wheels, preferably synchronized with the speed of the vehicle, so as to reduce the drag of the traveler on the conductor.

To avoid excessive looseness in the articulated arm, and facilitate passing a switching point as described for FIG. **7,** resilient biasing may be employed at the knee of the arm to urge it to the bent position, or friction bearings may be employed, etc., so as to impose a moderate degree of restraint to the arm movements.

Instead of using a single articulated arm as described hereinbefore, a double articulated arm may be employed to provide additional stability if required. Thus, in FIG. **13,** a second articulated arm with its knee extending toward the left may be added, end joining members **75** and **76** being common to both arms.

The invention has been described in connection with specific embodiments thereof. It will be understood that many changes in detail are possible within the spirit and scope of the invention.

I claim:

1. In an electric railroad system, the combination which comprises

a. an elevated conductor having sections mounted alongside a track and sections extending over the track and thence alongside the track,

b. and an electrically-powered vehicle adapted to run on said track and having an overhead traveler mounted on an extensible arm for obtaining power from said elevated conductor,

c. said extensible arm being pivotally mounted on top of said vehicle for movement about an axis of rotation extending longitudinally of the vehicle,

d. said traveler including means for engaging said conductor and holding the traveler in guided relationship with the conductor,

e. said extensible arm being adapted for movement of said traveler toward and away from the axis of rotation of the arm,

f. whereby said traveler can move to either side of the vehicle and to a central position to follow changes in position of said elevated conductor while remaining in engagement therewith.

2. Apparatus in accordance with claim **1** in which said sections of the conductor extending over the track rise to a higher level than the alongside level of the conductor.

3. Apparatus in accordance with claim **1** in which said traveler includes grooved means for engaging said conductor on opposite sides thereof and means for resiliently biasing the grooved means against the conductor.

4. Apparatus in accordance with claim **1** in which said traveler includes pairs of longitudinally spaced grooved wheels for engaging said conductor on respectively opposite sides thereof and means for resiliently biasing said wheels toward the conductor to maintain the traveler in guided relationship with the conductor.

5. Apparatus in accordance with claim **1** in which said traveler and arm are designed and adapted to maintain substantially the same orientation of the traveler with respect to a radius to said axis of rotation of the arm as the traveler moves between side and central positions of the vehicle and toward and away from said axis of rotation.

6. Apparatus in accordance with claim **5** in which said traveler includes grooved means for engaging said conductor on opposite sides thereof in a plane substantially perpendicular to a radius to said axis of rotation of the arm, and means for resiliently biasing the grooved means against the conductor.

7. Apparatus in accordance with claim **6** in which supports for said elevated conductor are attached thereto on the side thereof away from said traveler and arm in alongside and central positions of the conductor and in positions therebetween.

8. Apparatus in accordance with claim **6** in which said railroad system includes a track switching point for switching vehicles from one track to another, a conductor frog mounted beyond said track switching point in-

termediate the centers of said tracks, said frog having a pair of guide channels at respective angles from the horizontal corresponding to the traveler angles of vehicles traveling down respective tracks.

9. In an electric railroad system, the combination which comprises

a. an elevated conductor having sections mounted alongside a track and sections extending over the track and thence alongside the track,

b. and an electrically-powered vehicle adapted to run on said track and having an overhead traveler mounted on an articulated arm for obtaining power from said elevated conductor,

c. said traveler having grooved means for engaging said conductor on respectively opposite sides thereof and resiliently biased toward the conductor to maintain the traveler in guided relationship with the conductor,

d. said articulated arm being pivotally mounted on top of said vehicle about an axis of rotation extending longitudinally of the vehicle for angular movement between either side of the vehicle and a central position over the vehicle,

e. said articulated arm having at least two jointed sections allowing movement of said traveler toward and away from the axis of rotation of the arm and designed and adapted to maintain substantially the same orientation of the traveler with respect to a radius to the axis of rotation as the traveler moves between side and central positions of the vehicle and toward and away from the axis of rotation to follow changes in position of said elevated conductor while remaining in engagement therewith.

10. Apparatus in accordance with claim **9** in which the grooved means of said traveler comprises pairs of longitudinally spaced grooved wheels for engaging opposite sides of the conductor, the plane of said wheels being substantially perpendicular to a radius to said axis of rotation of the arm.

11. Apparatus in accordance with claim **10** in which said jointed sections of the articulated arm each comprise a pair of spaced parallel rods with respective end joining members and a common mid joining member forming two parallelogram sections, said rods being pivoted to said joining members for movement in the plane of said parallelogram sections, said traveler being mounted on one of said end joining members and the other end joining member being pivotally mounted on top of said vehicle about said axis of rotation of the arm, the length of said sections and the spacing of said elevated conductor from said axis of rotation being predetermined to maintain said sections in a bent knee configuration during normal operation.

12. Apparatus in accordance with claim **10** in which supports for said conductor are attached thereto on the side thereof away from said traveler and articulated arm in alongside and central positions of the conductor and in positions therebetween.

* * * * *

APPENDIX B

LITERATURE SEARCH LIST

Article Name - Authors - Date - Source

1. The Electrification of the Puget Sound Line of the Chicago, Milwaukee & St. Paul Railway, A. H. Armstrong, January, 1915, General Electric.

2. Overhead Wiring System for High Speed Operation, Ikuro Kumezawa, June, 1962, Railway Technical Research Insititute.

3. An Experimental Study of the Overhead Contact System for Electric Traction at 25kV, R. G. Sell, G. E. Princet, and D. Twine, 1964-65, Proc. Instn. Mech. Engrs.

4. The Application of an Analogue Computer to a Problem of Pantograph and Overhead Line Dynamics, R. B. Morris, 1964-65, Proc. Instn. Mech. Engrs.

5. Calculating the Behavior of an Overhead Catenary System for Railway Electrification, H. I. Andrews, 1964-65, Proc. Instn. Mech. Engrs.

6. Pantograph Motion on a Nearly Uniform Railway Overhead Line, G. Gilbert, and H.E.H. Davies, March, 1966, Proc. IEE.

7. British Railways Research on Current Collection, R. G. Sell, April, 1966, The Railway Gazette.

8. Overhead Line Equipment for Electric Railways, G. W. Wallace, October, 1966, The Railway Gazette.

9. Overhead Wire Structure for Superspeed Train Operation, Ikuro Kumezawa, 1966, RTRI.

10. Effect of Design Changes in Railway Catenary-Pantograph Systems on Power Collection at High Speed, R. T. Gray, S. Levy, J. A. Bain and E. J. Leclerc, March 27-28, 1968, ASME-IEEE.

11. Railway Overhead Contact Systems, Catenary-Pantograph Dynamics for Power Collection at High Speeds, S. Levy, J. A. Bain and E. J. Leclerc, March 27-28, 1968, ASME-IEEE.

12. Trolley Wire Overhead for Main Line Railways, A. Tustin and R. Broomfield, March 7, 1969, The Railway Gazette.

13. Current Collection at 200 KM/H, April, 1969, The Railway Gazette.

14. Single-wire Railway Overhead System, P. M. Caine, and P. R. Scott, July, 1969, Proc. IEE.

15. Power Collection Catenary/Pantograph Dynamics, September, 1969, U. S. Dept. of Transportation.

16. The Dynamic Behaviour of Overhead Catenary Wire Systems, Kelich Tsuchiya, 1969, RTRI.

17. Wear in High Speed Pantograph Current Collection, Masaru Iwase, and Kazuo Yokoi, 1969, RTRI.

18. Catenary Systems for High Voltage A-C Railroad Electrificatin, A. D. Suddards, T. H. Rosbotham, and T. B. Bamford, April 7-8, 1970, ASME-IEEE.

19. Dynamic-model Studies of Overhead Equipment for Electric Railway Traction, T. A. Willetis, A. D. Suddards, September, 1970, IEE Proceedings.

20. Numerical Method for Calculating the Dynamic behaviour of a Trolley Wire Overhead Contact System for Elecric Railways, M. R. Abbott, November, 1970, The Computer Journal.

21. British Railways' Experience with Pantographs for High-Speed Running, K. Taylor, August, 1971, Journal of the I. Mech. E. Railway Division.

22. Development of Overhead Equipment for British Railways 50 Hz A.C. Electrification Since 1960, A. G. Goldring and A. D. Suddards, August, 1971, Proc. IEE.

23. A survey of Western European A.C. Electrified Railway Supply Substation and Catenary System Techniques and Standards, Blair A. Ross, Sept./Oct., 1971, IEEE Transactions on Industry and General Applications.

24. The Development of the Pantograph for High-Speed Collection, D.J.W. Souch, October, 1971, Journal of the L. Mech. E. Railway Division.

25. The Analysis of the Overhead Contact System by Digital Computer Simulation, Katsushi Manabe, Hiromu Arimoto, 1971, RTRI.

26. Catenary for Today's Electric Railroads--Recent Developments in the Design of Overhead Equipment, A. D. Suddards, 1971, Railway Management Review.

27. Trolley-Wire Overhead Appears on an SNCF Main Line, October, 1971, Railway Gazette International.

28. The Development and Future Trends of the Underground Electric Trolley Locomotive Systems, S. Gilbert, 1972, December Mining Technology.

29. Recent Developments in the Design of Overhead Equipment, A. D. Suddards, 1972, Elektrische Bahnen.

30. Waves in the Periodic Overhead-Conductor Systems of Electrified Railways, A. J. Reynolds and P.G.A. Crick, July, 1973, Proc. IEE.

31. SNCF Applies Trolley-Wire Overhead to 130 km/h Electrified Lines, July, 1973, Rail Engineering International.

32. Performance Tests of Heavy Simple Catenary System, Takashi Ouchi, Kenji Horiki, Hikoshiro Furukawa, 1973, RTRI.

33. Computer Evaluation of Overhead Equipment for Electric Railroad Traction, Peter R. Scott and Maurice Rothman, September/October, 1974, IEEE Transactions on Industry Applications.

34. On Wave Solutions in Overhead Wire Dynamics, E. N. Fox, 1976, Int. J. Mech. Sci.

35. New Developments in Understanding the Dynamics of Overhead Current Collection Equipment for Electric Railways, A.E.W. Hobbs, R. Illingworth and A. J. Peters, February, 1977, Closed Loop.

36. Accurate Prediction of Overhead Line Behaviour, A.E.W. Hobbs, September, 1977, Railway Gazette International.

37. A Study of Pantograph for High-Speed Running, Tetsuo Shimomae, Masami Aihara, 1977, RTRI.

38. A Study of the Motion of Overhead Contact Wire at Crossing, Takeshi Yoshizawa, 1977, RTRI.

39. Simulation of Overhead Contact Wire and Pantograph as a System, Tsutomu Sakaguchi, 1978, Japanese Railway Engineering.

40. Beitrag Zur Quantitativen Beschreibung des Dynamischen Verhaltens von Fahrleitungssystemen, January, Carl Bopp, January, 1981, Hestra-Verlag-Darmstadt.

41. A Review of Some Recent Articles on Railroad Catenaries and Pantographs, Robert Wagner, January 30, 1981, U. S. Dept. of Transportation, Federal Railroad Administration.

42. The Planning of Research and Development of Electrical Traction for Railroads in the Light of the Energy Shortage, Mathew Guarino, Jr., April, 1981, Federal Railroad Administration.

43. Catenary Tension and High Speed Power Collection, Michel A. Thomet, Bechtel, Incorporated.

44. Hard Alloy Aluminum in Contact Wires - An Engineering Feasibility Study, L. E. Carlson and G. E. Griggs, April, 1981, IEEE/ASME.

APPENDIX C

DEVELOPMENT OF ARM LENGTH FOR TRAVELLER ARM ASSEMBLY

This study is made to determine a reasonable length of a traveller arm connecting the wheel assembly current collector to the rail vehicle. The contact conductor is assumed to be (1) beside the track at a height required for 25kV to 50kV line-to-ground voltage, (2) supported by a horizontal post insulator mounted directly on a vertical pole, and (3) approximately horizontal from the low point of sag to the arm mounting on the vehicle.

Vertical Height of Contact Conductor

The National Electrical Safety Code (ANSI C2-1981) table 232-1 lists Minimum Vertical Clearance of Wires, Conductor and Cables Above Ground, Rails, or Water. For "Item 5. Spaces or ways accessible to pedestrians only" which may be reasonable for private right-of-way, 5.4 m (18 ft) clearance is listed. For our calculations this value is used at 65.5 C (150 F) conductor sag conditions for the height above rails. We used a conservatively high temperature since the 61 m (200 ft) span length is greater than the 175 ft length listed in the code. It is recognized that for road crossings, clearance normally is increased to 6.1 m (20 ft). Also it is recognized that the ground level, directly under the side mounted contact conductor, may be somewhat lower than the rails because of rail and ballast height. However, this space between pole and rail may be used by maintenance vehicles. Therefore, the 5.4 m (18 ft) clearance above rails seems reasonable for private right-of-way.

Horizontal Clearance - Pole to Track

Rules have been developed over the years to cover such eventualities as clearance for brakeman riding at the side of cars and needs of maintenance crews. These rules vary from state to state and many exceptions are granted; for example, bridges and underpasses already in existence may have reduced clearance. Track arrangement in multitrack territory or industrial sidings also may have limited clearance to poles.

Our calculations are based on typical practice for new construction in the United States which is 3.2 m (126 in.) from centerline of track to inside of pole. This is slightly greater than most state requirements and will allow maintenance vehicles to pass between rail and pole. Added clearance for curves and for super-elevation of track also is provided.

Clearance Allowances

The clearances are developed for tangent track, (Figure C-1), and for track having a three degree curve (Figure C-2). For the tangent track allowances, lateral displacements are based on values for multiple unit (MU) cars in accordance with American Railway Engineering Association (AREA) Manual for Railway Engineering Chapter 33, page 33-2-7. Wind blow out of the contact conductor is based on 61 m (200 ft) spans, 15.9 mm (0.625 in.) in diameter solid hard drawn copper conductor, sag at 65.5 C (150 F), wind velocity pressure of 383 Pa (8 lb/ft^2) and fixed support of wire at insulators. Pole rake is 102 mm (4 in.).

For curved track similar allowances are included except no pole rake. The contact conductor is placed inside the curve so that the conductor chord will be away from the track. Actual values are calculated for a three degree curve and 127 mm (5 in.) super-elevation for car body tilt and overhang.

The following summarizes these calculations. The greatest lateral dimension for the arm is 3923 mm (154.45 in.) for the three degree curve. If an allowance of about 330 mm (13 in.) is granted for construction tolerance and height variations, then a maximum lateral arm dimension of 4270 mm (14 ft) is reasonable.

Vehicle and Track Tolerances. (reference: AREA Manual for Railway Engineering, Chapter 33, Part 2-1978, p.33-2-7, Chart 1A - Multiple Unit Cars)

Allowance for lateral shift of track	51 mm (2 in.)
Car body roll (18 ft x sin 3°)	287 mm (11.3 in.)
Rails - 1/2 in. difference in height at 56-1/2 in. gage related to 18 ft height	48 mm (1.9 in.)

Allowance for Wind Blow Out. Assume fixed support of conductor, and temperature of 65.5 C (150 F)

Sag 955 mm (37.61 in.), 15.9 mm (0.625 in.) diameter solid Hard Drawn Copper, 61 m (200 ft) span.

Wind 383 Pa (8 lb/ft^2)

$$\text{Wind blow out} = \frac{\text{wind load x sag}}{[\text{wind load}^2 + \text{weight}^2]^{1/2}}$$

$$= \frac{(8 \times 0.625/12) \times 37.61}{[(8 \times 0.625/12)^2 + (1.18)^2]^{1/2}}$$

$$= 12.5 \text{ in. or } 318 \text{ mm}$$

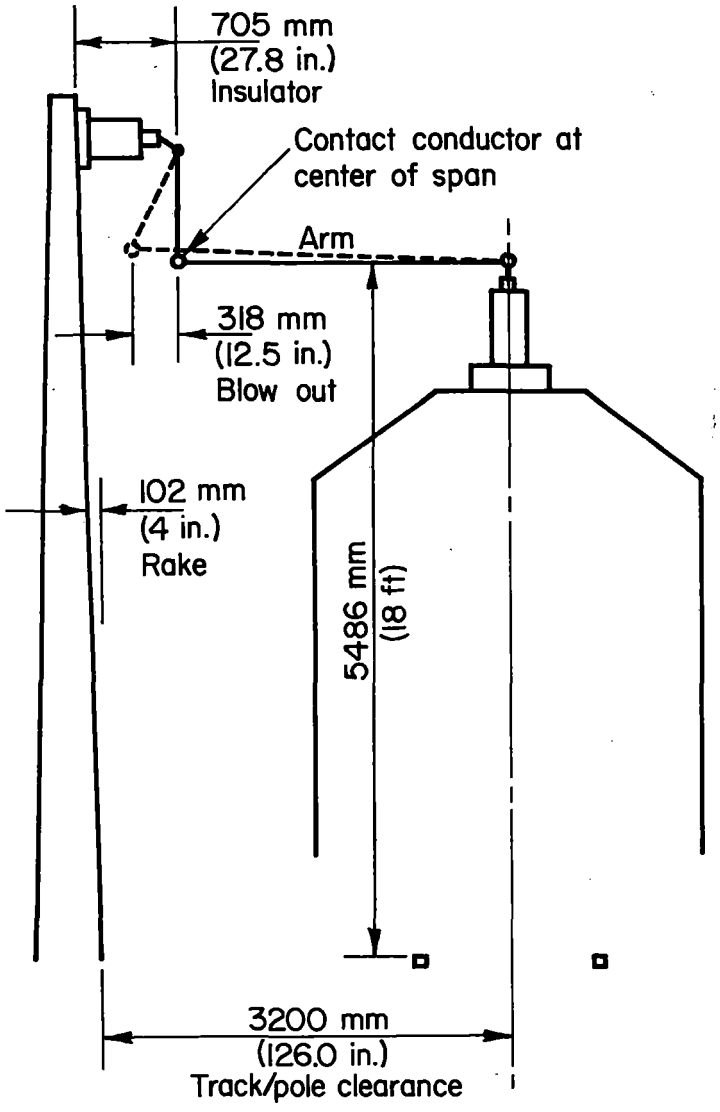

Track/pole clearance	3200 mm	(126.0 in.)
Insulator	−705 mm	(−27.8 in.)
Blow out	318 mm	(12.5 in.)
Rake	102 mm	(4.0 in.)
Lateral shift of track	51 mm	(2.0 in.)
Car body roll	287 mm	(11.3 in.)
Rail height difference	48 mm	(1.9 in.)
Arm length required	3301 mm	(129.9 in.)

FIGURE C-1. TRAVELLER ARM LENGTH REQUIREMENTS FOR TANGENT TRACK WITH 15.9 mm (0.625 in.) DIAMETER HARD DRAWN COPPER CONDUCTOR AT 65.5 ℃ (150 F), 61 m (200 ft) SPANS AND WIND VELOCITY PRESSURE OF 383 Pa (8 lb/ft^2)

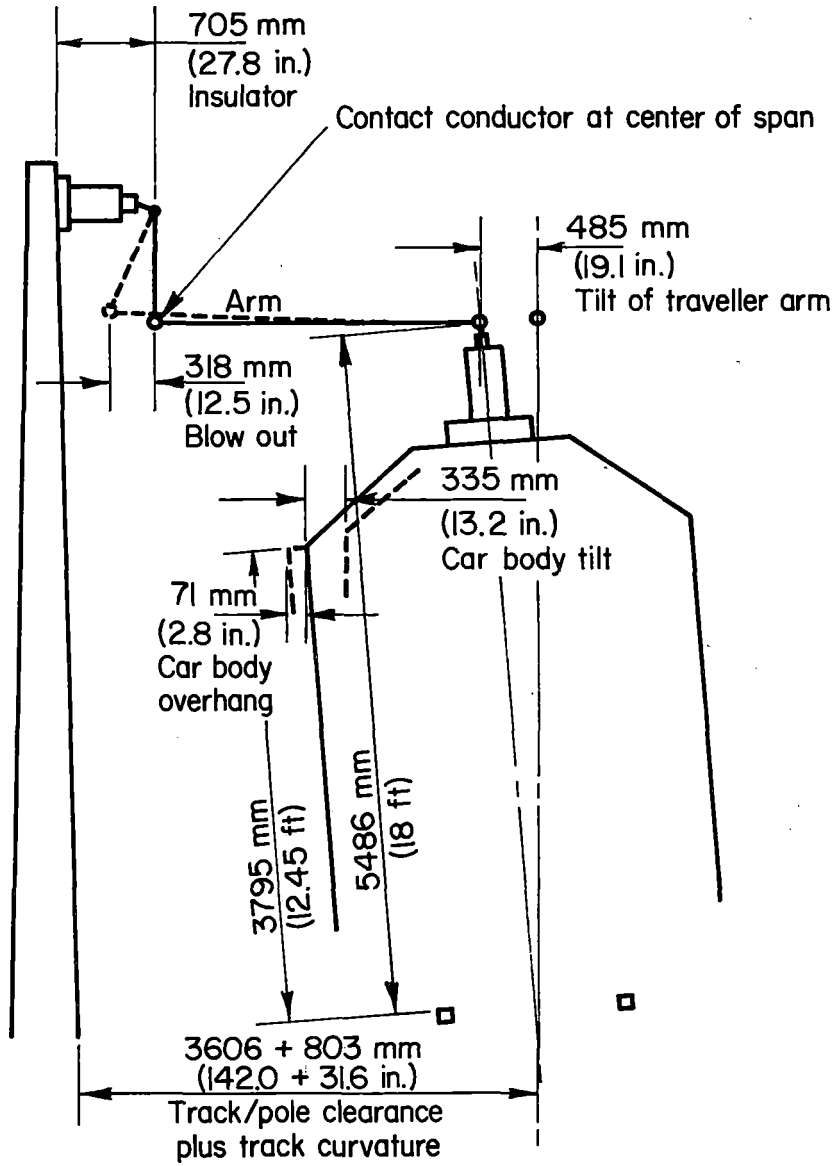

Track/pole clearance	3606 mm (142.0 in.)
Insulator	−705 mm (−27.8 in.)
Tilt of traveller arm	−485 mm (−19.1 in.)
Track curvature	803 mm (31.6 in.)
Blow out	318 mm (12.5 in.)
Lateral shift of track	51 mm (2.0 in.)
Car body roll	287 mm (11.3 in.)
Rail height difference	48 mm (1.9 in.)
Arm length required	3923 mm (154.4 in.)

Tangent pole to track ℄	3200 mm (126.0 in.)
Car body tilt	335 mm (13.2 in.)
Car body overhang	71 mm (2.8 in.)
Track/pole clearance	3606 mm (142.0 in.)

FIGURE C-2. TRAVELLER ARM LENGTH REQUIREMENTS FOR THREE DEGREE CURVE WITH 15.9 mm (0.625 in.) DIAMETER HARD DRAWN COPPER CONDUCTOR AT 65.5 C (150 F), 61 m (200 ft) SPANS AND WIND VELOCITY PRESSURE OF 383 Pa (8 lb/ft^2)

Allowance for Track Curvature (Contact conductor inside of curve)

3 degree curve, 61 m (200 ft) span
Lateral displacement = $7/8\ h^2d$
h = chains to span center (chain = 100 ft)
d = degree curvature
$= 7/8\ (1)^2\ 3$
= 2.63 ft = 31.6 in. or 803 mm

Increase in Pole to Track Clearance (for 3 degree curve)

Assume 127 mm (5 in.) super-elevation
Pole on inside of curve.

Car Body Tilt (TILT) at 3795 mm (12.45 ft) height

$$\frac{56\text{-}1/2}{5} = \frac{12.45 \times 12}{TILT}$$

TILT = 13.2 in. or 335 mm

Car Body Overhang (OH) on curve

Assume truck centers - 60 ft

$OH = 7/8\ h^2d$

$$= \frac{7}{8}\left(\frac{30}{100}\right)^2 \times 3$$

= 0.24 ft = 2.8 in. or 71 mm

Tilt of Traveller Arm (TTA) support point

$$\frac{56\text{-}1/2}{5} = \frac{18 \times 12}{TTA}$$

TTA = 19.1 in. or 485 mm

APPENDIX D

ANALYTICAL SIMULATIONS

The dynamics of the traveller/conductor system is a difficult problem to solve in its entirety. It involves the motion of the traveller mechanism (lumped masses, springs, dampers, and continuous beams), the conductor wire (a continuous catenary), and the support structure (pole, insulator, and clamp). Perhaps the most difficult area to analyze is the relative motion between the traveller mechanism and the conductor - at each instant in time the forcing function not only changes magnitude and direction, it also changes point of application. To perform the dynamic analysis of the traveller/conductor system, a multi-model approach was employed. The benefits of using several models are: simple models give general characteristics of the dynamics and help establish limits; moderately complex models include most of the details and can be used to make parametric studies important to design; and very complex models simulate the system very accurately, and can be used as a final check on the design.

The models used in this analysis include simple geometric equations, one degree of freedom exact solutions, a six degree of freedom lumped-mass computer simulation, and a finite element computer simulation.

1. Catenary Geometry

Figure D-1 shows the shape of a simple catenary. If it is assumed that the conductor is pin-attached (no moments) at the poles, it will assume the shape of a catenary whose functional relation can be expressed as

$$y = a\left[\cosh\left(\frac{x}{a}\right) - 1\right], \qquad \text{(D-1)}$$

where

$a = 4T/\rho\pi d^2$

T = tension in wire

ρ = weight density

d = diameter of catenary.

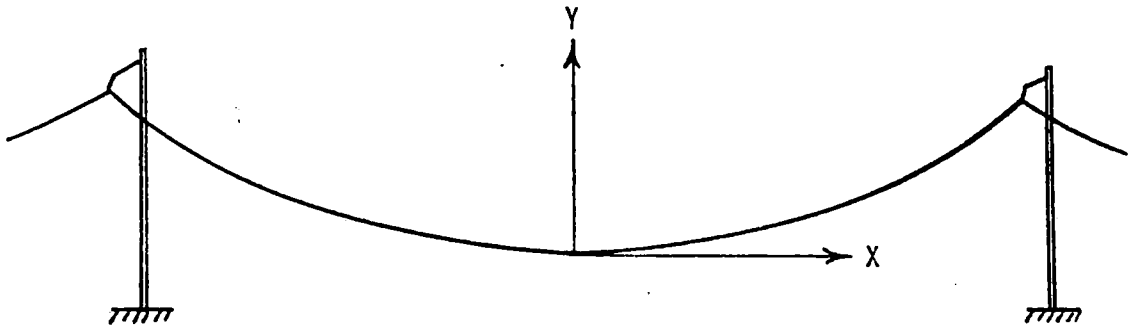

FIGURE D-1. GEOMETRY OF SIMPLE CATENARY

For small values of x/a, cosh (x/a) can be approximated very accurately by the first two terms in its power series expansion. Equation (D-1) then simplifies to

$$y = x^2/2a. \qquad \text{(D-2)}$$

The slope of the catenary is given by the spatial derivative of Equation (D-2)

$$\frac{dy}{dx} = \frac{x}{a} . \qquad \text{(D-3)}$$

From Equation (D-3) and the definition of the variable a, it can be seen that the slope at any point on the catenary depends on tension, density, and diameter.

The vertical velocity of an object following the catenary is given by the time derivative of Equation (D-2)

$$\frac{dy}{dt} = \frac{\dot{x}x}{a} . \qquad \text{(D-4)}$$

It is the effective change in vertical velocity of the catenary shape at the pole insulator, that acts as a forcing function on any device that is attempting to follow it. Using Equation (D-4) the net change in vertical velocity at the hard point is

$$\Delta\dot{y} = \frac{2dy}{dt} = \frac{\rho\pi d^2 SV}{4T} , \qquad \text{(D-5)}$$

where

S = pole span

V = forward velocity

2. Single Degree of Freedom Simulation

To establish an upper bound for the force needed to change the direction of the traveller device, a simple mass/spring/dashpot system is considered, Figure D-2.

The equation of motion for the system in Figure D-2 is

$$\ddot{MX} + C(\dot{x}-\dot{y}) + K(x-y) = 0 \; . \qquad \text{(D-6)}$$

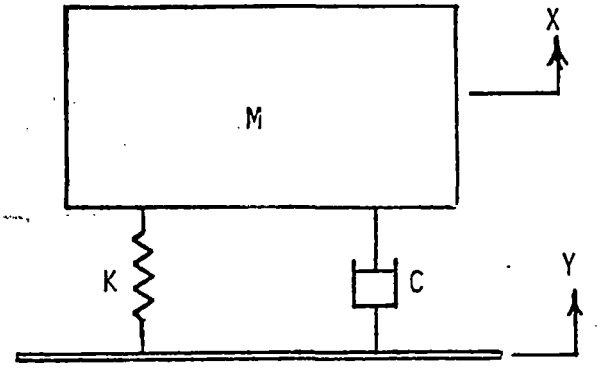

FIGURE D-2. BASE-EXCITED 1 DOF MASS/SPRING/DASHPOT MODEL

Considering the case where the support base is given an instantaneous vertical velocity as an approximation to the change in velocity experienced when the attached device traverses the hard point on the catenary [Equation (D-5)], the initial conditions are

$$x(0) = \dot{x}(0) = y(o) = 0 \; . \qquad \text{(D-7)}$$

$$\dot{y}(0) = -\Delta\dot{y} \; . \qquad \text{(D-8)}$$

If the base velocity is held constant, and a substitution of variables is made ($u = x - y$), Equation (D-6) can be rewritten as

$$\ddot{Mu} + \dot{Cu} + Ku = 0 \; . \qquad \text{(D-9)}$$

Equation (D-9) has the following general solutions:

$$u(t) = e^{-\xi\omega_d t}\left[A \sin \omega_d t + B \cos \omega_d t\right] \qquad \text{(D-10)}$$

where

$$\xi = \frac{C}{2\sqrt{KM}}$$

$$\omega_d = \omega_n \sqrt{1-\xi^2}$$

$$\omega_n = [K/M]^{\frac{1}{2}} .$$

The initial conditions from Equations (D-7) and (D-8) are

$$u(0) = 0 \qquad \text{(D-11)}$$

$$\dot{u}(0) = \Delta\dot{y} \qquad \text{(D-12)}$$

Substituting the initial conditions of Equation (D-11) and (D-12) into Equation (D-10) yields

$$B = 0 , \qquad \text{(D-13)}$$

$$A = \Delta\dot{y}/\omega_d . \qquad \text{(D-14)}$$

Therefore, the solution to Equation (D-9) is

$$u = e^{-\xi\omega_d t}\left[\frac{\Delta\dot{y}}{\omega_d} \sin \omega_d t\right] . \qquad \text{(D-15)}$$

Differentiating Equation (D-15) to find the time of maximum displacement, it was determined that

$$u(t) = u_{max} \text{ when } \omega_d t = \tan^{-1} \frac{1}{\xi} \qquad \text{(D-16)}$$

The maximum force in the stiffness element between the mass and the base is then given by

$$F = Ku_{max} = Ke^{-\xi \tan^{-1}\left(\frac{1}{\xi}\right)} \left[\frac{\dot{\Delta y}}{\omega_d} \sin\left(\tan^{-1}\left(\frac{1}{\xi}\right)\right)\right]. \qquad \text{(D-17)}$$

Rearranging Equation (D-17) gives

$$F = F_o \left[\frac{e^{-\xi \tan^{-1}\left(\frac{1}{\xi}\right)}}{(1-\xi^2)^{\frac{1}{2}}}\right] \sin\left(\tan^{-1}\left(\frac{1}{\xi}\right)\right) \qquad \text{(D-18)}$$

where

$$F_o = \dot{\Delta y}\left[\frac{KW}{g}\right]^{\frac{1}{2}} . \qquad \text{(D-19)}$$

The coefficient of F_o in Equation (D-18) is tabulated, for appropriate values of the damping ratio ξ, in Table D-1.

TABLE D-1. EVALUATION OF COEFFICIENT OF F_o IN EQUATION (D-18)

ξ	$\left[\frac{e^{-\xi \tan^{-1}\left(\frac{1}{\xi}\right)}}{(1-\xi^2)^{\frac{1}{2}}}\right] \sin\left(\tan^{-1}\left(\frac{1}{\xi}\right)\right)$
0	1.00
.05	0.93
.10	0.86
.15	0.81
.20	0.76

From Table D-1 it can be seen that even damping ratios that would be considered very high for normal materials do not reduce the maximum force significantly. Therefore, as a conservative estimate the maximum force can be taken as F_o in Equation (D-19). Substituting

Equation (D-5) into Equation (D-19) yields the maximum conservative force needed to change the direction of an object traversing the hard point of a catenary, assuming that there is a slope discontinuity in the catenary at that point.

$$F_o = \frac{\rho \pi d^2 \, SV}{4T} \left[\frac{KW}{g}\right]^{\frac{1}{2}} . \qquad \text{(D-20)}$$

Although Equation (D-20) included many of the system parameters, and was a simple expression to calculate a maximum force under severe dynamic loading conditions, it did not include several very important parameters that could reduce the force levels required. Those parameters include: wheel spacing, insulator flexibility at the hard point, a smooth conductor transition at the hard point, and the effect of providing more flexibility between components (multi-degrees of freedom).

3. Six Degree of Freedom Simulation

Equations of Motion

The six degree of freedom simulation included independent degrees of freedom for the yoke assembly (vertical and pitch), the wheel assembly (vertical and pitch), and the insulator/conductor under each wheel (vertical). A schematic of the model is shown in Figure D-3.

The equations of motion for the six degree of freedom simulation are

$$M_1\ddot{y}_1 + K_{y2}(y_1-y_2) + C_{y2}(\dot{y}_1-\dot{y}_2) = 0 \qquad \text{(D-21)}$$

$$I_1\ddot{\theta}_1 + K_{\theta 2}(\theta_1-\theta_2) + C_{\theta 2}(\dot{\theta}_1-\dot{\theta}_2) = 0 \qquad \text{(D-22)}$$

$$M_2\ddot{y}_2 + K_{y2}(y_2-y_1) + K_{y3}(2y_2-y_6-y_5) + C_{y2}(\dot{y}_2-\dot{y}_1) + C_{y3}(2\dot{y}_2-\dot{y}_6-\dot{y}_5) = 0 \qquad \text{(D-23)}$$

$$I_2\ddot{\theta}_2 + K_{\theta 2}(\theta_2-\theta_1) + K_{y3}b(2b\theta_2+y_6-y_5) + C_{\theta 2}(\dot{\theta}_2-\dot{\theta}_1) + C_{y3}b(2b\dot{\theta}_2+\dot{y}_6-\dot{y}_5) = 0 \qquad \text{(D-24)}$$

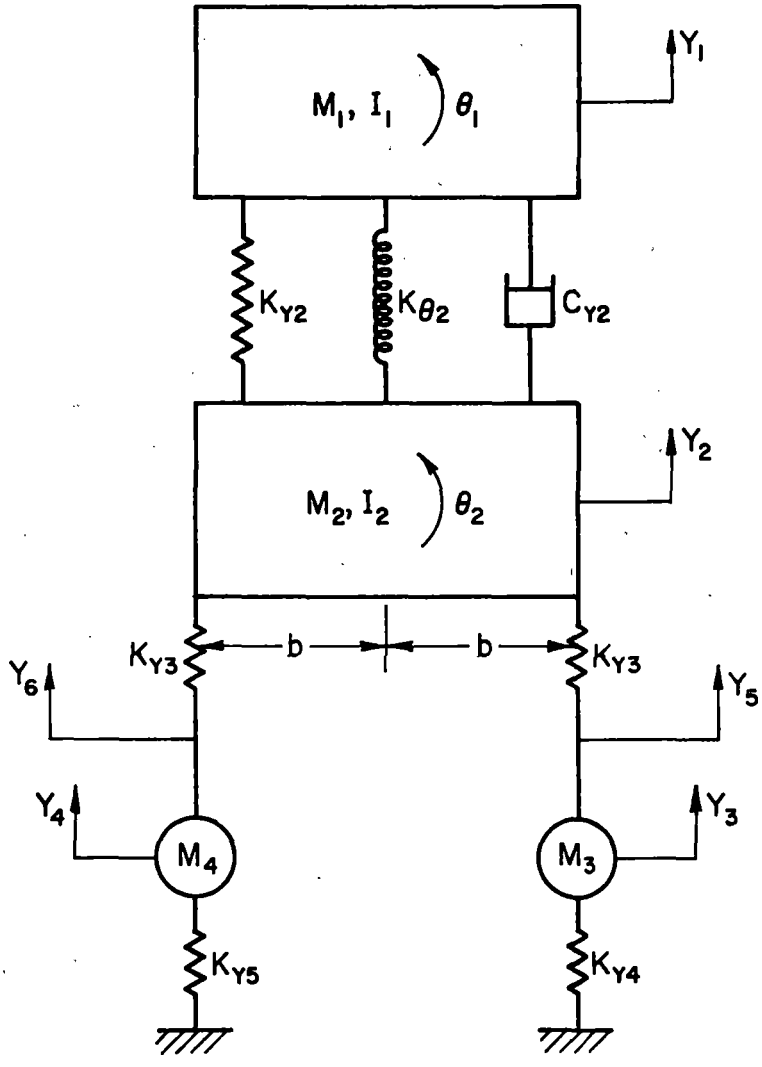

FIGURE D-3. 6-DOF MODEL FOR TRAVELLER/CONDUCTOR

$$M_3\ddot{y}_3 + K_{y3}\,(y_5 - y_2 - b\theta_2) + K_{y4}\,y_3 \qquad \text{(D-25)}$$

$$+ C_{y3}\,(\dot{y}_5 - \dot{y}_2 - b\dot{\theta}_2) + C_{y4}\,\dot{y}_3 = 0$$

$$M_4\ddot{Y}_4 + K_{y3}\,(Y_6 - Y_2 + b\theta_2) + K_{y5}\,Y_4 \qquad \text{(D-26)}$$

$$+ C_{y3}\,(\dot{Y}_6 - \dot{Y}_2 + b\dot{\theta}_2) + C_{y5}\dot{Y}_4 = 0\ .$$

The variables Y_5 and Y_6 in the above equations are the forcing functions due to the effective shape of the conductor.

Transition Geometry. A true catenary shape will have a discontinuous slope at the hard point. To provide a smooth transition at the hard point, it was assumed that the catenary shape was continuous in position and slope with a circular arc at some distance from the hard point, Figure D-4.

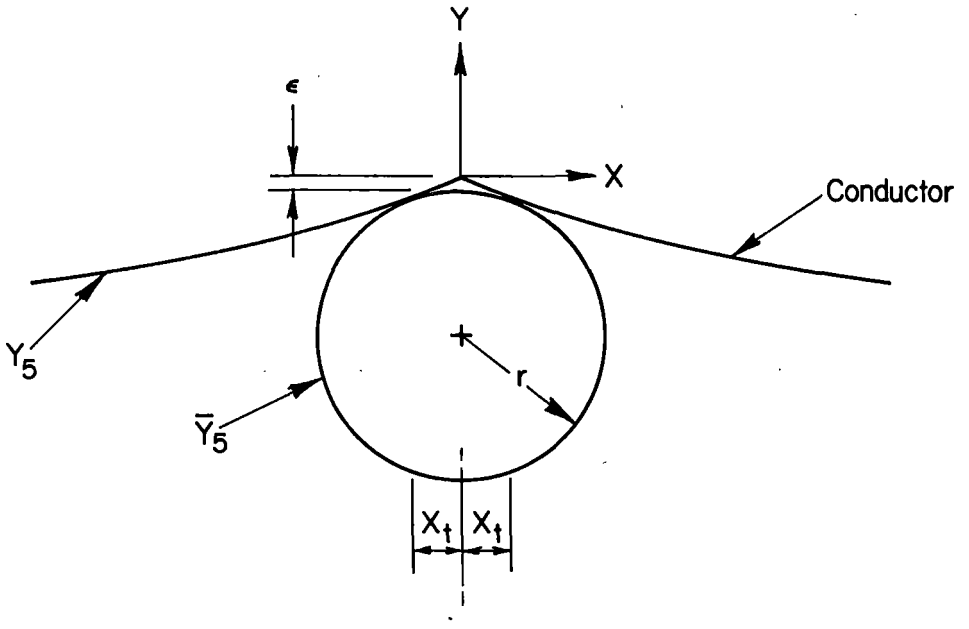

FIGURE D-4. TRANSITION GEOMETRY OF CONDUCTOR AT INSULATOR

In Figure D-1 the origin of the catenary slope was defined at the lowest point of the catenary. Transferring the origin to the hard point, the catenary equation is

$$Y_5(X) = \frac{\left(X-\frac{S}{2}\right)^2}{2a} - \frac{S^2}{8a} \qquad X \geq 0, \tag{D-27}$$

$$Y_5(X) = \frac{\left(X+\frac{S}{2}\right)^2}{2a} - \frac{S^2}{8a} \qquad X \leq 0, \tag{D-28}$$

The equation of a circle tangent to the catenary is given as

$$(\overline{Y}_5-A)^2 + (X-B)^2 = r^2 \ . \tag{D-29}$$

The boundary conditions are

$$\overline{Y}_5(0) = -\varepsilon, \ \overline{Y}_5'(0) = 0 \ . \tag{D-30}$$

Substituting Equations (D-30) into Equation (D-29) and its spatial derivative gave the final form of the circle.

$$\overline{Y}_5 = (r^2-X^2)^{\frac{1}{2}} - (r+\varepsilon) \tag{D-31}$$

To provide a smooth transition between the circular arc and the catenary, the displacement and slope were set equal at some given longitudinal distance, X_t, from the hard point. The total transition length was $2X_t$.

$$Y_5(X_t) = \overline{Y}_5(X_t) \tag{D-32}$$

$$Y_5'(X_t) = \overline{Y}_5'(X_t) \tag{D-33}$$

For X>0 Equations (D-27) and (D-31) were equated according to the boundary conditions of Equation (D-32) and (D-33). The results were the radius of curvature, r, and offset, ε.

$$r = \left[X_t^2 + \left(\frac{AX_t}{X_t - S/2} \right)^2 \right]^{\frac{1}{2}} , \tag{D-34}$$

$$\varepsilon = \frac{S^2}{8a} + (r^2 - X_t^2)^{\frac{1}{2}} - r - \frac{\left(X_t - \frac{S}{2}\right)^2}{2a} . \tag{D-35}$$

With r and ε defined, the forcing function for the circular part of the transition was available from Equation (D-31). A similar expression with a time delay due to the wheel spacing held for Y_6.

Insulator/Conductor Stiffness. The effective stiffness of the pole insulator and conductor was established by assuming that the insulator and conductor were two stiffnesses in series. The stiffness of the insulator remained constant throughout a simulation, but the conductor became more flexible at further distances from the pole. The stiffness of the conductor was approximated by assuming that it was a tensioned beam with bending stiffness, pin-supported at the pole insulators. Standard beam deflection equations were used to find its stiffness based on its deflection due to a unit load at some point away from the insulator.

At the insulator the stiffness of the conductor was infinite, so that the effective stiffness of the insulator/conductor was equal to the stiffness of the insulator. As a wheel moved beyond the insulator, the effective stiffness of the insulator/conductor decreased rapidly to the stiffness of the conductor only.

4. Lateral Forces in Curves

Track Curvature

In accordance with railroad practice, track curvature is defined as the angle subtended by a 30.48 m (100 ft) chord, Figure D-5.

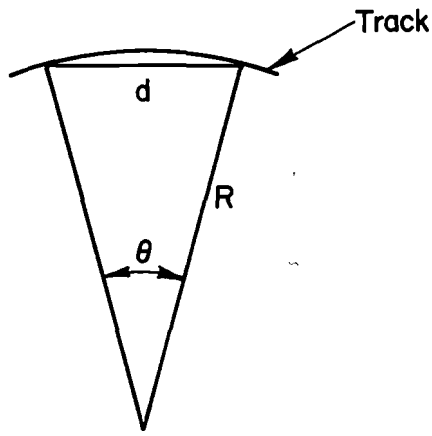

FIGURE D-5. TRACK CURVATURE DEFINITION

The degree of curvature is given by

$$\theta = 2 \sin^{-1} (d/2R) . \qquad \text{(D-36)}$$

For small angles the radius of curvature is approximated by

$$R = 57.3d/\theta , \qquad \text{(D-37)}$$

where

θ = track degree of curvature, degree

R = radius of curvature, m (ft)

d = cord length, 30.48 m (100 ft).

Conductor Lateral Angular Deflection

The lateral load on the traveller is produced by the conductor's angular change in the lateral direction at each pole. The geometry of that change is shown in Figure D-6.

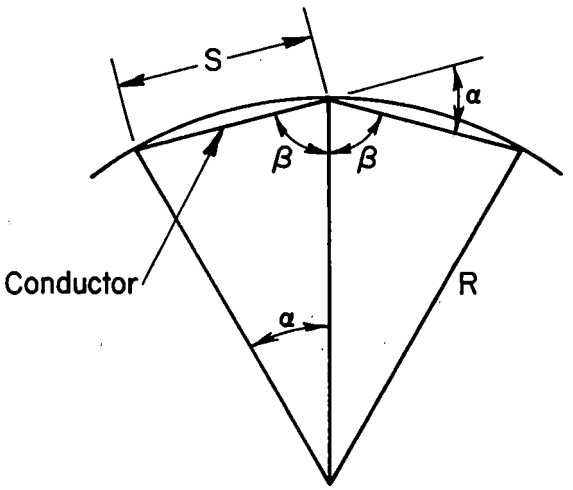

FIGURE D-6. LATERAL GEOMETRY OF CONDUCTOR FOR CURVED TRACK

The conductor's angular change in the lateral direction is given by

$$\alpha = \pi - 2\beta = \pi - 2 \cos^{-1} (S/2R), \text{ rad.} \qquad \text{(D-38)}$$

where

S = pole spacing

R = radius of curvature.

Assuming small angles of conductor deflection, α, and substituting Equation (D-37) into Equation (D-38) yields

$$\alpha = \theta S/57.3d, \text{ rad.} \qquad \text{(D-39)}$$

The change in direction at the pole is produced by a velocity change in the lateral direction given by

$$\Delta \dot{X} = V\alpha = \frac{V\theta S}{57.3d} \qquad \text{(D-40)}$$

If there is no gradual transition, the effect on the traveller due to the change in lateral velocity at the pole is similar to the change in vertical velocity at the pole, i.e., an instantaneous initial

base velocity acting on a single degree of freedom system, Figure D-2. Using the same derivation technique as illustrated in Equations (D-6) through (D-19), the maximum conservative lateral force on the traveller is given as

$$\overline{F}_o = \Delta\dot{X}\left[\frac{KW}{g}\right]^{\frac{1}{2}}$$

Substituting Equation (D-40) into Equation (D-42) gives

$$\overline{F}_o = \frac{V\theta S}{57.3d}\left[\frac{KW}{g}\right]^{\frac{1}{2}} .$$

6525

DYNAMIC ANALYSIS OF A LOW-COST CATENARY SYSTEM FOR ELECTRIC RAILROADS

George R. Doyle, Jr.
BATTELLE
Columbus Laboratories
505 King Avenue
Columbus, Ohio 43201

ABSTRACT

A simplified railroad electrification system has been suggested to reduce the construction and maintenance complexities and cost associated with the conventional collector/conductor system. The new system includes a single-conductor catenary and a collector attached to the conductor by two sets of rotating wheels. Based on experience and dynamic analyses, a preliminary design has been established. The dynamic analyses determined the mechanical loads in the system as a function of several parametric variations. This paper outlines the dynamic models, presents the parametric study, and recommends several guidelines to follow in designing the traveller/conductor system.

NOMENCLATURE

- $a = 4T/\rho\pi d^2$
- c = Damping coefficient
- d = Conductor diameter
- F = Maximum damped force between mass and base
- F_o = Maximum undamped force between mass and base
- g = Acceleration of gravity
- I = Moment of inertia
- K = Stiffness
- M = Mass
- r = Radius of circular transition
- S = Span between poles
- t = Time
- T = Conductor tension
- V = Vehicle velocity
- W = Weight of wheel or yoke assembly
- x = Longitudinal displacement
- X_t = Half transition length
- y = Vertical displacement
- $\Delta\dot{y}$ = Change in vertical velocity
- ϵ = Vertical offset of circular transition from catenary
- ζ = Damping ratio
- θ = Rotational displacement
- ρ = Conductor density
- ω_d = Damped natural frequency
- ω_n = Natural frequency

INTRODUCTION

Electrification has long been recognized as a means to supply clean energy to power the nation's railroads. The major economic drawback to electrification is the large capital investment and maintenance costs associated with the power distribution system (poles, conductor, and insulators). A simplified railway electrification system has been suggested that would substantially reduce those costs(1)*.

While the typical overhead electrification system includes poles, insulators, droppers, a catenary, and the contact conductor, the new design eliminates the droppers, and the catenary becomes the contact conductor. Because the conductor does not maintain a constant elevation above the track, a capture system is necessary to assure contact between the collector and the conductor, Figure 1.

With the incentive of large cost reductions, preliminary design, dynamic, and cost analyses were conducted to determine the feasibility of operation(2). The results of that study were a basic hardware design and estimated mechanical loads. The dynamic analyses, described herein, defined the mechanical loads and design guidelines to reduce those loads. All of the results are based on tangent track operations with no anomalies in the catenary-shaped, contact conductor. The details of the design are described in a companion paper(3).

ANALYSES

Single-Degree-of-Freedom Simulation

The traveller system consisted of a yoke assembly and a wheel assembly with two sets of flanged wheels riding on the conductor, Figure 2. The wheel assembly was attached to the yoke assembly through two yoke bushings.

* Underlined numbers in parentheses designate References at end of paper.

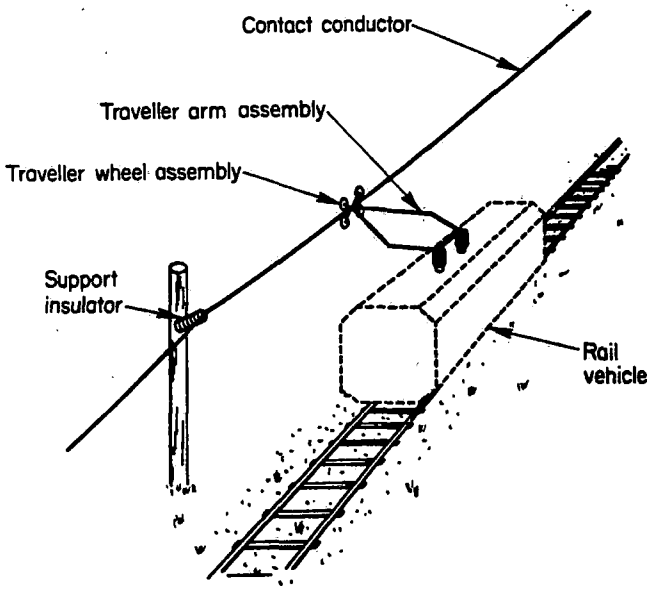

FIGURE 1. GENERAL ARRANGEMENT OF SUBASSEMBLIES FOR A LOW-COST ELECTRIFICATION SYSTEM

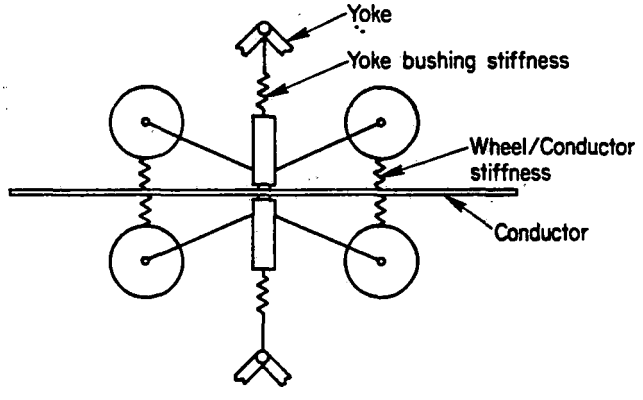

FIGURE 2. TRAVELLER/CONDUCTOR CONFIGURATION

It was recognized that the greatest potential dynamic problem would occur at the pole insulator where the traveller motion changed from its maximum upward velocity to its maximum downward velocity, Figure 3. Therefore, a worst case scenario was assumed, i.e., the traveller system experienced a step input in velocity equal to the conductor's vertical velocity change at the insulator (see Appendix). The maximum force between the traveller and conductor for a step change in velocity of a single-degree-of-freedom system (1-DOF) is given by

$$F_o = \frac{\rho\pi d^2 SV}{4T}\left[\frac{KW}{g}\right]^{1/2} \qquad (1)$$

It can be seen from Eq. (1) that the maximum force depends on seven variables. Although the derivation considered the variables ρ, d, T, and S to be independent, "real world" constraints would dictate changes in one or more of these variables if any other one was changed. The other variables V, K, W, are independent.

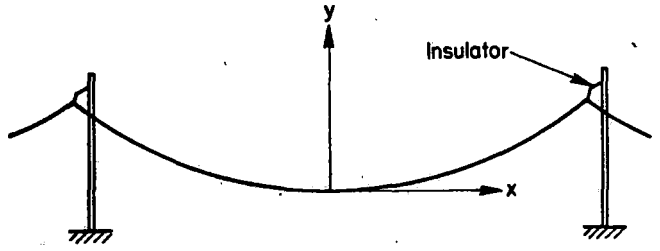

FIGURE 3. GEOMETRY OF SIMPLE CATENARY

They indicate that for a specified maximum speed of the rail vehicle: (1) the weight of the traveller system should be as light as possible, and (2) the stiffness in the traveller system should be as low as possible.

The real significance of Eq. (1) is that the term $\rho\pi d^2 S/4T$ defines the total change in slope of a simple catenary at its support, see Appendix, Eq. (A-3). Therefore, to reduce forces, the slope of the conductor should be minimized.

Although Eq. (1) was useful for indicating general trends of several parameters of the traveller/conductor system, it could not account for the effects of multi-degree-of-freedom response, wheel spacing, nonlinearities in the insulator/conductor stiffness and a more gradual change in vertical velocity at the insulator.

Six-Degree-of-Freedom Simulation

The six-degree-of-freedom simulation (6-DOF) provided an approximate model of the traveller's and insulator/conductor's vertical dynamics (Figure 4). A time-domain solution of the six differential equations of motion (given in the Appendix) was accomplished by a computer program using a 4th-order, Runge-Kutta, numerical integration technique. The excitation was the changing displacement of the conductor, which was modeled as a catenary with a circular transition at the insulator (see Appendix).

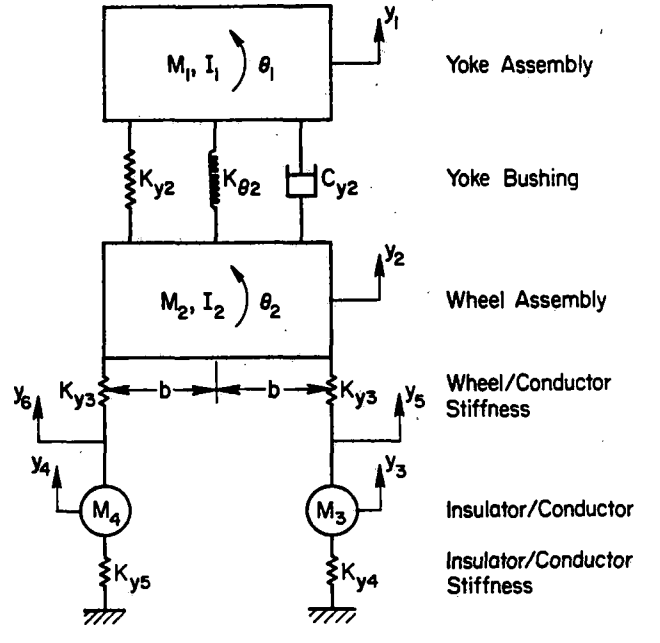

FIGURE 4. 6-DOF MODEL FOR TRAVELLER/CONDUCTOR

TABLE 1. VARIABLES FOR 6-DOF PARAMETRIC STUDY

Variable	Nominal	Minimum	Maximum
Yoke assembly weight, N (lb)	40.0 (9.00)	22.2 (5.00)	133 (30.0)
Wheel assembly weight, N (lb)	53.4 (12.0)	22.2 (5.00)	133 (30.0)
Insulator/conductor weight, N (lb)	66.7 (15.0)	22.2 (5.00)	133 (30.0)
Yoke bushing stiffness, N/mm (lb/in.)	17.5 (100)	8.75 (50.0)	70.0 (400)
Wheel/conductor stiffness, N/mm (lb/in.)	875 (5000)	175 (1000)	5250 (30,000)
Insulator stiffness, N/mm (lb/in.)	52.5 (300)	17.5 (100)	280 (1600)
Conductor diameter, mm (in.)	15.9 (0.625)	12.7 (0.50)	25.4 (1.00)
Conductor tension, N (lb)	8900 (2000)*	4450 (1000)	44,500 (10,000)
Pole Span, m (ft)	61.0 (200)	15.2 (50)	122 (400)
Wheel spacing, mm (in.)	280 (11.0)	150 (6.00)	610 (24.0)
Transition length, mm (in.)	510 (20.0)	0.00 (0.00)	1520 (60.0)
Vehicle Speed, kph (mph)	81 (50.0)	16 (10.0)	145 (90.0)
Conductor density, N/m^3 ($lb/in.^3$)	8.74×10^4 (0.322)	--not varied--	

*Assumes a maximum atmospheric temperature of 60 C (140 F).

Finite Element Simulation

The 1- and 6-DOF models discussed previously required several simplifying assumptions which did not represent the actual physical model, especially the 1-DOF model. To verify the results of the simplifying assumptions, a finite element approach was used.

The conductor geometry, including the transition, was modeled by pretensioned trusses (no bending stiffness) and with weightless beams (with bending stiffness) in the vicinity of the transition. The pole, insulators, clamp, and arms of the traveller were also modeled with beam elements. Spring and damping elements were used to model the yoke bushing, while a special follower element was used to model the wheels that contacted the conductor. The model was three dimensional, and had 303 degrees of freedom.

ANALYSES RESULTS

Parameter Definition

The major results of the dynamic analyses were provided by a parametric study using the 6-DOF time domain model. The nominal parameters and their variations are listed in Table 1.

Parametric Study

Based on the variable limits given in Table 1, a series of time domain computer runs were made with the 6-DOF model. Each run established the maximum dynamic forces in the yoke bushing, at each wheel/conductor interface, and in the insulator as the front and rear wheels passed through the transition and beyond. In all cases the dynamic forces associated with the rear wheel were somewhat greater than those associated with the front wheel. Therefore, only the maximum rear wheel dynamic forces were plotted for each independent parametric variation.

Graphical results of some of the parametric variations are not shown in this paper, but can be found in reference (2).

Effect of Yoke Assembly Weight. The effect of varying the yoke assembly weight is illustrated in Figure 5. As the yoke assembly weight increased, the maximum force in the yoke bushing increased rapidly. The maximum forces at the wheel/conductor interface and at the insulator increased somewhat, but the effect was not significant. The yoke bushing force, based on the 1-DOF model, indicated greater magnitudes, but a similar trend to the 6-DOF model.

Effect of Wheel Assembly Weight. When the wheel assembly weight was increased, Figure 6, the maximum wheel/conductor interface force increased rapidly, but the yoke bushing force actually decreased. The maximum force on the insulator also increased moderately with wheel assembly weight.

Effect of Yoke Bushing Stiffness. Figure 7 shows a slowly increasing maximum force with increasing yoke bushing stiffness. The poor comparison with the 1-DOF model was due to the nonzero transition length in the 6-DOF model.

Effect of Wheel/Conductor Stiffness. Figure 8 shows that the maximum forces developed were nearly independent of the wheel/conductor stiffness. The reason for these results was that for a large transition time, the system would respond gradually rather than undergo a large transient.

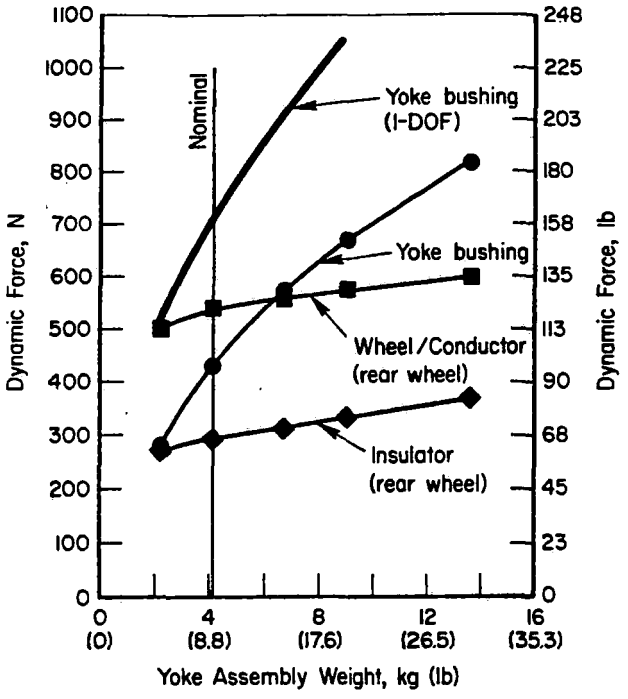

FIGURE 5. EFFECT OF YOKE ASSEMBLY WEIGHT ON YOKE BUSHING, WHEEL/CONDUCTOR, AND INSULATOR FORCES

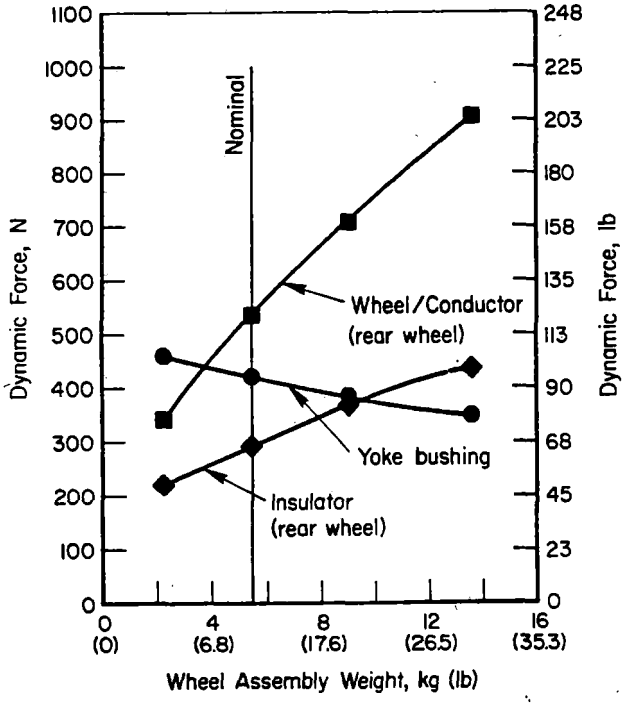

FIGURE 6. EFFECT OF WHEEL ASSEMBLY WEIGHT ON YOKE BUSHING, WHEEL/CONDUCTOR, AND INSULATOR FORCES, 1Kg = 9.8 N

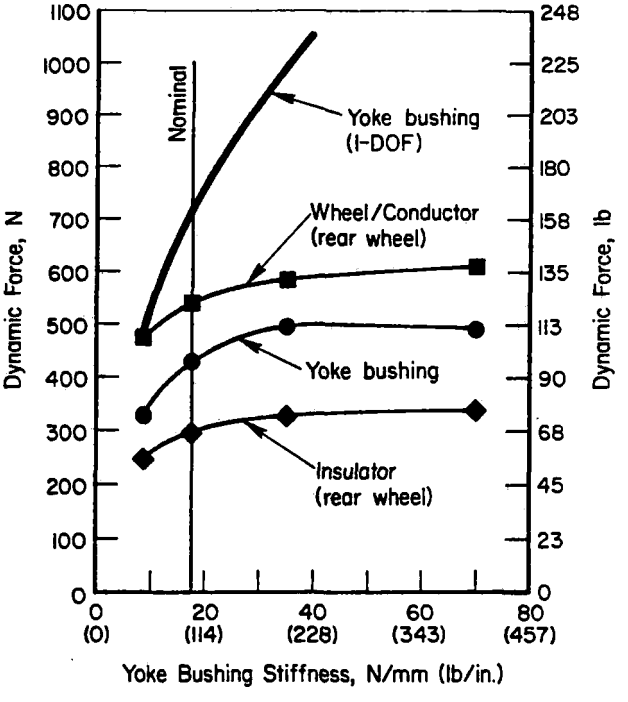

FIGURE 7. EFFECT OF YOKE BUSHING STIFFNESS ON YOKE BUSHING, WHEEL/CONDUCTOR, AND INSULATOR FORCES, 1Kg = 9.8 N

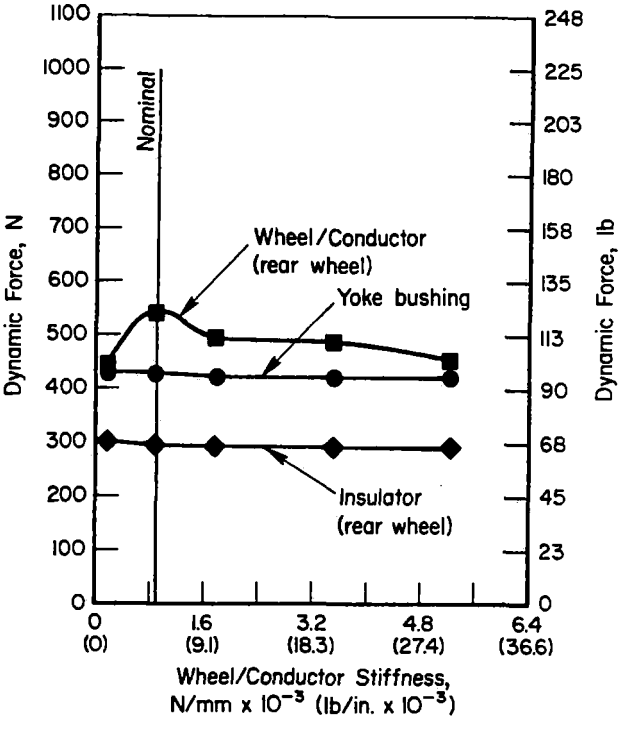

FIGURE 8. EFFECT OF WHEEL/CONDUCTOR STIFFNESS ON YOKE BUSHING, WHEEL/CONDUCTOR, AND INSULATOR FORCES

Effect of Conductor Diameter. Based on Eq. (1), the maximum force developed is proportional to the square of the conductor diameter. The 6-DOF model verified that preliminary determination, and predicted force levels somewhat less than the 1-DOF model(2).

Effect of Conductor Tension. The effect of changing the conductor tension was shown in Eq.(1) to be inversely proportional to the tension. This was verified by the 6-DOF model which predicted forces somewhat less than the 1-DOF model(2).

Effect of Pole Span. Eq. (1) indicates that the yoke bushing force is linearly proportional to pole span, which the 6-DOF model also predicted. The wheel/conductor and insulator forces were also linear functions of pole span(2).

Effect of Wheel Spacing. An increase in wheel spacing decreased the yoke bushing force somewhat, Figure 9. The insulator force did not show a strong trend with wheel spacing, but the wheel/conductor force increased substantially at small wheel spacing.

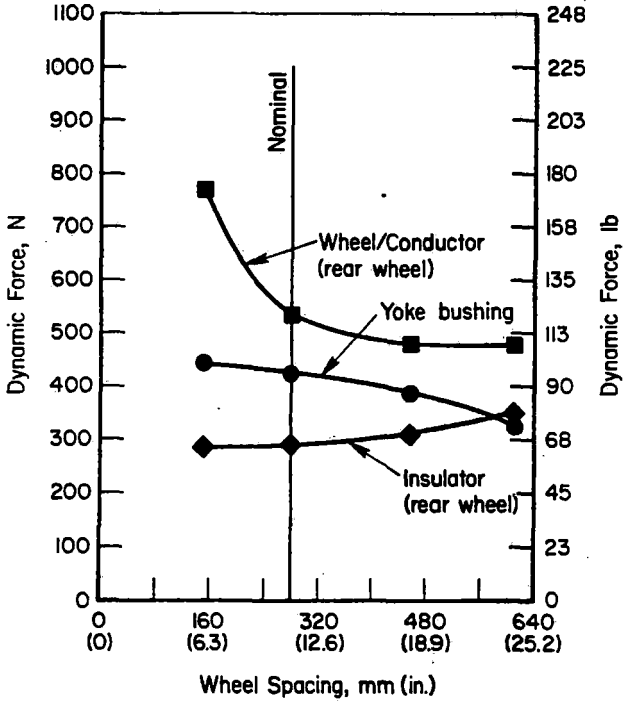

FIGURE 9. EFFECT OF WHEEL SPACING ON YOKE BUSHING, WHEEL/CONDUCTOR AND INSULATOR FORCES

Effect of Conductor Transition Length. Figure 10 illustrates the effect of transition length on the forces generated in the system. Most of the gain was produced by a 508-mm (20-in.) transition. It is of particular interest to note that the yoke bushing and insulator forces had only a slightly decreasing trend with increasing transition length.

Effect of Vehicle Speed. Based on Eq. (1) the yoke bushing force should increase as a linear function of vehicle speed, and as shown in Figure 11, it did. However, the force at the wheel/conductor interface increased more rapidly while the force at the insulator increased less rapidly.

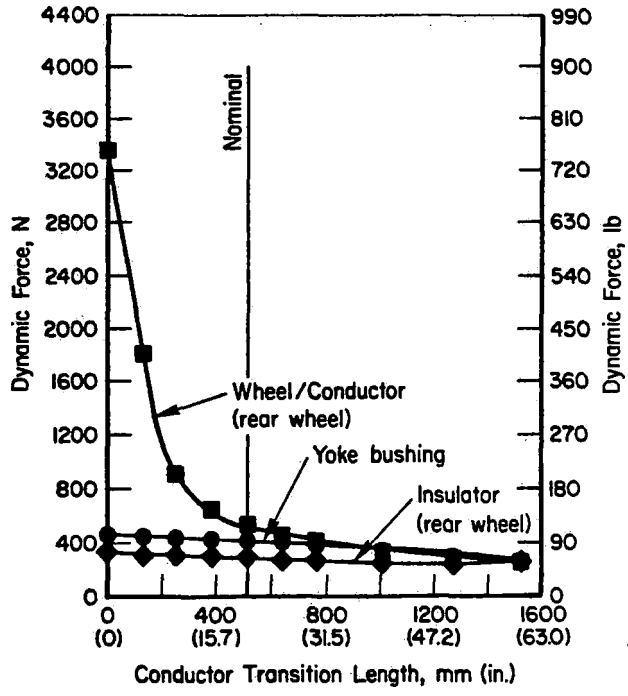

FIGURE 10. EFFECT OF CONDUCTOR TRANSITION LENGTH ON YOKE BUSHING, WHEEL/CONDUCTOR, AND INSULATOR FORCES

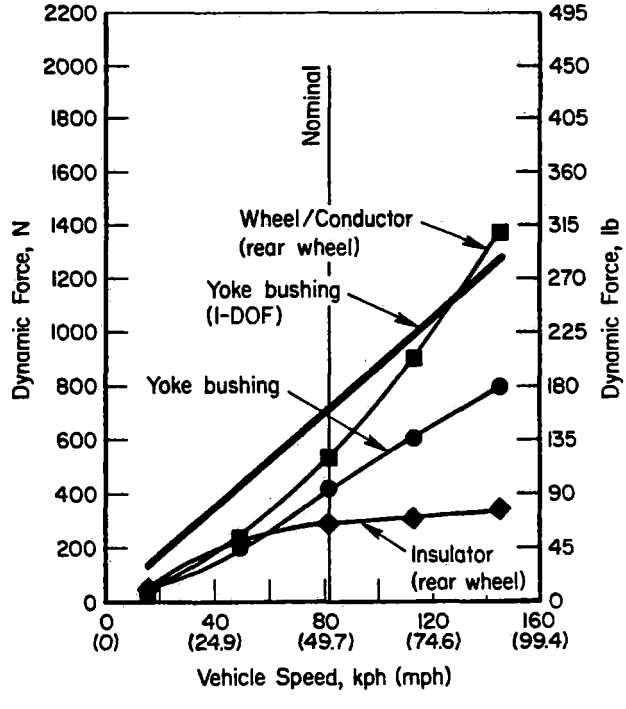

FIGURE 11. EFFECT OF VEHICLE SPEED ON YOKE BUSHING, WHEEL/CONDUCTOR, AND INSULATOR FORCES

Finite Element Model

Two principal results were obtained from the finite element simulation: the time histories of the

yoke bushing and the wheel/conductor forces. The simulation was compared to the 6-DOF model and is presented as a verification that the 6-DOF model gave reasonably accurate results. The results of the finite element simulation are based on the nominal parameters listed in Table 1.

Yoke Bushing Force. In Figure 12 the total yoke bushing force is plotted for the finite element and the 6-DOF models. It is apparent that the two responses are identical in the first mode frequency (12 Hz), and are reasonably close in the maximum amplitude. Extending the force time history further than shown in Figure 12 showed a slowly damped oscillation.

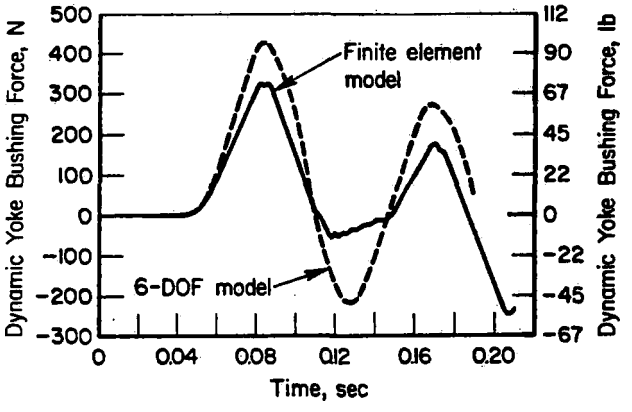

FIGURE 12. COMPARISON OF YOKE BUSHING FORCE TIME HISTORY OVER CONDUCTOR TRANSITION FOR FINITE ELEMENT AND 6-DOF MODEL

Wheel/Conductor Force. Figure 13 compares the finite element and 6-DOF model time histories for the force at the rear wheel/conductor interface. The comparison of the results from the two models was not good at any arbitrary time in the simulation; however, the frequency content of the two simulations was similar; and more important, the force magnitudes were similar.

SUMMARY

Three mathematical simulations were used to investigate the dynamics of a traveller system riding on a tensioned conductor. The 1-DOF and finite element models verified the trends and magnitudes of the forces predicted by the 6-DOF model.

The results of the 6-DOF model parametric study are summarized qualitatively in Table 2. The force trends are indicated for increases in the specified parameter. Large increases in the yoke bushing force can be expected from increases in yoke assembly weight, conductor diameter, pole span, and vehicle speed. Large increases in the wheel/conductor interface force can be expected for increases in wheel assembly weight, conductor diameter, pole span, and vehicle speed. Large increases in the wheel/conductor force can also be expected from a decrease in wheel spacing, and especially from decreased transition length. Large increases in the insulator force can be expected from increases in conductor diameter, and pole span. Decreasing tension increases all force levels.

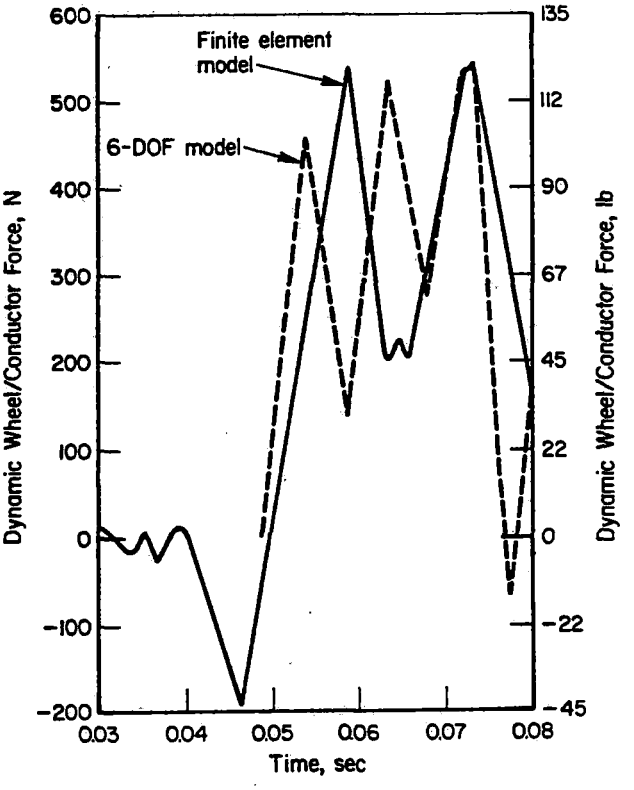

FIGURE 13. COMPARISON OF REAR WHEEL/CONDUCTOR FORCE TIME HISTORY OVER TRANSITION FOR FINITE ELEMENT AND 6-DOF MODELS

RECOMMENDATIONS

Based on the preliminary analytical studies, the following recommendations were made:

- An 805-mm (20-in.) circular transition should be built into the conductor at each pole attachment.
- A preload of at least half of the maximum wheel/conductor force should be built into the wheel assembly to prevent wheel/conductor separation. The recommended preload between each wheel and the conductor should be 270 to 445 N (60 to 100 lb).
- The traveller system weight should be minimized.
- The slope of the conductor should be minimized.

ACKNOWLEDGEMENTS

The author would like to thank the Federal Railroad Administration and the U.S. Department of Energy for sponsoring this study, and Mr. Robert Retallack of American Electric Power Service Corporation for his suggestions during the study. He would also like to thank his colleagues: Mr. Willard Kaiser, who made several recommendations pertinent to the design and dynamic analysis of the electrification system; and to Dr. George Workman, who contributed to the development of the finite element model.

TABLE 2. QUALITATIVE SUMMARY OF 6-DOF MODEL PARAMETRIC STUDY

Increasing Parameter	Yoke Bushing Force	Wheel/Conductor Force	Insulator Force
Yoke Assembly Weight	Increase rapidly	Increase slightly	Increase slightly
Wheel Assembly Weight	Decrease slightly	Increase rapidly	Increase moderately
Insulator Weight	Small change	Increase slightly	Decrease moderately
Yoke Bushing Stiffness	Increase slightly	Increase slightly	Increase slightly
Wheel/Conductor Stiffness	Small change	Small change	Small change
Insulator Stiffness	Increase slightly	Increase slightly	Increase moderately
Conductor Diameter	Increase rapidly	Increase rapidly	Increase rapidly
Conductor Tension	Decrease rapidly	Decrease rapidly	Decrease moderately
Pole Span	Increase rapidly	Increase rapidly	Increase rapidly
Wheel Spacing	Decrease slightly	Small change*	Increase slightly
Transition Length	Decrease slightly	Decrease slightly*	Small change
Vehicle Speed	Increase rapidly	Increase rapidly	Increase slightly

*A decrease in the parameter will result in a rapid increase in force.

REFERENCES

(1) Retallack, R. L., "Electric Railroad System with Elevated Conductor Alongside the Track", United States Patent 3,829,631, August 13, 1974.

(2) Retallack, R. L., Doyle, George R., Jr., Schneider, Lynn A., and Sheadel, John M., "A Low Cost Catenary Design-Analysis", FRA/ORD-81/73, October, 1981.

(3) Retallack, R. L., and Sheadel, J. M., "A Low-Cost Catenary System for Electric Railroads", to be presented at the ASME 1982 Winter Annual Meeting.

APPENDIX

Catenary Geometry

If it is assumed that the conductor is pin-attached at the poles, it will assume the shape of a catenary, Figure 3, whose functional relation can be expressed as

$$y = a\left[\cosh\left(\frac{x}{a}\right) - 1\right] \quad . \qquad (A\text{-}1)$$

For small values of x/a, Eq. (A-1) simplifies to

$$y = x^2/2a \quad . \qquad (A\text{-}2)$$

The slope of the catenary is given by the spatial derivative of Eq. (A-2)

$$\frac{dy}{dx} = \frac{x}{a} \quad . \qquad (A\text{-}3)$$

The vertical velocity of an object following the catenary is given by the time derivative of Eq. (A-2)

$$\frac{dy}{dt} = \frac{x\dot{x}}{a} \quad . \qquad (A\text{-}4)$$

The net change in vertical velocity at the insulator is

$$\Delta\dot{y} = \frac{2dy}{dt} = \frac{\rho\pi d^2 SV}{4T} \quad . \qquad (A\text{-}5)$$

Single-Degree-of-Freedom Simulation

The equation of motion for the system in Figure A-1 is

$$M\ddot{X} + C(\dot{x}-\dot{y}) + K(x-y) = 0 \quad . \qquad (A\text{-}6)$$

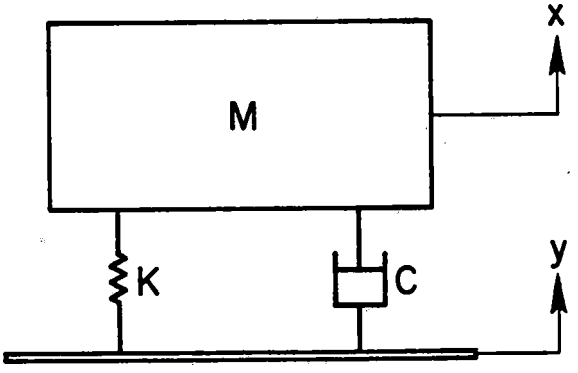

FIGURE A-1. BASE-EXCITED 1-DOF MASS/SRING/DASHPOT MODEL

Considering the case where the support base is given an instantaneous vertical velocity, the initial conditions are

$$x(0) = \dot{x}(0) = y(o) = 0;\ y(o) = -\Delta\dot{y} \qquad (A\text{-}7)$$

If the base velocity is held constant, and a substitution of variables is made ($u = x - y$), Eq. (A-6) can be rewritten as

$$M\ddot{u} + C\dot{u} + Ku = 0 \quad . \tag{A-8}$$

The solution to Eq. (A-8), with the initial conditions given in Eq. (A-7), is

$$u = e^{-\zeta\omega_d t}\left[\frac{\Delta\dot{y}}{\omega_d}\sin\omega_d t\right] \quad . \tag{A-9}$$

Differentiating Equation (A-9) to find the time of maximum displacement, it was determined that

$$u(t) = u_{max}, \text{ when } \omega_d t = \tan^{-1}\left(\frac{1}{\zeta}\right) \tag{A-10}$$

The maximum damped force in the stiffness element between the mass and the base is then given by

$$F = Ku_{max}$$

$$= F_o\left[\frac{e^{-\zeta\,\tan^{-1}\left(\frac{1}{\zeta}\right)}}{\left(1-\zeta^2\right)^{1/2}}\sin\left(\tan^{-1}\left(\frac{1}{\zeta}\right)\right)\right], \tag{A-11}$$

where

$$F_o = \Delta\dot{y}\left[\frac{KW}{g}\right]^{1/2} \quad . \tag{A-12}$$

The coefficient of F_o in Eq. (A-11) was evaluated for low damping ratios and found to be approximately 1.0.(2). Therefore, as a conservative estimate, the maximum force can be taken as F_o, in Eq. (A-12). Substituting Eq. (A-5) into Eq. (A-12) yields the maximum conservative force needed to change the direction of an object traversing the cusp of two adjacent catenaries.

$$F_o = \frac{\rho\pi d^2 SV}{4T}\left[\frac{KW}{g}\right]^{1/2} \quad . \tag{A-13}$$

Six-Degree-of-Freedom Simulation

Equations of Motion. The six-degree-of-freedom simulation included independent degrees of freedom for the yoke assembly (vertical and pitch), the wheel assembly (vertical and pitch), and the insulator/conductor under each wheel (vertical). A schematic of the model and the system parameters are shown in Figure 4.

The equations of motion for the six-degree-of-freedom simulation are:

$$M_1\ddot{y}_1 + K_{y2}(y_1-y_2) + C_{y2}(\dot{y}_1-\dot{y}_2) = 0 \tag{A-14}$$

$$I_1\ddot{\theta}_1 + K_{\theta 2}(\theta_1-\theta_2) + C_{\theta 2}(\dot{\theta}_1-\dot{\theta}_2) = 0 \tag{A-15}$$

$$M_2\ddot{y}_2 + K_{y2}(y_2-y_1) + K_{y3}(2y_2-y_6-y_5) + C_{y2}(\dot{y}_2-\dot{y}_1) + C_{y3}(2\dot{y}_2-\dot{y}_6-\dot{y}_5) = 0 \tag{A-16}$$

$$I_2\ddot{\theta}_2 + K_{\theta 2}(\theta_2-\theta_1) + K_{y3}b(2b\theta_2+y_6-y_5) + C_{\theta 2}(\dot{\theta}_2-\dot{\theta}_1) + C_{y3}b(2b\dot{\theta}_2+\dot{y}_6-\dot{y}_5) = 0 \tag{A-17}$$

$$M_3\ddot{y}_3 + K_{y3}(y_5-y_2-b\theta_2) + K_{y4}y_3 + C_{y3}(\dot{y}_5-\dot{y}_2-b\dot{\theta}_2) + C_{y4}\dot{y}_3 = 0 \tag{A-18}$$

$$M_4\ddot{y}_4 + K_{y3}(y_6-y_2+b\theta_2) + K_{y5}y_4 + C_{y3}(\dot{y}_6-\dot{y}_2+b\dot{\theta}_2) + C_{y5}\dot{y}_4 = 0 \quad . \tag{A-19}$$

The variables y_5 and y_6 in the above equations are the forcing functions due to the effective shape of the conductor.

Transition Geometry. To provide a smooth transition at the insulator, it was assumed that the catenary shape was continuous in position and slope with a circular arc at some distance from the insulator, Figure A-2.

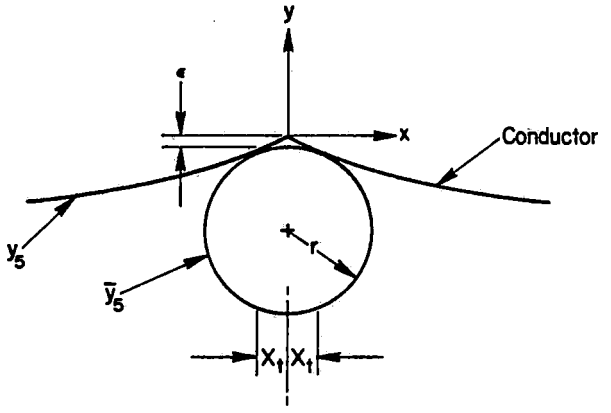

FIGURE A-2. TRANSITION GEOMETRY OF CONDUCTOR AT INSULATOR

The catenary equation, based on the coordinate system shown in Figure A-2, is

$$Y_5(X) = \frac{\left(X-\frac{S}{2}\right)^2}{2a} - \frac{S^2}{8a} \qquad X>0 \quad . \tag{A-20}$$

The equation of the circle is given by

$$\bar{Y}_5(x) = (r^2-X^2)^{1/2} - (r+\varepsilon) \quad . \tag{A-21}$$

For X>0, Eqs. (A-20) and (A-21) and their derivatives were equated at the half transition length, X_t. The results were the radius of curvature, r, and offset ε.

$$r = \left[X_t^2 + \left(\frac{aX_t}{X_t-S/2}\right)^2\right]^{1/2} \quad , \tag{A-22}$$

$$\varepsilon = \frac{S^2}{8a} + (r^2-X_t^2)^{1/2} - r - \frac{\left(X_t-\frac{S}{2}\right)^2}{2a} \quad . \tag{A-23}$$

The forcing functions, y_5 and y_6, depend on the effective shape and deflection of the catenary at the wheel location. For example, when the front wheel is on the circular transition,

$$y_5 = \bar{Y}_5 + y_3 \tag{A-24}$$